

FOR REFERENCE

NOT TO BE TAKEN FROM THIS ROOM

THE SOLUTION OF NONHOMOGENEOUS STATE OF STRESS
STRAIN AND SWELLING PROBLEM IN AMORPHOUS
POLYMER NETWORKS

by

CENGİZ ÖMER KAHRAMANOĞLU

B.S. in M.E., Boğaziçi University, 1983

Bogazici University Library



14

39001100315301

Submitted to the Institute for Graduate Studies in
Science and Engineering in partial fulfillment of
the requirements for the degree of

Master of Science

in

Mechanical Engineering

Boğaziçi University

1984

ACKNOWLEDGEMENTS

I would like to mention my gratitude to two marvelous people, Prof.Dr. Akın Tezel, Chairman of the Mechanical Engineering Department at Boğaziçi University and Doç.Dr. Burak Erman from Civil Engineering Department for their contribution and leadership.

Cengiz Kahramanoğlu

ABSTRACT

The total free energy a swollen and deformed amorphous cross-linked polymer network is given as $\Delta E = \Delta E_m + \Delta E_{ph} + \Delta E_c$ where ΔE_m is the free energy of mixing of polymer and solvent; ΔE_{ph} indicates the first part of elastic energy by representing ideal conditions called as 'Phantom Case'; ΔE_c covers the local constraints and completes the total free energy as a second part of elastic free energy. The explicit form of all free energies are obtained from molecular theory of rubber elasticity by including their recent developments. Expressions for stress in terms of strain and swelling ratio are obtained from free energy. Bending of a cross-linked amorphous cuboid is formulated as a boundary value problem and the distribution of solvent and stresses are numerically calculated for six distinct solvents. The magnitude of bending moments are found for different degrees of flexures up to 180° . Results are compared with each other and also with their linear solutions. As swelling increases a decrease in elasticity modulus is observed.

Ö Z E T

Düzensiz, çapraz bağlı, polimer zincirlerden oluşan malzemelerin şişmiş ve şekil değiştirmiş durumdaki toplam serbest enerjileri $\Delta E = \Delta E_m + \Delta E_{ph} + \Delta E_c$ ifadesi ile verilir. Burada ΔE_m karışım serbest enerjisidir; ΔE_{ph} elastik serbest enerjinin ilk kısmı olup, ideal şartlardan oluşan ve 'phantom' adı verilen durumu temsil eder, ΔE_c ise elastik serbest enerjinin ikinci kısmı olarak bölgesel etkilerin toplam serbest enerjiye katkısını belirtir. Serbest enerjinin açık denklemleri, son gelişmeler gözönüne alınarak moleküler teoriden elde edilmişlerdir. Uzama oranı ve şişme derecesi ile bağıntılı gerilme denklemleri serbest enerjiden çıkarılmıştır. Düzensiz çapraz bağlı polimer malzemeden yapılmış çubuğun eğilmesi, sınırdeğer problemi olarak formüle edilip, gerilmeler ve solvent dağılımı nümerik olarak altı değişik solvent değeri için hesaplanmıştır. Eğilme momenti 180^0 eğilme değerine kadar incelenmiştir. Sonuçlar birbirleri ve lineer çözümleri ile, bir ilişki gözlemek için karşılaştırılmış ve şişme arttıkça elastisite modülünün azaldığı gözlenmiştir.

TABLE OF CONTENTS

	<u>Page</u>
ACKNOWLEDGEMENTS	iii
ABSTRACT	iv
ÖZET	v
LIST OF FIGURES	ix
LIST OF TABLES	xii
LIST OF SYMBOLS	xiii
I. INTRODUCTION	1
II.. RUBBER ELASTICITY	3
2.1 General Physical Properties of Rubber	3
2.1.1 Elastic and Thermoelastic Properties	3
2.1.2 Chemical Constitution of Rubber	5
2.1.3 General Conditions for Rubber-like Elasticity	5
2.1.4 Network Formation	6
2.2 Internal Energy and Entropy Changes on Deformation	6
2.2.1 Stress Temperature Relations	6
2.2.2 Thermodynamic Analysis	7
2.3 The Elasticity of Molecular Network	9
2.3.1 General Approach and Fundamental Assumption of the Theory	9
2.3.2 Calculation of Entropy of Deformation	11
2.3.3 Work of Deformation	13
2.3.4 The Elastic Properties of Swollen Rubber	13
2.4 Swelling Phenomena	14

	<u>Page</u>	
2.4.1	General Thermodynamic Principles and Their Significance	15
2.4.2	Statistical Treatment of Swelling	17
2.4.3	The swelling of Cross-linked Polymers	20
2.4.4	The Dependence of Swelling on Strain	21
2.4.5	Recent Developments	23
2.4.6	The ' χ ' Parameter	25
III.	CONTINUUM MECHANICS MODEL	28
3.1	Flexure of an Incompressible Cuboid	28
3.1.1	Continuum Solution	28
3.2	Flexure of Compressible Cuboid	32
3.2.1	Solution of a Compressible Cuboid Problem	32
IV.	SOLUTION OF PROBLEMS OF ELASTICITY WITH SWELLINGS	35
4.1	General Approaches and Finite Bending of Swollen Beam	35
4.1.1	General Treatments	35
4.1.2	Description of Finite Bending of Swollen Beam Problem	36
4.1.3	Formulation of Problem	38
4.1.4	Numerical Calculation Method	40
4.2	The Uniqueness of Problem	41
4.2.1	General Differences	41
V.	RESULTS AND DISCUSSION	43
5.1	Swelling Ratio	43
5.2	Stresses	52
5.2.1	Stress t_1 in X Direction	52
5.2.2	Stress t_2 in Y Direction	56
5.2.3	Stress t_3 in Z Direction	60
5.2.4	Stresses and ' χ ' Parameter	64
5.3	General Results	67
5.4	Bending Moment M	69

	<u>Page</u>
VI. LINEAR APPROACH	73
6.1 Linear Theory	73
6.2 Comparasion of Linear and Nonlinear Solutions	76
VII. CONCLUSION	83
APPENDICES	85
APPENDIX A	86
APPENDIX B	101
BIBLIOGRAPHY	103
REFERENCES NOT CITED	104

LIST OF FIGURES

	<u>Page</u>	
FIGURE 2.1.1	Typical force-extension curve for the vulcanized rubber	4
FIGURE 2.2.1	Force at constant length as a function of temperature and elongation	7
FIGURE 2.3.1	Unstrained and strained case for unit cube	11
FIGURE 2.3.2	Affain deformation of chain	11
FIGURE 2.4.1	Free energy, heat, and entropy dilution for Rubber-Benzene	16
FIGURE 2.4.2	Schematic presentation of Flory model	18
FIGURE 2.4.3	The unit cube for strain-swelling relation	21
FIGURE 2.4.4	Interaction parameter ' χ ' for PDME-Benzene	27
FIGURE 3.1.1	Coordinate system for incompressible cuboid deformation	29
FIGURE 4.1.1	Sample swelling and deformation	37
FIGURE 5.1.1	Bending of a block at different degrees	44
FIGURE 5.1.2	Locations of ten equally spaced stations	45
FIGURE 5.1.3	Equilibrium swelling of a block for different χ 's	45
FIGURE 5.1.4	' χ ' parameter versus degree of swelling	46
FIGURE 5.1.5	Solvent distribution in terms of $v_2(r)$ for $\chi = 1.0$	48

	<u>Page</u>
FIGURE 5.1.6 Solvent distribution in terms of $v_2(r)$ for $\chi = 0.75$	48
FIGURE 5.1.7 Solvent distribution in terms of $v_2(r)$ for $\chi = 0.63$	49
FIGURE 5.1.8 Solvent distribution in terms of $v_2(r)$ for $\chi = 0.50$	49
FIGURE 5.1.9 Solvent distribution in terms of $v_2(r)$ for $\chi = 0.25$	50
FIGURE 5.1.10 Solvent distribution in terms of $v_2(r)$ for $\chi = 0.00$	50
FIGURE 5.1.11 Nondimensional polymer fraction $v_2(r)/v_{20}$ for every individual ' χ 's'	51
FIGURE 5.2.1 Radial distribution of t_1 for $\chi = 1.00$	53
FIGURE 5.2.2 Radial distribution of t_1 for $\chi = 0.75$	54
FIGURE 5.2.3 Radial distribution of t_1 for $\chi = 0.63$	54
FIGURE 5.2.4 Radial distribution of t_1 for $\chi = 0.50$	55
FIGURE 5.2.5 Radial distribution of t_1 for $\chi = 0.25$	55
FIGURE 5.2.6 Radial distribution of t_1 for $\chi = 0.00$	56
FIGURE 5.2.7 Stress t_2 curves for $\chi = 1.00$	57
FIGURE 5.2.8 Stress t_2 curves for $\chi = 0.75$	58
FIGURE 5.2.9 Stress t_2 curves for $\chi = 0.63$	58
FIGURE 5.2.10 Stress t_2 curves for $\chi = 0.50$	59
FIGURE 5.2.11 Stress t_2 curves for $\chi = 0.25$	59
FIGURE 5.2.12 Stress t_2 curves for $\chi = 0.00$	60
FIGURE 5.2.13 Pointing effects for $\chi = 1.00$	61
FIGURE 5.2.14 Pointing effects for $\chi = 0.75$	62
FIGURE 5.2.15 Pointing effects for $\chi = 0.63$	62
FIGURE 5.2.16 Pointing effects for $\chi = 0.50$	63
FIGURE 5.2.17 Pointing effects for $\chi = 0.25$	63
FIGURE 5.2.18 Pointing effects for $\chi = 0.00$	64
FIGURE 5.2.19 Stress t_1 for different χ 's at $\theta_0 = 90^\circ$	65

	<u>Page</u>
FIGURE 5.2.20 Stress t_2 for different χ 's at $\theta_0 = 90^\circ$	66
FIGURE 5.2.21 Stress t_3 for different χ 's at $\theta_0 = 90^\circ$	66
FIGURE 5.4.1 Moment-Flexure degree curves for every ' χ ' parameters	70
FIGURE 5.4.2 Moment behaviour respect to swelling degree	71
FIGURE 5.4.3 Maximum t_2 values for different a/b ratio	72
FIGURE 6.1.1 A typical beam for linear approach	74
FIGURE 6.2.1 Comparison of linear and nonlinear solutions for $\chi = 1.00$	77
FIGURE 6.2.2 Comparison of linear and nonlinear solutions for $\chi = 0.75$	78
FIGURE 6.2.3 Comparison of linear and nonlinear solutions for $\chi = 0.50$	79
FIGURE 6.2.4 Comparison of linear and nonlinear solutions for $\chi = 0.25$	79
FIGURE 6.2.5 Comparison of linear and nonlinear solutions for $\chi = 0.00$	80
FIGURE 6.2.6 Swelling effect on bending parameter and components	81
FIGURE 6.2.7 Elasticity modulus and swelling degree curve in nonlinear theory	82

LIST OF TABLES

	<u>Page</u>
TABLE 2.4.1 Sample values for ' χ ' parameter	27
TABLE 5.3.1 General results for deformed geometry	68

LIST OF SYMBOLS

a	: The width of swollen beam
a_0	: The width of unswollen beam
a_D	: The width of swollen and deformed beam
dA	: Change in Helmholtz free energy
b	: The length of swollen beam
b_0	: The length of unswollen beam
C	: Bending parameter
C_L^K	: Deformation tensor
$C_{(L)}^{(K)}$: Deformation tensor in physical components
E	: Elasticity modulus
ΔE	: Total free energy
ΔE_m	: Mixing free energy
ΔE_e	: Elastic free energy
ΔE_{ph}	: Phantom free energy
ΔE_c	: Constraints free energy
F	: Force
G	: Constant for elastically stored free energy
G_{KL}	: Metric tensor for X^K coordinate system
g_{kl}	: Metric tensor for x^k coordinate system
ΔH	: Change in heat constant

I	: Moment of inertia of beam
I, II, III	: Invariants of deformation tensor
L	: Length of a link
L_s	: Length of a swollen specimen
L_{us}	: Length of a unswollen specimen
l	: Length of specimen
M	: Flexure couple-moment
M_c	: Average molecular weight
m	: Constant depends on number of links
N	: Number of polymer molecules
n	: Number of links, number of solvent molecules
δn	: Transferred solvent moles
P	: Static pressure
dQ	: Change in heat energy
R	: Universal gas constant
r_1	: Inner radius of deformed beam
r_2	: Outer radius of deformed beam
S	: Entropy
dS	: Change in entropy
T	: Absolute temperature
t_i	: Stress
dU	: Change in internal energy
v	: Volume fraction
v_1	: Solvent volume fraction
v_2	: Polymer volume fraction

v_{20}	: Initial swelling degree
V	: Volume
V_0	: Initial volume
V_s	: Swollen and deformed volume
V_{us}	: Unswollen volume
V_1	: Molecular volume
\bar{W}	: Total conformation of N molecules
dW	: Change in work done on system
$x^i = (r, \theta, z)$: Coordinate system for deformed state
$X^i = (X, Y, Z)$: Coordinate system for undeformed state
x, y, z, r	: Notations for deformed chain
x_0, y_0, z_0, r_0	: Notations for undeformed chain
<u>Greek symbols</u>	
α	: Flory's constant
α_i	: Distorsion referenced from swollen state
δ	: Cohesive energy density
ϵ	: Strain
ζ	: Constant for effects of structural inhomoneties
θ_0	: Flexure degree
κ	: Material constant
λ_i	: Deformation gradient or stretch, referenced from unswollen and undeformed state
λ_0	: Deformation gradient between unswollen and swollen states
μ	: Number of junctions in network
ξ	: Network cycle rank

ρ	: Final density
ρ_0	: Initial density
ψ	: Nondimensional radius = $r - r_1/r_2 - r_1$
χ	: Swelling parameter
$\bar{\chi}$: Interaction parameter for system
$\bar{\chi}_1$: Interaction parameter for solvent
$\bar{\chi}_2$: Interaction parameter for polymer

I. INTRODUCTION

Rubber is obtained in the form of latex from the tree named "Hevea Braziliensis". "Caoutchouc" is another and more expressive term which means 'weeping wood' in Maya Indians' Language. As it can be easily guessed, it is something from the new world. Europeans learned rubber during the travels of Christopher Columbus.

Today 75 per cent of rubber production is consumed by the tire sector. It is also the main material of waterproof products and isolation processes and the textile industry is another field where rubber threads are commonly used to produce flexible clothes.

The term rubber is not restricted to the original natural rubber because of the technological developments, especially the progress achieved during the second world war enabled the industry to manufacture artificial rubber and rubber-like materials so the term is applied to any material having mechanical properties similar to those of natural rubber regardless of its chemical constitution.

Rubber is essentially a polymer network which is created by linking individual polymer chains into solid structure. It swells when exposed to the action of solvent. This is not a chemical reaction, just a physical

mixing which causes isotropic swelling. The configurational entropy of the expanding chains is decreased upon swelling. On the other hand the mixing of polymers with solvent increases the entropy. When the two entropies are equal, the state of equilibrium is reached. This state is treated by Flory and Rehner [1]. It is possible to observe a further change in the amount of solvent absorbed when the swollen network is deformed to different states. The network-solvent system shows nonhomogeneous state of stress, strain and degree of swelling at every material point when external forces are applied in technical and biological problems.

In the treatment of these problems, stress strain and swelling relations are taken from molecular theory of rubber elasticity which is reasonably in good agreement with experimental results.

In following sections the rubber elasticity is examined on the basis of molecular and statistical theory and then a solution model is developed for solving nonhomogeneous state of stress and strain by using continuum mechanics principles. The solutions are found for a specific problem which is the flexure of an amorphous polymer beam and the study is completed with comparative discussions on results.

II. RUBBER ELASTICITY

In this section we will give a brief summary of L.R.G. Treloar's study, including physical properties of rubber, internal energy and entropy change on deformation, the elasticity of network, swelling phenomena, and the recent developments related to rubber-like behaviour [2].

2.1 GENERAL PHYSICAL PROPERTIES OF RUBBER

2.1.1 Elastic and Thermoelastic Properties

The rubber or rubber-like material has one obvious and important physical characteristic; it shows large deformations when even small stresses are applied. A typical force-extension curve is shown in Fig. 2.1.1. The nonlinearity prohibits the use of a single value of elasticity modulus. When a point, at the origin, is considered in terms of quantitative values, the difference from conventional solids becomes more clear. The slope of this curve at the origin is in the order of 1.0 N/mm^2 which is very low compared with a typical hard solid that has a Young's Modulus in the order of $2 \times 10^5 \text{ N/mm}^2$ [2].

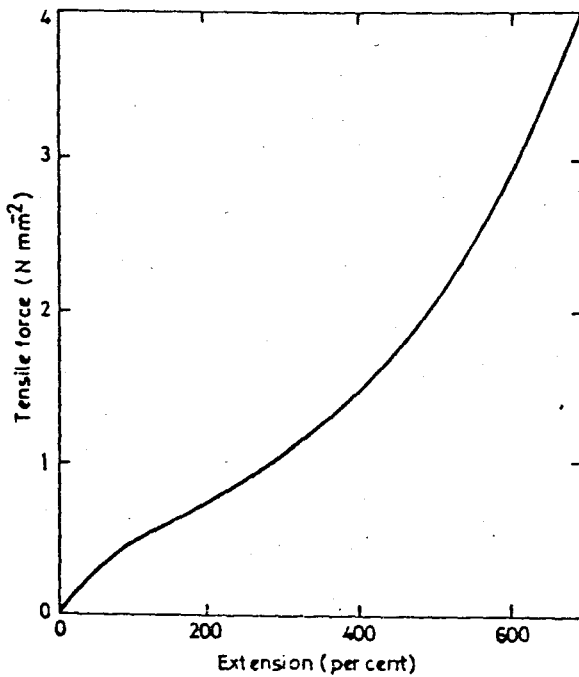


Figure 2.1.1 - Typical force-extension curve for vulcanized rubber [2].

The study of thermoelastic properties goes back to Gough (1805) who made the following observations;

1. The stretched rubber, under a constant load contracts (reversibly) on heating and
2. The rubber gives out heat (reversibly) when it is stretched.

These results were confirmed by Joule (1859). A more detailed explanation of thermoelasticity will be given in Section 2.2.

2.1.2 Chemical Constitution of Rubber

The rubber exist in latex in the form of small globules having diameters of micron size suspended in liquid. The rubber, usually 35 per cent of mixture, can be obtained by drying the liquid parts. It is essentially a hydrocarbon identified by the chemical formula $(C_5H_8)_n$. Chemically the rubber hydrocarbon is a polymer of isoprene built up in the form of continuous chains. In a chain, double bonds exist and every fourth carbon atom carries the methyl (CH_3) side-group. The double bonds are important during the reactions with sulfur or with other reagents in the vulcanization process.

Polyvinyl chloride, polystyrene, Butadiene-styrene, Polypropylene are some common synthetic rubbers which have very large utility fields.

2.1.3 General Conditions for Rubber-like Elasticity

Under the guidance of the previous works which were carried out by Haller (1931) and Karrer (1933), the below conditions for the rubber-like state are stated by L.R.G. Treloar.

1. The presence of long-chain molecules, with freely rotating links;
2. Weak forces between the molecules;
3. An interlocking of the molecules at a few places along their length to form a three dimensional network.

The above conditions define the rubber-like state in fact the first two conditions not only identify the rubber state but also apply to the liquid state as well. The last condition states the difference between rubber and liquid by restricting the movement of molecules.

2.1.4 Network Formation

The necessary cross-links between chains are normally introduced by the vulcanization process. This is a simple reaction with sulfur which was discovered by Charles Goodyear. Different reagents and methods have been used but the vulcanization is the main production method to create cross-linkages. In rubber technology articles are moulded or extruded while they are semi-liquid or in any convenient form. Then their final form is fixed by securing desired properties.

2.2 INTERNAL ENERGY AND ENTROPY CHANGES ON DEFORMATION

2.2.1 Stress-Temperature Relations

When the system of long chain molecules pass from the unstrained state to the strained state, the elasticity of rubber changes because of differences in the configuration of chains. In fact these changes are related to the configurational entropy of the system, and the internal energy is assumed to be constant during the deformation. When only entropy change is involved, the stretching force for a given state of strain should be proportional to absolute temperature as shown in Figure 2.2.1 which is obtained experimentally by Antony (1942). In this figure, in order to

distinguish low and high strain regions, the 10 per cent extension is accepted as a boundary of the so-called 'thermoelastic inversion' region. At low strains, stress shows decrease for higher temperatures and at high strains stress increases as the temperature increases.

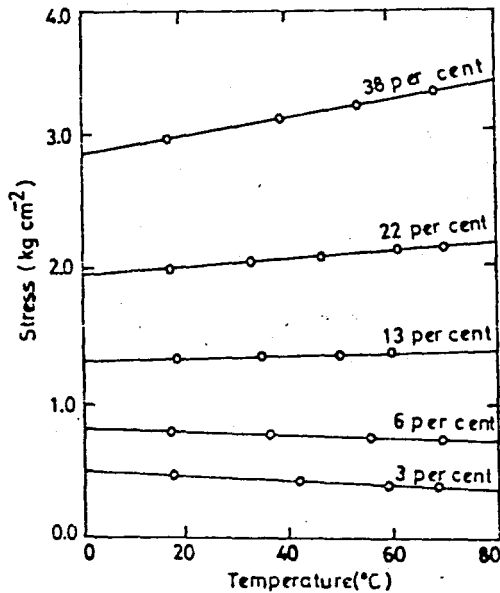


Figure 2.2.1 - The change in force at constant length for different elongations is indicated. (Antony, 1942).

2.2.2 Thermodynamic Analysis

Using first and second laws of thermodynamics it is possible to obtain a relationship between force, length and the temperature in the following order by assuming a reversible process;

$$dU = dQ + dW$$

and $TdS = dQ$

(2.1)

where dQ and dW are respectively heat observed by the system and work done on the system by external forces, T is the absolute temperature and dS is the entropy. The Helmholtz free energy may be defined for infinitesimal changes as

$$dA = dU - TdS \quad (2.2)$$

By using Eqs. (2.1) and (2.2) we obtain the classical results for an isothermal reversible process in which Helmholtz free energy is equal to the work done on the system;

$$dA = dW \quad (2.3)$$

Similarly the work done will be expressed in terms of the static pressure and tensile force, 'F', acting on a specimen.

$$dW = Fd\ell - pdV \quad (2.4)$$

In the case of rubber elasticity, the last term may be neglected and the force may be found as;

$$F = \frac{dW}{d\ell} = \frac{dA}{d\ell} \quad (2.5)$$

Eq. (2.5) shows that tensile force is equal to change in Helmholtz free energy per unit increase in length of specimen. When the force or change in Helmholtz free energy is zero, the unstretched state is obtained;

$$\frac{dA}{d\ell} = 0 \quad (2.6)$$

On the other hand, according to Joule's observations, the heat must be given as a response to extension. When the internal energy change is assumed to be zero, according to kinetic theory, the first law becomes

$$dW = -dQ . \quad (2.7)$$

Since the stretching work is positive, the heat observed should be negative which means that heat is evolved during the extension.

2.3 THE ELASTICITY OF MOLECULAR NETWORK

In order to express the mechanical properties of rubber in terms of molecular constitution it is necessary to develop kinetic theory which brings the quantitative side of the subject into the picture.

2.3.1 General Approach and Fundamental Assumptions of the Theory

The following assumptions which are based on Kuhn theory have been used by Treloar to develop a new theory [2].

1. A chain is defined as a segment of molecule between cross-linkages and the network contains N chains per unit volume.
2. The end-to-end distance which is known as the mean square distance is the same for all assemblies of unstrained chains and it is given by the formula;

$$\bar{r} = \frac{\int_0^{\infty} rP(r)dr}{\int_0^{\infty} P(r)dr} = \frac{3}{2m^2} = nL^2 \quad (2.8)$$

where

$$P(r) = (4m^3/\pi^{3/2})\exp(-m^2r^2)\pi r^2 \quad (2.9)$$

$$m^2 = 3/2 nL^2 \quad (2.10)$$

and 'r' is the end-to-end distance for a set of free chains. P(r) indicates the probability distribution of r and m is a constant which depends on the number of links 'n' and the length of a link, 'L'.

3. During the deformation no volume change occurs.
4. The junction points between chains move as if they were imbedded in an elastic continuum. So during the deformation every part of the chain changes in the same ratio. This case is the so-called affine case.
5. The total entropy of the network is equal to the totality of individual chain's entropy which is given as

$$s = k\{\ln P(r)dv\}$$

or when Eq. (2.9) is used, its implicit final form becomes,

$$s = C - km^2r^2 \quad (2.11)$$

where k is a proportionality constant obtained from Eq. (2.9) and C is an arbitrary constant.

2.3.2 Calculation of Entropy of Deformation

In order to obtain energy expressions the main variable entropy should be calculated. A specimen in the form of a unit cube is taken as in Fig. 2.3.1 and instead of simple tension a more general case is taken into account. The cube is strained and transformed into a rectangular parallel-piped having three unequal edges $\lambda_1, \lambda_2, \lambda_3$.

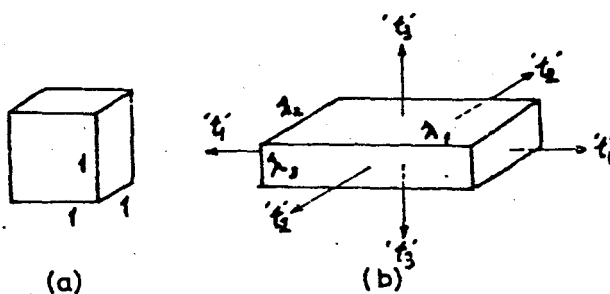


Figure 2.3.1 - Unstrained and strained case for unit cube.

Since the specimen was unit cube before the deformation λ 's will be equal to stretches. Because of the third assumption i.e. no volume change during the deformation the following equality can be stated.

$$\lambda_1 \lambda_2 \lambda_3 = 1 \quad (2.12)$$

If an individual chain in the specimen is considered

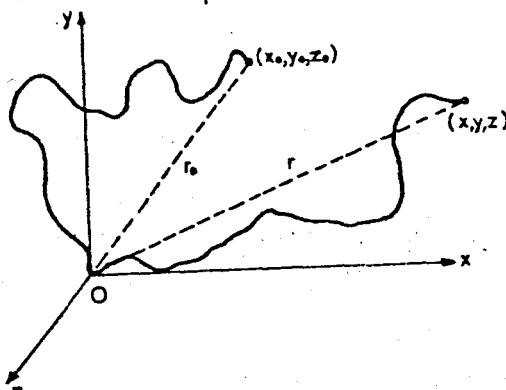


Figure 2.3.2 - Affine deformation of chain.

as in figure 2.3.2; r_0 is the end-to-end distance before deformation and r is the end-to-end distance after deformation. The components of r can be expressed as

$$\begin{aligned}x &= \lambda_1 x_0 \\y &= \lambda_2 y_0 \\z &= \lambda_3 z_0\end{aligned}\tag{2.13}$$

where the principal axis coincides with the coordinate system. Since the entropy of initial state ' S_0 ' and the entropy of strained state ' S ' can be expressed as follows

$$S_0 = -km^2(x_0^2 + y_0^2 + z_0^2) + C\tag{2.14}$$

and

$$S = -km^2(\lambda_1^2 x_0^2 + \lambda_2^2 y_0^2 + \lambda_3^2 z_0^2) + C\tag{2.15}$$

the contribution of deformation to total entropy of network can be found easily as

$$\Delta S = S - S_0\tag{2.16}$$

Since r_0 is completely arbitrary, x_0 , y_0 , z_0 components can be considered as unity and N chains can be assumed to exist in the unit cube. If we substitute Eqs. (2.14) and (2.15) into Eq. (2.16) and multiply with N to get the total entropy contribution, we will have the following equation

$$\Delta S = - (1/2)Nk(\lambda_1^2 + \lambda_2^2 + \lambda_3^2 - 3)\tag{2.17}$$

where the 1/2 factor is obtained from insertion of r_0^2 which is equal to $3/(2m^2)$.

2.3.3 Work of Deformation

From Eq. (2.7) we already know that $dW = -TdS$, since there is no change in internal energy, Helmholtz free energy or work of deformation can be given directly as

$$dW = (1/2)NkT(\lambda_1^2 + \lambda_2^2 + \lambda_3^2 - 3) \quad (2.18)$$

where the dW is the elastically stored free energy in unit volume. The coefficient NkT in this equation may be expressed as $G = NkT$, where G is dependent only on N at constant temperature. The expression obtained above shows that the elastic properties of rubber is dependent on number of chains, N , and the G may be expressed in terms of the chains' average molecular weight

$$G = \rho RT/M_c \quad (2.19)$$

where ρ and R are density and gas constant respectively.

2.3.4 The Elastic Properties of Swollen Rubber

Although the phenomenon of swelling will be discussed in the following section a brief introduction to swollen rubber properties will be given here. If we take the previous unit cube and expose it to solvent action, it swells. The swelling degree may be defined as the volume ratio of rubber to solvent-rubber mixture and it will be equal to $V_0/V = v_2$. Hence the dimensions of unit cube after swelling can be easily found as

$$\lambda_0 = 1 \cdot v_2^{-1/3}.$$

Since there is no volume restriction in the derivation of entropy of deformation, it can be carried out to the swollen state. By following the method used in the preceding section and defining the final swollen stretch λ_i as

$$\lambda_i = \alpha_i \lambda_{i0} = v_2^{-1/3} \alpha_i \quad (2.20)$$

in which α_i 's are referenced to unstrained swollen state, the entropy of deformation ΔS per unit volume can be found with the multiplication of ΔS by v_2 . Finally the multiplication of ΔS with temperature will give the strain energy or free energy function as

$$dW = -T\Delta S = (1/2)NkTv^{1/3}(\alpha_1^2 + \alpha_2^2 + \alpha_3^2 - 3) \quad (2.21)$$

in which the stretches are referenced from swollen state.

2.4 SWELLING PHENOMENON

In swelling phenomenon the polymer and solvent mixture which strongly depends on the nature of the liquid is the most important concept. Like materials, natural and synthetic polymers can be divided into two groups as water-swelling polymers and organic swelling polymers. The first class includes the cellulose and proteins while the second class essentially consists of rubbers.

2.4.1 General Thermodynamic Principles and Their Significance

When the thermodynamics of the subject is examined, the state of equilibrium of swelling becomes important. In the case of rubber swelling; the mixed phase is the solid and the pure phase is the liquid. The equilibrium of the system has a very close relation with free energy, when the free energy is minimum with respect to changes in composition of mixed phase it means that the state of equilibrium is satisfied. A change in free energy may happen if a small quantity of liquid is transferred from the pure state to the mixed state. This transfer may be expressed with Gibbs free energy of dilution ΔE . For equilibrium condition it should be zero

$$\Delta E = 0 \quad (2.22)$$

The Gibbs energy can be written in terms of heat ΔH and entropy ΔS of dilution

$$\Delta E = \Delta H - T\Delta S \quad (2.23)$$

where ΔH is the change in the heat content and ΔS is the change in entropy per mole of liquid. The heat content can be given with $H = U + PV$ but because of fundamental assumption there is no change in volume so heat content is equal to internal energy. Since it is possible to obtain some thermodynamic quantities experimentally, with the help of following equalities we can calculate the Gibbs free energy and the heat content. As given in the following formulas they are related to the absolute temperature T , vapour pressure P and saturation vapour pressure P_0

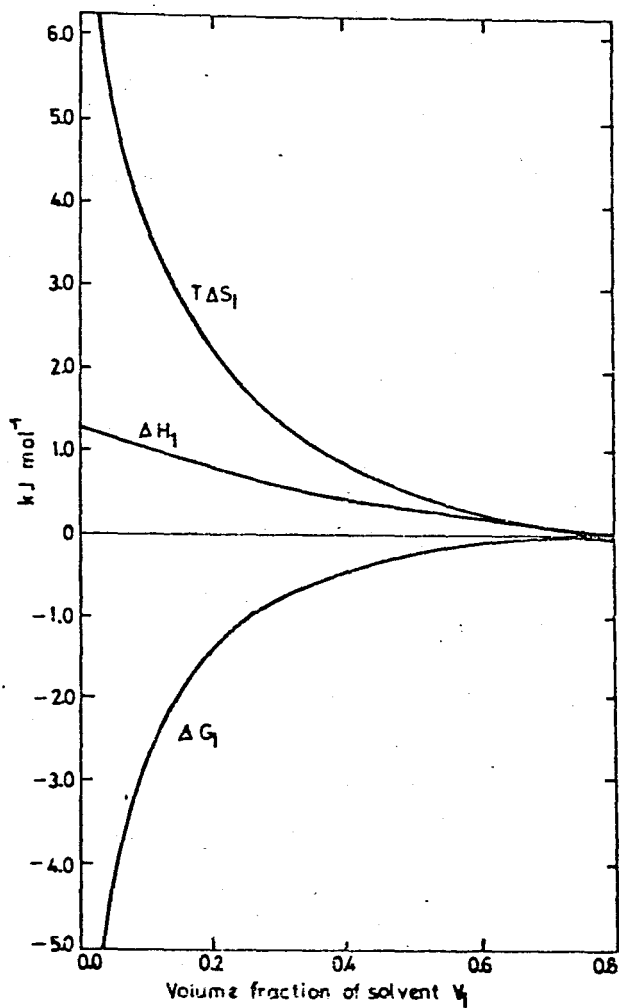


Figure 2.4.1 - Free energy, heat and entropy dilution for rubber-benzene.

$$\Delta E = RT \ln(P/P_0)$$

(2.24)

$$\Delta H = -RT^2 \frac{\partial [\ln(P/P_0)]}{\partial [T]}$$

The change in entropy ΔS may readily be found by combining Eqs. (2.23) and (2.24). In Figure 2.4.1 for rubber-benzene case, the free energy, heat and entropy of dilutions have been calculated from vapour pressure and osmotic data [2]. As it is seen from Figure 2.4.1, ΔE is always negative and ΔS is positive like ΔH which is comparatively small and has a tendency to reduce the energy (from Eq. (2.23)). Since ΔH corresponds to heat absorption of mixing, it tends to oppose swelling and the associated entropy becomes the 'driving force' of swelling.

2.4.2 Statistical Treatment of Swelling

It is easy to notice the close thermodynamic analogy between the elastic properties of rubber and the phenomenon of swelling. They are the manifestation of the configurational entropy of long chain molecule systems so the statistical treatment can be easily applied to the swelling phenomenon as well. A model for this case was prepared by Flory (1942) and further studies were done by Treloar. In this section the model and its results are introduced briefly.

A three dimensional lattice in which each site may be occupied either by a liquid molecule or by a single segment of a polymer chain is formed. Although the liquid molecules are free to occupy any vacant site, the polymer molecule segments are restricted to any adjacent site. This is illustrated in Figure 2.4.2 where individual circles represent solvent molecules and the rest are polymer chains.

If we let n_0 to be the total number of sites and N to be the number of polymer molecules, each consisting of x segments, the number of liquid

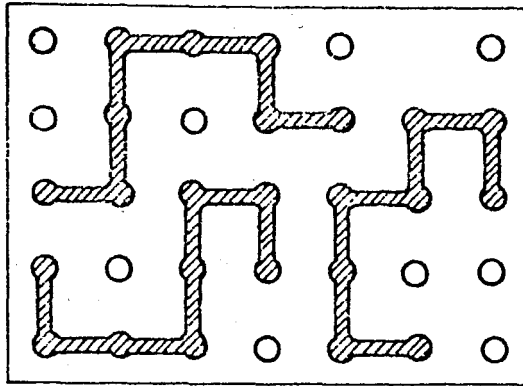


Figure 2.4.2 - Schematic presentation of Flory Model.

molecules will be $n_0 - xN$.

Under the guidance of Flory's model, Treloar found that the total conformation of N polymer molecule chain assembly is

$$\bar{W} = \frac{1}{N!} \sum_{j=1}^N \frac{1}{2} (n_0 - xN_j) \left(\frac{Z}{Z-1} \right)^{\alpha x - 1} \quad (2.25)$$

where the Z is nearest neighbouring site and α is the number of sites available. The configurational entropy ΔS which is essentially needed may be found from Boltzmann's relation

$$s = k \ln \bar{W} \quad (2.26)$$

Equation (2.26) consists of $n = n_0 - xN$ terms in \bar{W} and Boltzmann's constant k . When n is zero, it means that unswollen case is valid so it is possible to reach entropy S_0 of unswollen state by taking this term zero. Consequently the difference between ' S ' and ' S_0 ' will give the entropy of mixing process ΔS_m as;

$$\Delta S_m = -k(n \ln \frac{n}{n + xN} + N \ln \frac{xN}{n + xN}) \quad (2.27)$$

or

$$\Delta S_m = -k(n \ln v_1 + N \ln v_2) \quad (2.28)$$

where the v_1 and v_2 are volume fractions of solvent and polymer respectively Eq. (2.28) can be expressed with respect to liquid component by differentiating ΔS_m with respect to n .

$$\Delta S_{\ell} = -R(\ln(1 - v_2) + (1 - (1/x))v_2) \quad (2.29)$$

On the other hand for free energy calculations the heat dilution ΔH is given on a semi-empirical base by Flory with the following formula

$$\Delta H = \alpha v_2^2 . \quad (2.30)$$

The combination of Eqs. (2.30), (2.29) and (2.23) will give the total mixing energy. Hence

$$\Delta E_m = RT\{\ln(1 - v_2) + (1 - (1/x))v_2 + (\alpha/RT)v_2^2\} \quad (2.31)$$

is obtained. The term in front of the v_2^2 may be considered as a constant χ and when the chains are assumed sufficiently long, L and x will increase which means that the term $1/x$ may be neglected. Therefore we have

$$\Delta E_m = RT\{\ln(1 - v_2) + v_2 + \chi v_2^2\} \quad (2.32)$$

Flory (1953) had found a similar equation, by using Eq. (2.28). He expressed the mixing free energy as follows;

$$\Delta E_m = kT(n \ln v_1 + N \ln v_2 + \bar{X} n v_2) \quad (2.33)$$

where $\bar{\chi}$ is the so-called interaction parameter which will be discussed in a separate section.

2.4.3 The Swelling of Cross-linked Polymers

In the preceding discussion the system was not cross-linked; since the interconnection in polymers prevents the possibility of solution, Eq. (2.32) or (2.33) are not sufficient for the cross-linked case. When the total entropy of this condition is considered the total free energy of dilution becomes

$$\Delta\varepsilon = \Delta E_m + \Delta E_e \quad (2.34)$$

where ΔE_m represents the free energy of dilution for the polymer before the cross-linking and ΔE_e is the change of free energy per mole of liquid observed because of the elastic expansion of the network. In order to satisfy isotropic expansion of the network, we must have

$$\lambda_1 = \lambda_2 = \lambda_3 = 1/v_2^{1/3} = \lambda_0 \quad (2.35)$$

and also we know that, elastically stored free energy W , in Gaussian network, is given by Eq. (2.18). Substituting Eqs. (2.35) and (2.19) in Eq. (2.18) and taking $v_2^{-1} = 1 + nV_1$ in which V_1 is the molar volume of liquid and 'n' is the number of liquid molecules. Differentiation of W with respect to n will give the change in elastic free energy ΔE_e ,

$$\Delta E_e = \frac{\rho RT}{M_c} V_1 v_2^{1/3} \quad (2.36)$$

and total free energy of dilution is found as:

$$\Delta E = RT\{\ln(1 - v_2) + v_2 + \chi v_2^2 + \frac{\rho V_1}{M_c} v_2^{1/3}\} \quad (2.37)$$

2.4.4 The Dependence of Swelling on Strain

Up to this section the equilibrium of swelling of cross-linked polymers and the strain free state were considered. Additionally in this section the presence of stress or other mechanical constraints will be examined. This problem was solved by Flory and Rehner (1944) for simple tension case and its more complicated case corresponding to pure homogeneous multiaxial strain was solved by Treloar (1950). In order to give short summary of Treloar's work a unit cube is taken. The cube is in contact with the liquid and bounded by normal forces applied to its faces to form a rectangular block with dimensions l_1, l_2, l_3 where edges are accepted as in the direction of principle strains as in Figure 2.4.3.

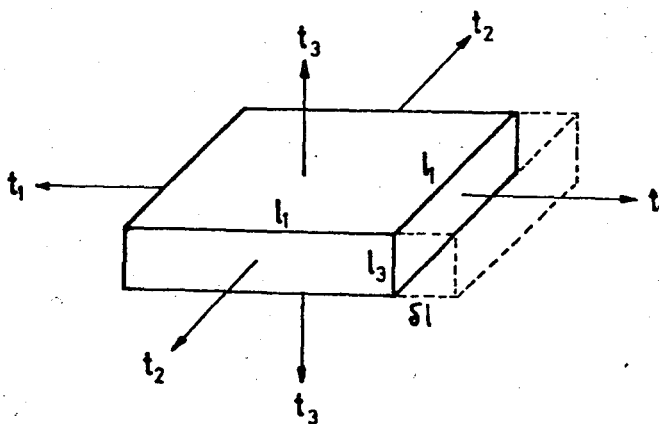


Figure 2.4.3 - Equilibrium of swollen rubber under stress

From the conservation of mass principle we have

$$\ell_1 \ell_2 \ell_3 = 1/v_2 = \frac{V_p + V_s}{V_p} = 1 + V_1 n / NV_p \quad (2.38)$$

for which the terms were defined previously. The Eq. (2.34) or the total Gibbs energy, for the transformation from unswollen and unstrained state to swollen and strained state may be written in terms of partial derivatives with respect to the number of moles of liquid. We have;

$$\left. \frac{\partial \Delta E}{\partial n} \right|_{\ell_2, \ell_3} = \frac{\partial \Delta E_m}{\partial n} + \frac{\partial \Delta E_e}{\partial \ell_1} \left. \frac{\partial \ell_1}{\partial n} \right|_{\ell_2, \ell_3} \quad (2.39)$$

where absorption of a small quantity δn moles of liquid is considered under the condition that ℓ_2 and ℓ_3 are constants while ℓ_1 is increased by $\delta \ell_1$ because of applied stress t_1 so the work done by t_1 is obtained as,

$$\delta W = t_1 \ell_1 \ell_2 \delta \ell_3 = t_1 V_1 \delta n \quad (2.40)$$

On the other hand from Eq. (2.3) the change of Helmholtz free energy ΔA for this displacement will be equal to work done by external forces. Additionally this will be equal to Gibbs free energy since it is expressed as $\Delta E = \Delta A + P\Delta V$ and volume change is assumed to be zero. Therefore we have

$$\delta W = \delta A = \delta \nabla E = t_1 V_1 \delta n \quad (2.41)$$

or

$$t_1 = \frac{1}{V_1} \frac{\partial \Delta E}{\partial n} \quad (2.42)$$

The term $\partial \Delta E / \partial n$ is given with Eq. (2.39) which consists of two parts. First part corresponds to Eq. (2.32). Second part of Eq. (2.39) may be found by taking partial derivative of Eq. (2.36) and (2.38). Insertion of their

final forms into Eq. (2.42) will give the t_1 expression which is referred to swollen but unstrained case where λ_i 's are defined in terms of principal stretches as in Eq. (2.20). So the final and general form of t_1 stress equation becomes [2]

$$t_1 = \frac{RT}{V_1} \{ \ln(1 - v_2) + v_2 + \chi v_2^2 + (\rho V_1 / M_c) v_2^{1/3} \lambda_i \} . \quad (2.43)$$

2.4.5 Recent Developments

In recent years there have been further studies which have been achieved by Flory and B. Erman in which the phantom case is defined and the domains of constraints are concerned separately. These constraints occur because of entanglements and steric requirements of real polymer chains. When phantom case is taken into account, each chain fluctuates freely about its equilibrium end-to-end vectors which are spanning the distance between two junctions. For any deformation, only the mean end-to-end vectors are deformed and the structure at ends are preserved then the 'phantom case' is obtained.

According to these new studies the elastic free energy of a polymer network can be represented as the sum of two terms [3,4]

$$\Delta E_e = \Delta E_{ph} + \Delta E_c \quad (2.44)$$

where the ΔE_{ph} is elastic free energy of hypothetical phantom network and ΔE_c represents the elastic free energy of constraints arising from the material properties of real chains. Following the statistical methods and

assuming Gaussian distribution the free energy for the phantom network is found as [4]

$$\Delta E_{ph} = (1/2)\xi kT(\lambda_1^2 + \lambda_2^2 + \lambda_3^2 - 3) \quad (2.45)$$

where ξ is the cycle rank or the number of independent circuits of the network, k is the Boltzmann's constant, and the free energy of constraints is found [4]

$$(kT)^{-1}\Delta E_c = (\mu/2)\sum_i \{(1 + g_i)B_i - \ln[(B_i + 1)(g_i B_i + 1)]\} \quad (2.46)$$

$$g_i = \lambda_i^2 [\kappa^{-1} + \zeta(\lambda_i - 1)] \quad (2.47)$$

$$B_i = (\lambda_i - 1)(1 + \lambda_i - \zeta\lambda_i^2)/(1 + g_i)^2 \quad (2.48)$$

in which μ is the number of junctions, κ and ζ are two new material parameters, κ varies between zero to infinity. $\kappa = 0$ case corresponds to 'phantom case', infinite value represents the affine case.

' ζ ' shows the effect of structural inhomogeneties. In recent studies the free energy of constraints ΔE_c are included in total free energy to obtain improved stress-strain relation. The derivative of ΔE_c may be found as

$$\frac{\partial \Delta E_c}{\partial n} = \frac{\partial \Delta E_c}{\partial \lambda_i^2} \frac{\partial \lambda_i^2}{\partial n} \quad (2.49)$$

and $\partial \Delta E_c / \partial \lambda_i^2$ can be calculated from Eq. (2.46) [6]

$$\frac{\partial \Delta E_c}{\partial \lambda_i^2} = (\mu/2)kTK(\lambda_i^2) \quad (2.50)$$

where

$$K(\lambda_i^2) = B[\dot{B}(B + 1)^{-1} + g(\dot{g}B + \dot{B}g)(gB + 1)^{-1}] \quad (2.51)$$

in which the definitions

$$\dot{B}_i = B_i \{ [2\lambda_i(\lambda_i - 1)]^{-1} + (1 - 2\zeta\lambda_i)[2\lambda_i(1 + \lambda_i - \zeta\lambda_i^2)]^{-1} - 2\dot{g}_i(1 + g_i)^{-1} \} \quad (2.52)$$

and

$$\dot{g}_i = \kappa^{-1} \zeta(1 - (3/2)\lambda_i) \quad (2.53)$$

has been used.

In this recent approach the total free energy becomes equal to;

$$\Delta E = \Delta E_m + \Delta E_{ph} + \Delta E_c \quad (2.54)$$

If we substitute Eq. (2.54) into Eq. (2.42) we can obtain the improved stress-strain and swelling relation in the form given below

$$t_i = \frac{RT}{V_1} [\ln(1 - v_2) + v_2 + \chi v_2^2] + \lambda_i^2 v_2 \frac{\xi kT}{V_0} (1 + (\mu/\xi)k(\lambda)) \quad (2.55)$$

as referred to swollen but unstrained case.

2.4.6 The 'χ' Parameter

So far the specific difference between the swelling process of various polymer-solvent systems were expressed with the aid of the

empirical parameter χ which is related with energy of mixing. The interactions between polymer and solvent molecules depend strongly on the forces between atoms. In order to understand the role of interactions in swelling, the cohesive energy density concept was introduced by Gee (1942).

In further studies the solubility parameter ' δ ' was defined as the square root of the cohesive energy density. It was found out that polymers may easily dissolve in solvents which have similar chemical structure to the polymer. The following relation between ' δ ' and ' χ ' was stated by Shvartz (1958).

$$\delta_1 = \delta_2 \pm [(kT/V_1)(\chi - \chi_s)]^{1/2} \quad (2.56)$$

in which the entropic effects is included by (χ_s) and finally the parameter χ is expressed in terms of the interaction parameter $\bar{\chi}$ which is in good agreement with experimental results [9]. We further have;

$$\chi = \bar{\chi} + nv_2^{-1} \frac{\partial \bar{\chi}}{\partial n} \quad (2.57)$$

where n is the number of liquid molecules as before. Some χ values are given in Table 2.4.1 [2]. Since parameter χ is not constant with respect to solvent it has been examined with respect to polymer volume fraction for PDMS-Benzene system at 25°C by Shih and Flory [9]. The results are given in Fig. 2.4.1.

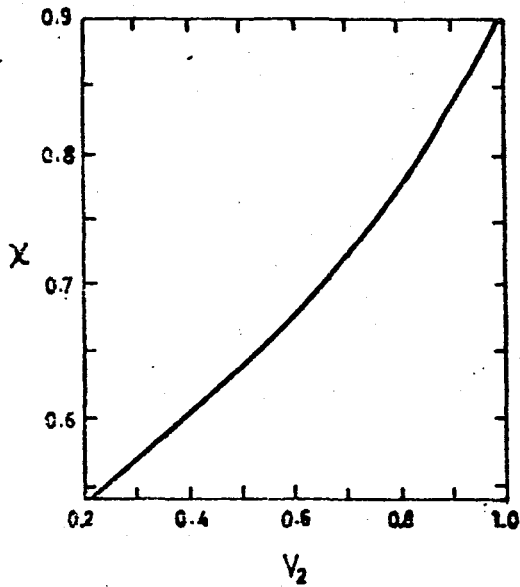
It is also possible to express the χ parameter in terms of χ_1 and χ_2 parameters which are dependent on the solvent and polymer respectively.

$$\chi = \chi_1 + \chi_2 v_2 \quad (2.58)$$

where χ_1 and χ_2 are known empirical values.

TABLE 2.4.1 - Sample Values for χ Parameter

Liquid	Natural Rubber	Poly-chloroprene (Neoprene)	Butyl Rubber	Silicone Rubber
Benzene	0.421	0.263	0.578	0.52
Toluene	0.393	-	0.557	0.465
Hexane	0.480	0.891	0.516	0.40
Dichloromethane	0.494	0.533	0.474	-
Carbon tetrachloride	0.307	-	0.362	0.450

Figure 2.4.4 - χ versus v_2 for PDMS-Benzene system.

III. CONTINUUM MECHANICS MODEL

In this section the flexure of amorphous swollen cuboid will be considered. At the beginning, pure bending of an incompressible beam will be examined under the guidance of C. Eringen's study [10] and then the model which was formally developed by Green and Adkins [11,12] for compressible materials will be applied to our problem.

3.1 FLEXURE OF AN INCOMPRESSIBLE CUBOID

3.1.1 Continuum Solution

Suppose we deform a rectangular parallel-piped in such a way that $X = \text{constant}$ planes become circles, $Y = \text{constant}$ planes become radial lines where $Z = \text{constant}$ planes are preserved as is shown in Figure 3.1.1. Such a deformation may be represented by two coordinate systems.

$$\begin{array}{ll}
 x^1 = r & X^1 = X \\
 x^2 = \theta & X^2 = Y \\
 x^3 = z & X^3 = Z
 \end{array} \tag{3.1}$$

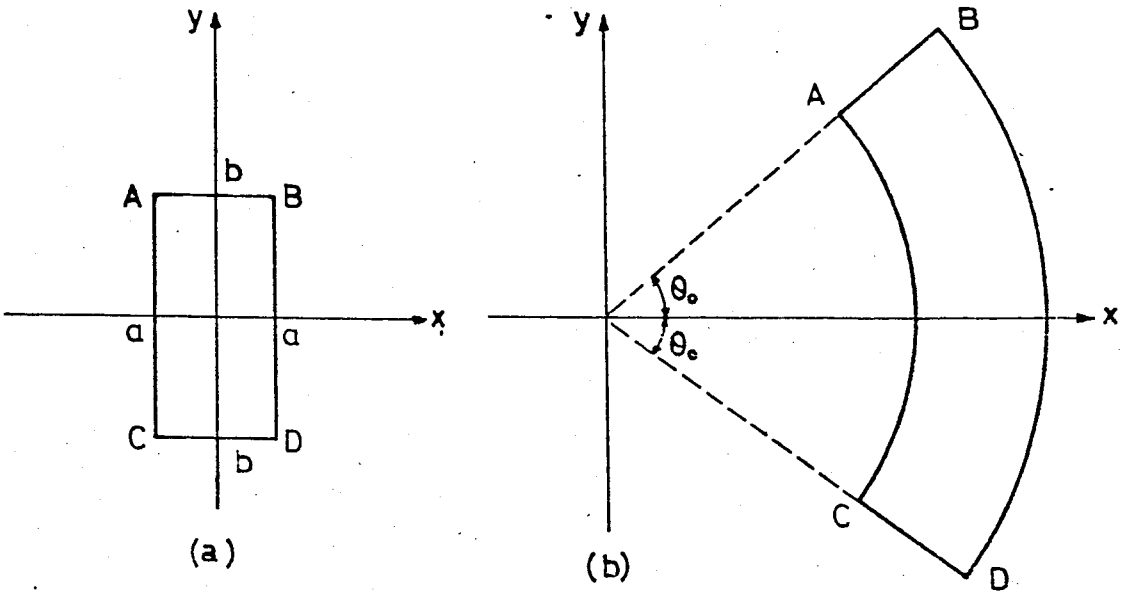


Figure 3.1.1 - Incompressible block (a) undeformed, (b) deformed.

where r, θ, z are cylindrical coordinates for the deformed state having the same origin with rectangular coordinates X, Y, Z and the deformation is described by

$$\begin{aligned}
 r &= x^1 = x^1(X^1) = f(X) \\
 \theta &= x^2 = x^2(X^2) = g(Y) \\
 z &= x^3 = x^3(X^3) = h(Z)
 \end{aligned}
 \tag{3.2}$$

The metric tensors in two coordinate systems can be easily found as

$$||G_{KL}|| = \begin{vmatrix} 1 & 0 & 0 \\ 0 & 1 & 0 \\ 0 & 0 & 1 \end{vmatrix} \quad ; \quad ||g_{kl}|| = \begin{vmatrix} 1 & 0 & 0 \\ 0 & r & 0 \\ 0 & 0 & 1 \end{vmatrix}
 \tag{3.3}$$

Since we are dealing with a real problem, the deformation tensor C_L^K should be stated in physical components which can be obtained from the formula below:

$$C_{(L)}^{(K)} = C_L^K \frac{\sqrt{G_{\underline{K}\underline{K}}}}{\sqrt{G_{\underline{L}\underline{L}}}} \quad (3.4)$$

where underscores are placed under the indices to indicate suspension of the summation. On the other hand the deformation tensor in terms of the derivatives of motion is given by,

$$C_L^K = G^{KM} C_{ML} = G^{KM} g_{kl} x_{,K}^k x_{,L}^l \quad (3.5)$$

If we substitute the required partial derivatives of Eq. (3.2) in Eq. (3.5). The deformation tensor becomes;

$$||C_L^K|| = \begin{vmatrix} f'^2 & 0 & 0 \\ 0 & r^2 g'^2 & 0 \\ 0 & 0 & h'^2 \end{vmatrix} \quad (3.6)$$

From the values of the metric tensor, given in Eq. (3.3) and Eq. (3.4), it will be observed that the tensor components of deformation in its diagonal form are identical with its physical components. i.e.,

$$C_{(L)}^{(K)} = C_L^K \quad (3.7)$$

It is also clear that the deformation tensor contains only diagonal terms. Invariants of the deformation tensor can be found by using Eq. (3.6) as,

$$\begin{aligned}
I_C &= \lambda_1^2 + \lambda_2^2 + \lambda_3^2 = f'^2 + r^2 g'^2 + h'^2 \\
II_C &= \lambda_1 \lambda_2 + \lambda_2 \lambda_3 + \lambda_3 \lambda_1 = f'^2 h'^2 + r^2 g'^2 (f'^2 + h'^2) \\
III_C &= \lambda_1^2 \lambda_2^2 \lambda_3^2 = f'^2 h'^2 g'^2 r^2
\end{aligned} \tag{3.8}$$

Also for the principal stretches we have

$$\lambda_1 = f' \quad \lambda_2 = rg' \quad \lambda_3 = h' \tag{3.9}$$

In order to satisfy isotropic deformation, $f(X)g(Y)h(Z) = 1$ should be satisfied so the third invariant must be equal to unity.

$$III_C = (f'rg'h')^2 = 1 \tag{3.10}$$

The differential equation can be separated by letting $ff' = A, g' = C,$
 $h' = (AC)^{-1} = D$ where A, C, D are constants. Integrating these equations and then allowing for two integration constants equal to zero in order to center the deformed block with respect to spatial coordinates, we obtain

$$r = f(X) = (2AX + B)^{1/2} \quad \theta = CY \quad z = DZ \tag{3.11}$$

and applying the following boundary conditions.

$$\begin{aligned}
r &= r_1 & X &= -a \\
r &= r_2 & X &= a \\
\theta &= \pm\theta_0 & Y &= \pm b
\end{aligned} \tag{3.12}$$

will yield the values of the constants A, B, C and D .

$$\begin{aligned}
A &= (1/4a)(r_2^2 - r_1^2) & C &= \theta_0/b \\
B &= (1/2)(r_1^2 + r_2^2) & D &= 4ab/(\theta_0(r_2^2 - r_1^2))
\end{aligned} \tag{3.13}$$

3.2 FLEXURE OF A COMPRESSIBLE CUBOID

3.2.1 Solution of a Compressible Cuboid Problem

This particular problem was treated by Green and Adkins. In our study we will follow the same procedure. Under the guidance of the previous section we can assume that the deformation of the compressible cuboid is similar to the incompressible one. Hence,

$$r = f(X) \quad \theta = (\theta_0/b)Y \quad Z = DZ \quad (3.14)$$

We also know that the constitutive equation for the stress-strain relation of a compressible material can be expressed in the form below by replacing deformation gradients by principal stretches. This constitutive equation is known as Neumann-Kirchoff form [10, p.146].

$$t_i = (\dot{\rho}/\rho_0)\lambda_i(\partial\Delta E/\partial\lambda_i) = v_2\lambda_i(\partial\Delta E/\partial\lambda_i) \quad (3.15)$$

accordingly the stress tensor becomes;

$$||t|| = \begin{vmatrix} v_2\lambda_1(\partial\Delta E/\partial\lambda_1) & 0 & 0 \\ 0 & v_2\lambda_2(\partial\Delta E/\partial\lambda_2) & \\ 0 & 0 & v_2\lambda_3(\partial\Delta E/\partial\lambda_3) \end{vmatrix} \quad (3.16)$$

Since the strain component and the strain energy $\Delta E = F(I, II, III) = F(\lambda)$ are independent of θ and z but depends on r (or f), the equations of equilibrium reduce to a simple relation;

$$\frac{dt_1}{dr} + \frac{t_1 - t_2}{r} = 0 \quad \text{or} \quad t_2 = (d/dr)(rt_1) \quad (3.17)$$

and the derivative of strain energy can be written as

$$\frac{d\Delta E}{dr} = \frac{\partial \Delta E}{\partial \lambda_1} \frac{d\lambda_1}{dr} + \frac{\partial \Delta E}{\partial \lambda_2} \frac{d\lambda_2}{dr} \quad (3.18)$$

by substituting first Eq. (3.16) and then mass conservation principle

$$\lambda_1 \lambda_2 \lambda_3 = v_2^{-1} \quad (3.19)$$

into Eq. (3.18) and using Eq. (3.15) we can obtain the following final form

$$\frac{d\Delta E}{dr} = \lambda_3 \lambda_2 (d\lambda_1/dr) t_2 + \lambda_3 \lambda_1 (d\lambda_2/dr) t_2 \quad (3.20)$$

Here, we have defined the state of strain in terms of principal stretches for the swelling case. We can use the same representation of Eq. (2.20) for

$$\lambda_i = \lambda_0 \alpha_i \quad (3.21)$$

where λ_0 indicates equilibrium swelling stretches and α_i comes from distortion as previously used in Eq. (2.20). Now we have expressed α_i 's in deformation tensor so λ can be given with the following matrix

$$||\lambda|| = v_2^{-1/3} \begin{vmatrix} f' & 0 & 0 \\ 0 & rg' & 0 \\ 0 & 0 & h' \end{vmatrix} \quad (3.22)$$

using Eq. (3.22) into (3.20), we obtain

$$(d\Delta E/dr) = (v_{20}b)^{-1} \theta_0 (rf'' t_1 + f' t_2) \quad (3.23)$$

or

$$d\Delta E/dr = (v_{20}b)^{-1} \theta_0 [(d/dr)(rf't_1)] \quad (3.24)$$

Integration of Eq. (3.24) will yield,

$$t_1 = \frac{v_{20}b}{\theta_0 rf'} (\Delta E + \Delta E_0) \quad (3.25)$$

where ΔE_0 is an integration constant. Since the beam is bent at both ends the boundary conditions require that stress, ' t_1 ', at $r = r_1$ and $r = r_2$ should be zero. This implies that the force acting on $R = (X^2 + Y^2)^{1/2} =$ constant surface is zero or equivalently Eq. (3.25) is equal to zero. This implies;

$$\Delta E(r_1) = \Delta E(r_2) = - \Delta E \quad (3.26)$$

so that in the incompressible case the strain energy at the boundaries should be constant and equal to each other.

The flexural couple M per unit depth, can be calculated from,

$$M = \int_{r_1}^{r_2} r t_2 dr \quad (3.27)$$

In the study of pure bending of a beam we encounter Pointing effects in the form of stress component t_3 required to produce the desired pure flexure.

IV. SOLUTION OF PROBLEMS OF ELASTICITY WITH SWELLING

4.1 GENERAL APPROACHES AND FINITE BENDING OF SWOLLEN BEAM

4.1.1 General Treatment.

At the end of Section II the stress-strain and swelling relations are studied in detail and finalized with the most important and general Equation (2.55). When the problem is formulated referring to principal coordinates, there are seven unknowns to be determined as functions of position; three of them are components of the stress tensor; the other three are components of the strain tensor and the last one is the degree of swelling. Three of the required seven equations may be obtained from stress-strain and swelling relations and the fourth one from the conservation of mass principle and the rest of them may be obtained from equations of equilibrium so the boundary value problem of the network with swelling can be formulated in a consistent manner.

When the principle axes are not used then additional three of each stress and strain tensor components are involved in the problem. In this case we have 13 unknowns. It is possible to obtain ten of these equations

and from the conservation of mass principle, the remaining three may be obtained from compatibility equations. Torsion of a swollen rubber cylinder is an example of this case.[8].

Since the problem involves nonlinearity, the general solution of the above formulation is difficult to obtain. Instead of general solutions the inverse methods are employed in which a suitable deformation is assumed.

Some technological problems like expansion and inversion of spherical shells are treated according to inverse methods and the presence of swelling is only considered in the torsion of a rubber cylinder. The existence of the swelling agent as a second phase and the nonlinearity of the problem necessitate the use of numerical methods in solutions.

4.1.2 Description of Finite Bending of a Swollen Beam Problem

In this section we will introduce the finite bending of a swollen cuboid under the guidance of the continuum mechanics model which was outlined in the preceding section.

The undistorted beam is allowed to swell in a suitable solvent (equilibrium swelling) and then bent by applying a flexural couple M which is created by the system of normal forces distributed over the end surfaces. The geometries of deformed and undeformed state is shown in Figure 4.1.1.

Initially undeformed and unswollen cuboid has dimensions $2a_0$ and $2b_0$. When it is exposed to solvent dimensions become $2a$ and $2b$. If we define the equilibrium swelling degree as v_{20} which is the ratio of polymer volume to swollen total volume, the relation between initial and final dimensions

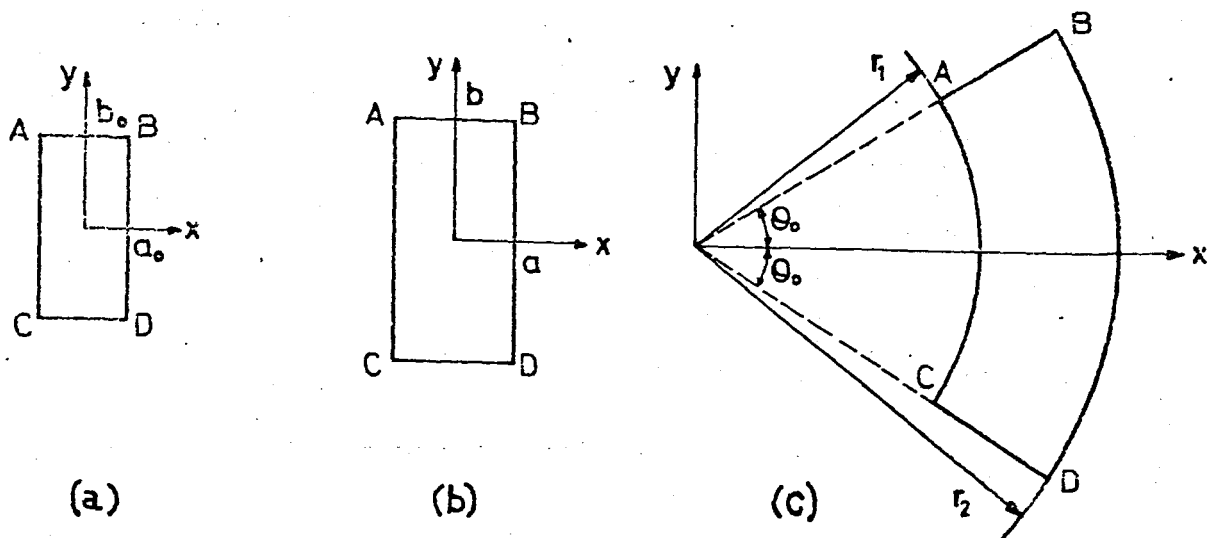


Figure 4.1.1 - a) Undistorted unswollen beam
 b) Undistorted swollen beam
 c) Distorted and swollen beam.

will be

$$a = v_{20}^{-1/3} a_0 \quad b = v_{20}^{-1/3} b_0 \quad (4.1)$$

We also have

$$\frac{V_s}{V_{us}} = \frac{(L_s)^3}{(L_{us})^3} = \frac{1}{v_2} \quad (4.2)$$

where V and L denote volume and length respectively and the subscripts 's' and 'us' indicate swollen and unswollen cases. In Eq. (4.1) swelling degree is denoted by v_{20} which corresponds to the initial value.

The material is chosen to be amorphous polymer network, the material parameters of which are available from previous experiments. There are mainly four parameters $\bar{\chi}$, $\xi kT/V_0$, κ and ζ . The values of these parameters

are taken from experiments for a typical amorphous polymer material as [8].

$\xi kT/V_0 = 0.2 \text{ Nmm}^2$ $\kappa = 8$ $\zeta = 0.12$ and for interaction parameter $\bar{\chi}$, six different values 0.0, 0.25, 0.50, 0.63, 0.75, 1.0 are used and considered independent of concentration of solvent in mixture. The network junction functionality is assumed to be tetrahedral which requires $\mu/\xi = 1$. The parameter relating solvent to molar volume V_1/RT is taken $0.04 \text{ mm}^2\text{N}^{-1}$. All the terms used in above parameters are same as stated before in Section 2.4.4. When the parameters have these values the network is called 'real' network [8].

For comparison purposes κ parameter was taken to be zero which corresponds to the phantom case. The initial ratio of a_0 to b_0 was taken generally as 1/2, but for large deformations mainly 180° flexures, the length of beam is increased while maintaining unit width.

4.1.3 Formulation of the Problem

The deformation of the cuboid which is shown in Fig. 4.1.1 is treated in the same way as is explained in Section 3.2. The deformation tensor is defined with principal stretches referring to swollen-undeformed state like in Eq. (2.20) and found by substituting Eq. (3.6) into Eq. (3.21). Hence,

$$||\lambda|| = \begin{vmatrix} v_{20}^{-1/3} f' & 0 & 0 \\ 0 & v_{20}^{-1/3} f g' & 0 \\ 0 & 0 & v_{20}^{-1/3} h' \end{vmatrix} \quad \text{or} \quad ||\lambda|| = v_{20}^{-1/3} \begin{vmatrix} f' & 0 & 0 \\ 0 & f g' & 0 \\ 0 & 0 & h' \end{vmatrix} \quad (4.3)$$

Second form of the representation in Eq. (4.3) indicates more clearly the initial equilibrium swelling from subsequent changes. For the swollen case the determinant of deformation tensor will be

$$\det||\lambda|| = 1/v_2(r)$$

or (4.4)

$$ff'g'h' = v_{20}/v_2(r)$$

where the $v_2(r)$ denotes the local polymer fraction which is a function of r . This implies that the swelling degree is nonlinear along the radius of curvature. We assume that there is no deformation along the z -direction after free swelling. Therefore

$$h' = 1 \quad (4.5)$$

and the pointing effect is provided as it was mentioned at the end of Section III. The assumption that plane sections remain plane and the results obtained from Eq. (3.14) will give

$$g' = \theta_0/b \quad (4.6)$$

Substituting Eq. (4.6) and (4.5) into Eq. (4.4) and using boundary conditions (3.13); the integration of Eq. (4.4) will yield the following equation

$$\int_{r_1}^{r_2} r \frac{v_2(r)}{v_{20}} \frac{1}{2a} dr = \frac{b}{\theta_0} \quad (4.7)$$

Expression (4.7) and the energy equivalence (Eq. (3.26)) at the inner and outer boundaries are two equations sufficient to determine the two unknown

radii. On the other hand stress t_1 can be found either by using Eq. (2.55) from molecular theory or Eq. (3.25) from continuum mechanics. The remaining stresses are usually found from Eq. (2.55). Finally the flexural couple M per unit swollen width can be calculated from Eq. (3.27).

4.1.4 Numerical Calculation Method

In order to solve the problem the degree of equilibrium swelling should be calculated first. This is the case when the strain energy is minimum $\partial\Delta E/\partial n = 0$ or equivalently the stresses are zero at the swollen and undeformed state. This can be obtained by using $t_1 = 0$, $v_2 = v_{20}$, and $\lambda = v_{20}^{-1/3}$ in Eq. (2.55). As a result we will have;

$$\frac{RT}{V_1} [\ln(1 - v_{20}) + v_{20} + \chi v_{20}^2] + v_{20}^{1/3} \frac{\xi kT}{V_0} [1 + \frac{\mu}{\xi} K(\lambda)] = 0 \quad (4.8)$$

Numerical solution of (4.8) will give the equilibrium swelling degree for a specific value of χ parameter. This leaves three more fundamental variables which are r_1 , r_2 and $v_2(r)$ for the desired flexure degree θ_0 .

As a first approximation the swelling ratio is assumed to be equal to v_{20} which means that it is independent of r . A trial value for r_1 is chosen and the corresponding r_2 is found from Eq. (4.7) and checked from Eq. (3.26) which implies the equality in energies at r_1 and r_2 . In calculations the energy is taken as a total free energy including mixing and elastic free energies.

In order to make energy calculations the states of strain are calculated from Eq. (4.3) and r_1 is changed until the Eq. (3.26) is satisfied.

Values of $\Delta E(r_i)$ and $t_1(r_i)$ are then calculated from Eq. (2.55) and Eq. (3.25) respectively for ten values of r_i equally spaced in the region $r_1 < r_i < r_2$. By using the $t_i(r_i)$ values, Eq. (2.55) is solved to find a new set of $v_2(r_i)$ values which are compared with the assumed initial v_{20} values. These calculations are continued from new strain, energy and stress calculations by using a new set of $v_2(r)$ values for ten equally spaced stations until convergence is obtained between the last two set of $v_2(r_i)$ values, this means that t_1 , the stress values which are calculated from Eqs. (2.55) and (3.25) are the same. After this convergence the r_1 and r_2 are checked again by using the final set of $v_2(r_i)$ in Eq. (4.7) which is one further back step of calculations.

This new iteration loop which is combined with the iterations on $v_2(r_i)$ is carried out until no difference is obtained between final and one before the final r_i values. In this way both r_i and $v_2(r)$ convergences are provided. A complete computer program which contains the above calculation steps is given in Appendix A and a sample output for $\theta = 120^\circ$ and $\chi = 0.25$ value is also provided.

4.2 THE UNIQUENESS OF PROBLEM

4.2.1 General Differences

Although the finite flexure of beam is a well-known problem, the case that is examined in this study differs from classical one in the way of its description and formulation.

The beam is exposed to solvent in order that it swells, and then is deformed. Because of the swelling, nonhomogeneity is involved in the problem. The results of molecular theory are applied to this nonhomogeneous state of stress and strain problem. According to the researcher's opinion this is new application of molecular theory to the present problem. Since up to present such studies have been carried out to include the homogeneous state of stress and strain only.

In the solution of our problem the solvent motion is considered and a continuum mechanics model is developed for the swelling problem which is another new application in swelling problems.

V. RESULTS AND DISCUSSION

5.1 SWELLING RATIO

The following two figures may be helpful to understand the problem and the numerical solution steps. Figure 5.1.1 shows that the flexure of cuboid which is exposed to a solvent with χ value of 0.50. As observed from Figure 5.1.1 the radius of curvature reduces when the degree of flexure θ_0 increased. In Figure 5.1.2 the subdivision of the block into ten finite elements is shown. When better solvents are used which means that χ parameter is close to zero the swelling increases as in Figure 5.1.3 so it is possible to follow swelling comparatively.

In the solution of the problem the procedure starts with equilibrium swelling degree, v_{20} , calculation which is carried out to six different χ 's and it is observed that when χ decreases v_{20} decreases as in Figure 5.1.4. Since the dimensions are related with reciprocal of swelling degree, an increase in χ or v_{20} will cause less swelling or vice-versa.

In the solution of problem various densities of certain quantities are defined at material points. Keeping this idea in mind in order to examine the solvent action in rubber we again use the ratio of polymer

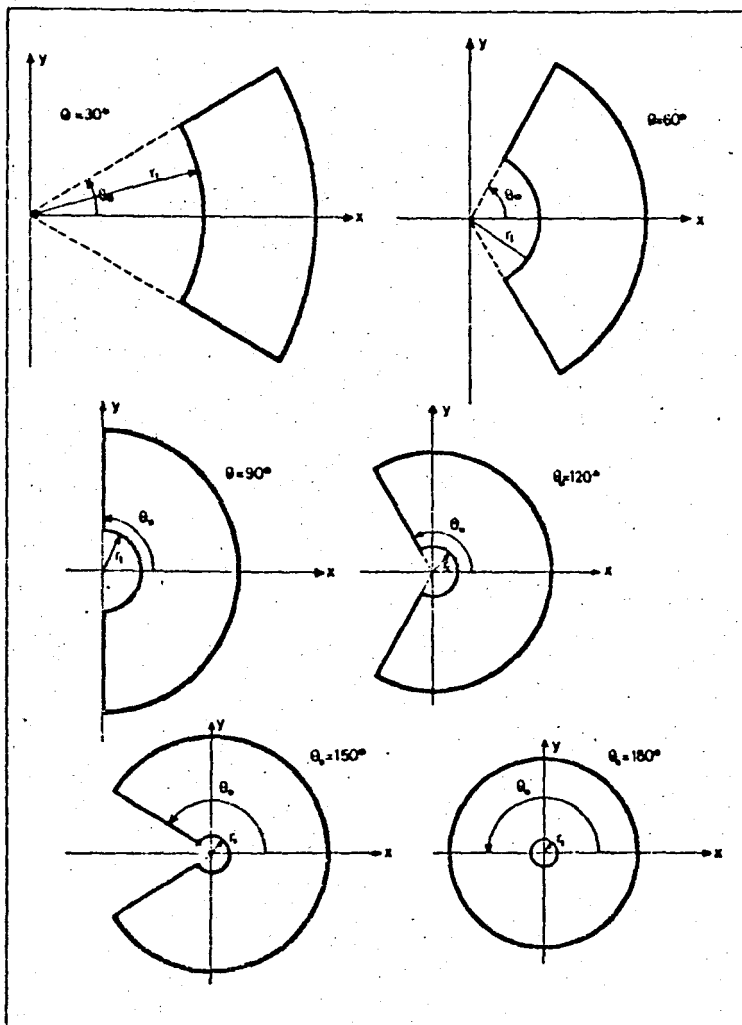


Figure 5.1.1 - Bending of a block for different degrees
($\chi = 0.50$)

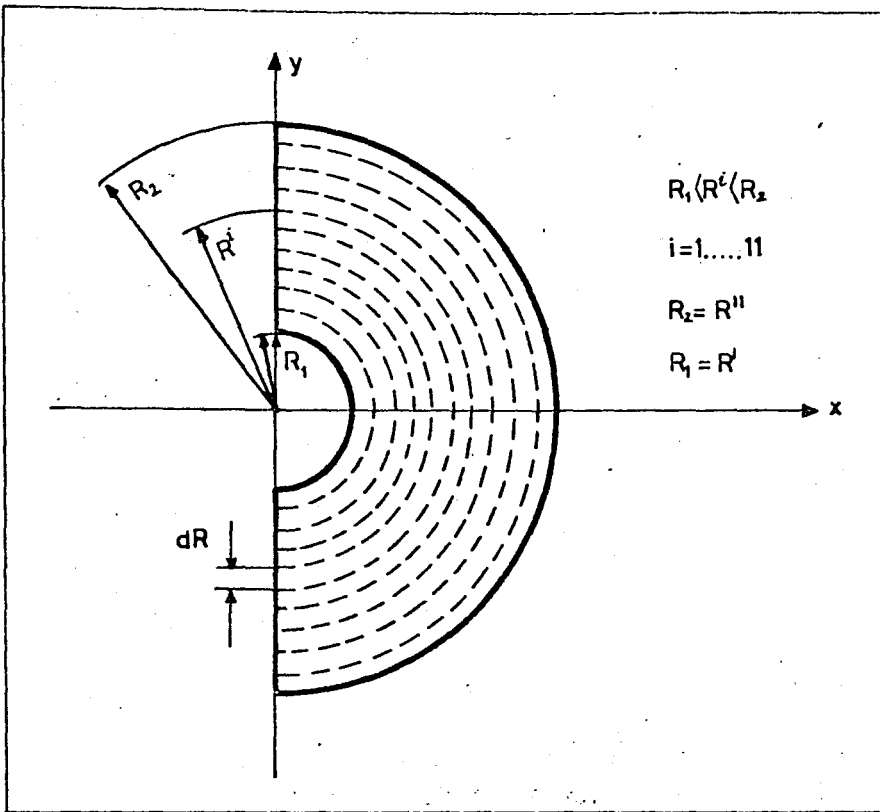


Figure 5.1.2 - Location of the 10 equally spaced stations in bent beam.

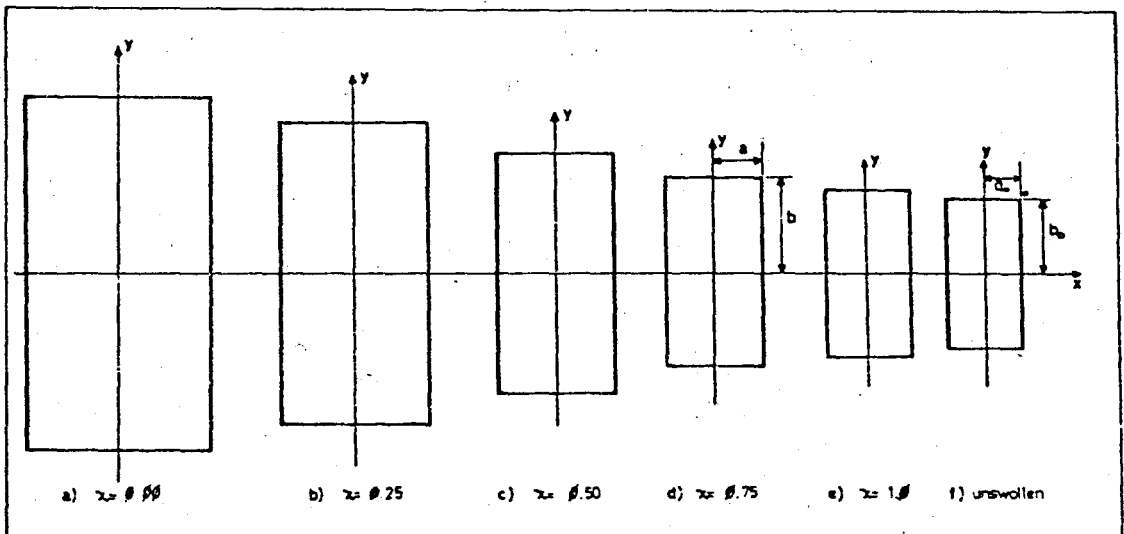


Figure 5.1.3 - Equilibrium swelling of a block for distant χ 's.

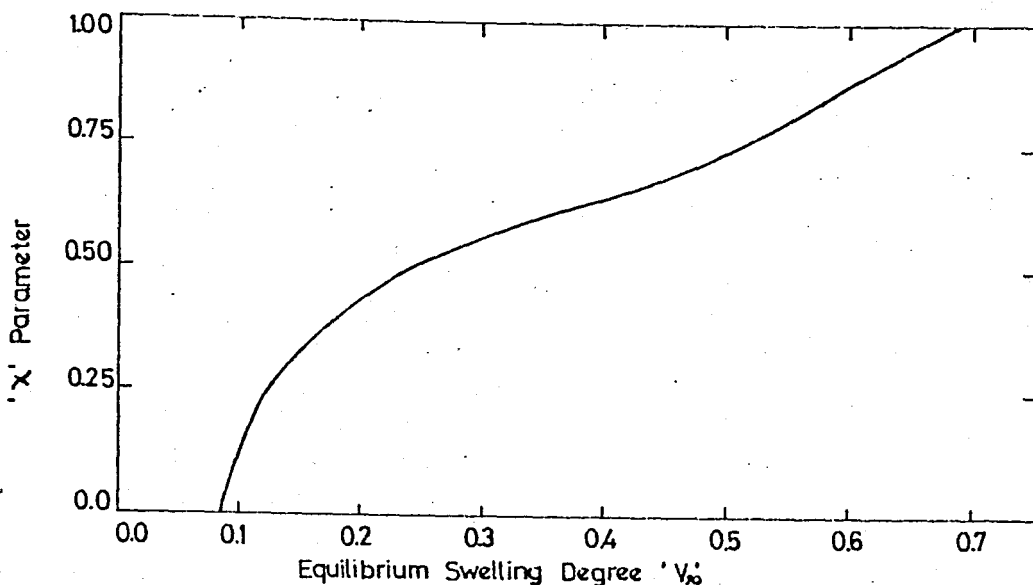


Figure 5.1.4 - ' χ ' parameter versus degree of swelling.

volume to total polymer and solvent volume. Basically two points are important in solvent action.

1. Solvent quantity in rubber cuboid or swelling magnitude.
2. Solvent motion in radial direction for different degree of flexures.

Under the guidance of the above points the solvent distribution, in terms of polymer volume fractions is calculated and plotted for six different degree of flexures up to 180° . This is repeated for every solvent which are mentioned before with their ' χ ' parameters. The following figures contain v_2 versus ψ graphs where ψ is nondimensionalized form of radius, defined as

$$\psi = \frac{r - r_1}{r_2 - r_1}$$

Figure 5.1.5 for $\chi = 1.00$

Figure 5.1.8 for $\chi = 0.50$

Figure 5.1.6 for $\chi = 0.75$

Figure 5.1.9 for $\chi = 0.25$

Figure 5.1.7 for $\chi = 0.63$

Figure 5.1.10 for $\chi = 0.00$

If we consider each figure by itself we notice that they have similar behaviour. When the flexure degree is increased, as expected, the solvent motion increases. At the inner layers which are close to the center of curvature, the polymer volume fraction increases and at the outer layer it decreases. This means that solvent quantity at the inner layers reduces but at the outer fibers it increases so solvent moves outwards. When the outer layers have more solvent, their swelling is more than those of the inner layers. We also know that we have tension at the outer part of the beam and compression at the inner part so it is apparent once again that tension has tendency to increase swelling.

When the last six figures are considered a decrease in polymer fraction v_2 and larger scattering can be followed as the value of parameter χ is decreased. More swelling or equivalently the existence of more solvent in the beam forms the reason for this behaviour.

The following alternative curve may be used for better presentation of these solvent distributions. The swelling ratio $v_2(r)$ can be put in nondimensional form referring to its equilibrium degree of swelling. In Figure 5.1.11 for each case, two sample degrees of flexure, one small value $\theta_0 = 30^\circ$ and the maximum value $\theta_0 = 180^\circ$ are taken. This presentation has an advantage that it is possible to follow all solvent actions from one figure even χ changes, and also it may give a

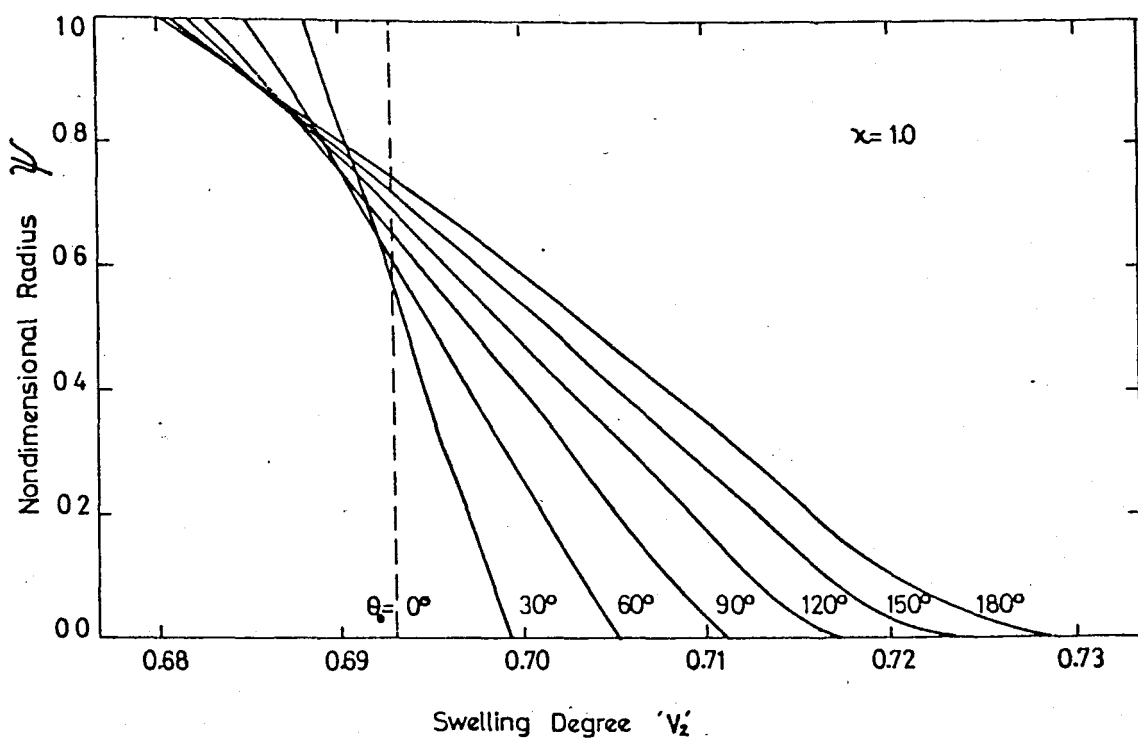


Figure 5.1.5 - $v_2(r)$ distribution in radial direction for $\chi = 1.00$.

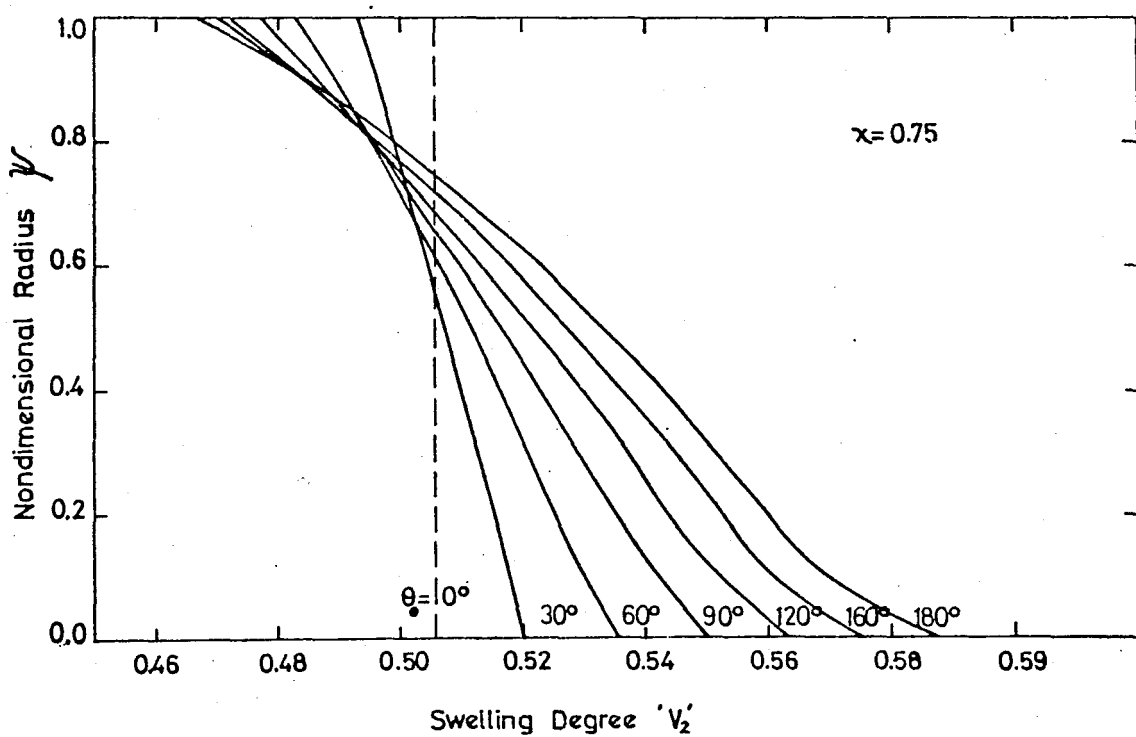


Figure 5.1.6 - $v_2(r)$ distribution in radial direction for $\chi = 0.75$.

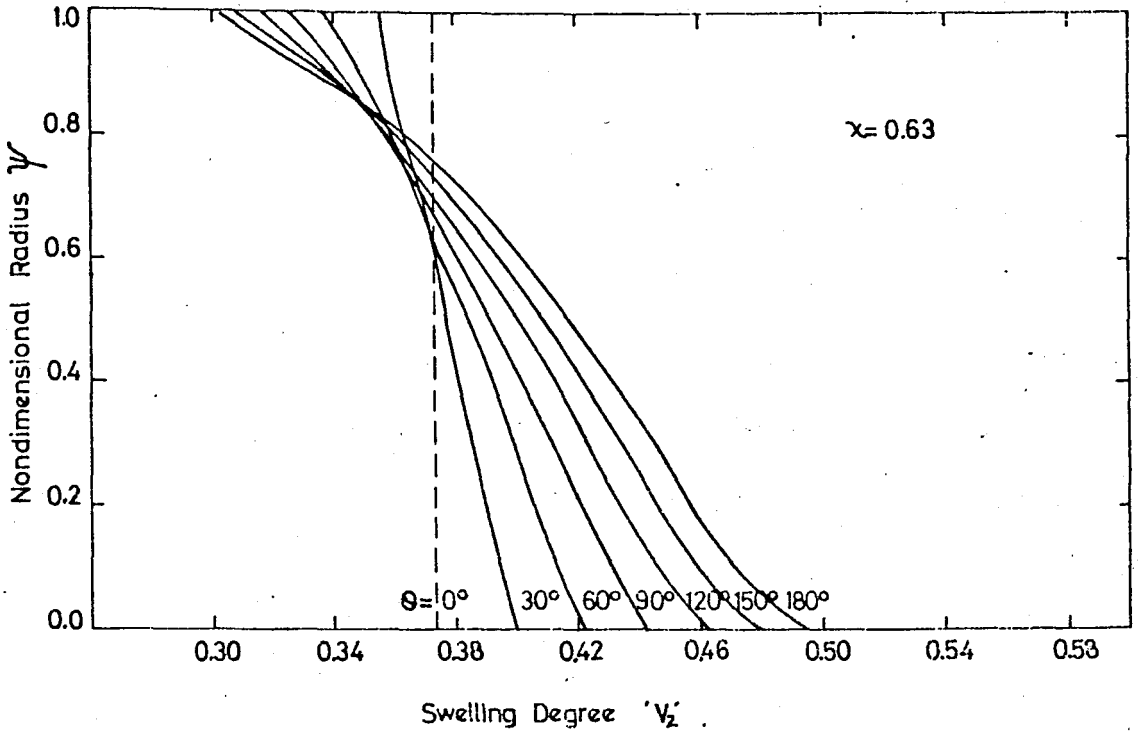


Figure 5.1.7 - $v_2(r)$ distribution in radial direction for $\chi = 0.63$.

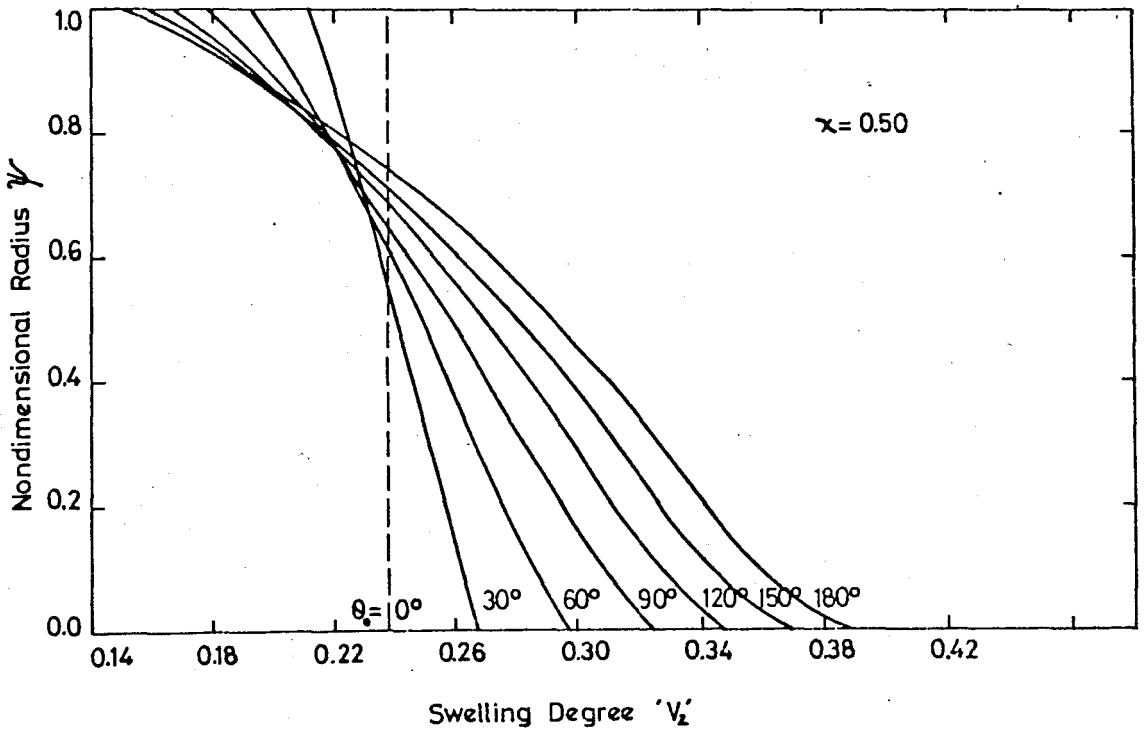


Figure 5.1.8 - $v_2(r)$ distribution in radial direction for $\chi = 0.50$.

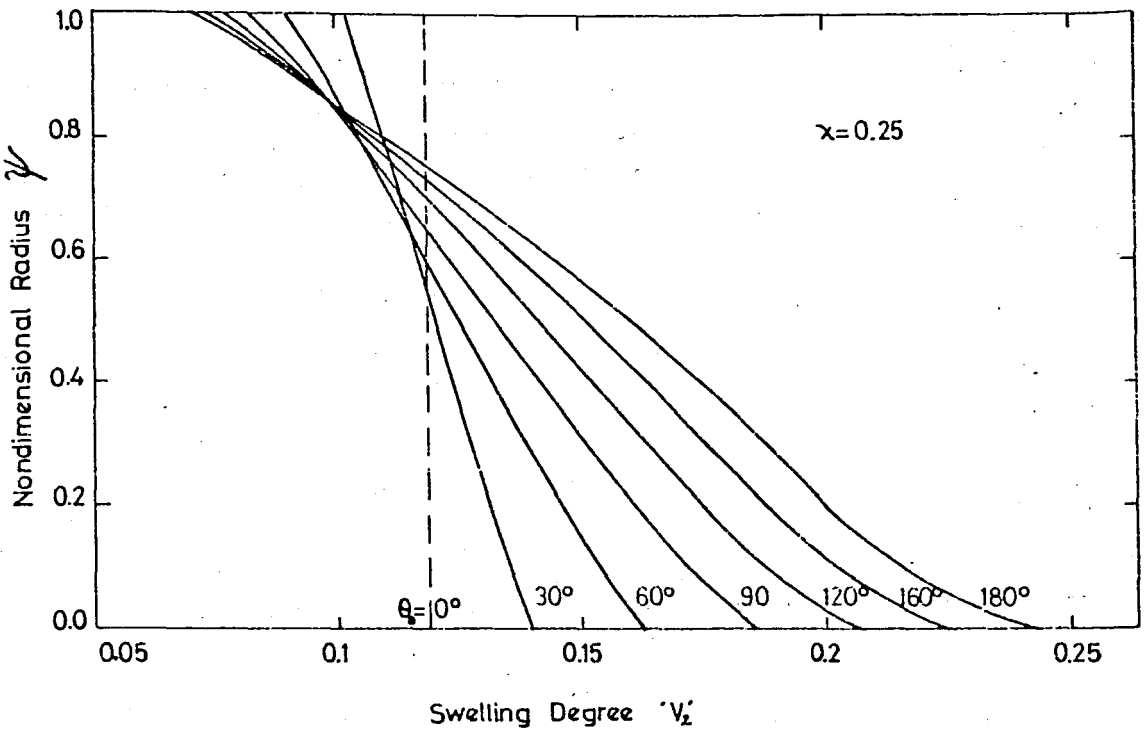


Figure 5.1.9 - $v_2(r)$ distribution in radial direction for $\chi = 0.25$.

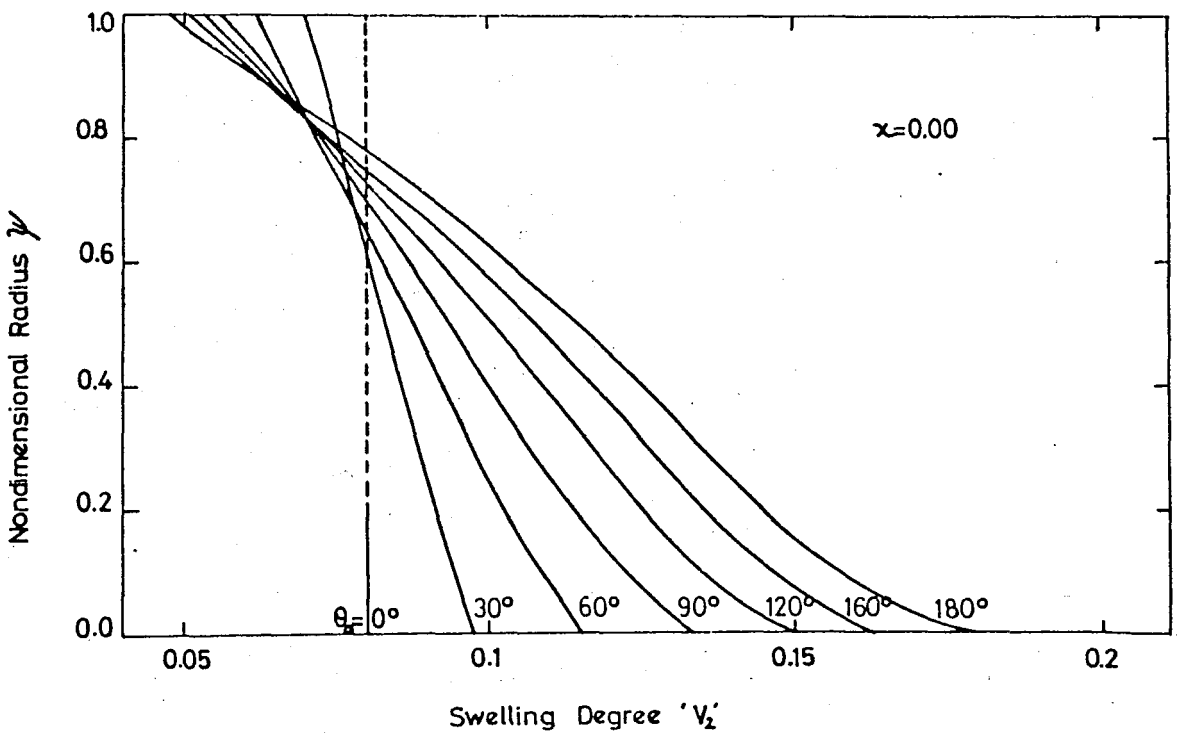


Figure 5.1.10 - $v_2(r)$ distribution in radial direction for $\chi = 0.00$.

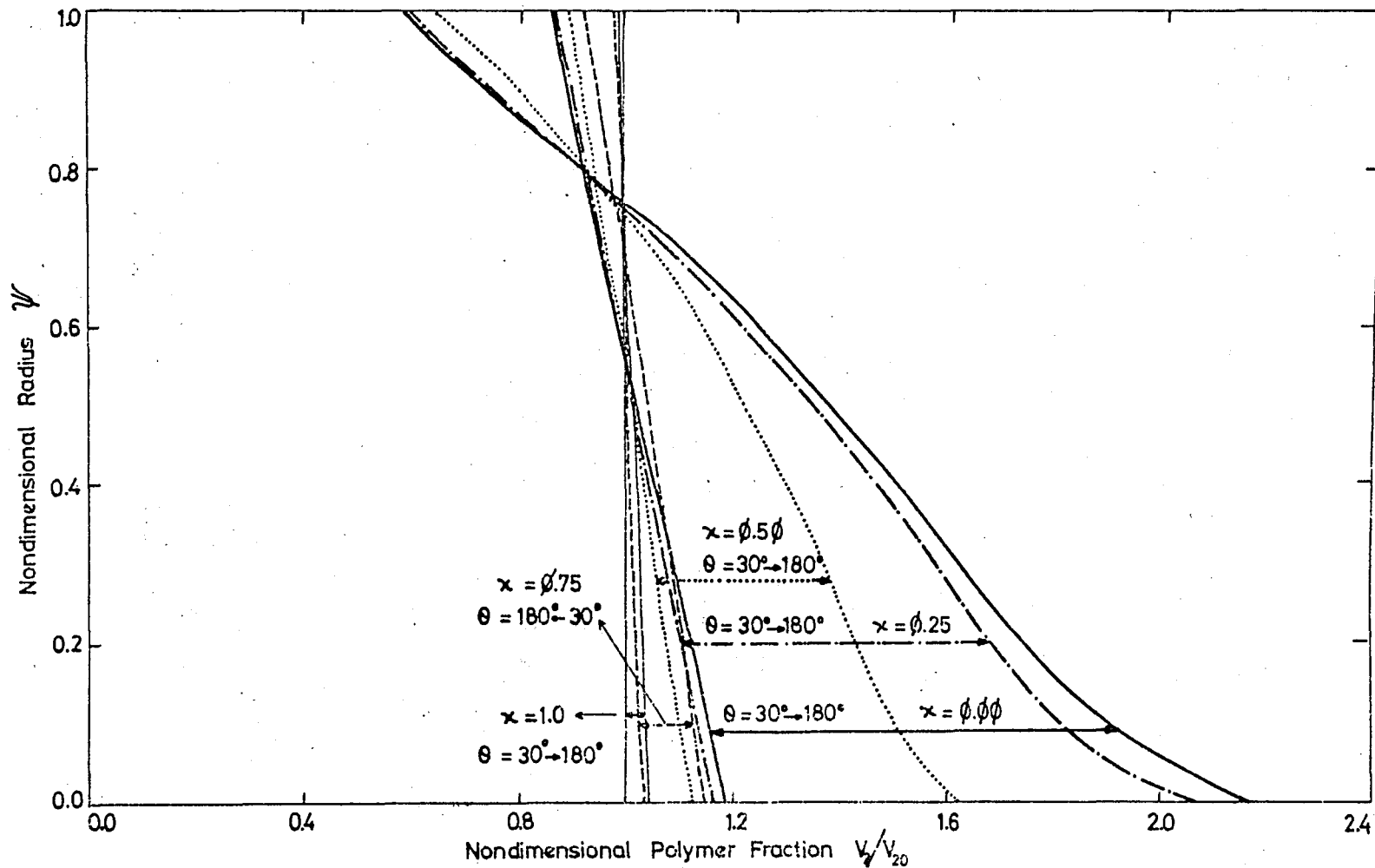


Figure 5.1.11 - χ versus nondimensional polymer fraction $v_2(r)/v_{20}$.

better idea for the above discussion which deals with more scattered solvent behaviour at inner and outer layers. The distribution of θ_0 equal to 30° and 180° are given in Appendix B on a separate graph.

5.2 STRESSES

5.2.1 Stress t_1 in X Direction

If we continue with the solution procedure next step is the calculation of stresses in three directions. Figure 5.2.1 shows the t_1 distribution along the radial direction for $\chi = 1.0$ at different degree of flexures up to 180° , in terms of nondimensional values of radii, ψ . The stress values may be followed in two scales. The bottom one is nondimensionalized by dividing t_1 to the modulus $\xi kT/V_0$ and the top one gives the absolute values in N/mm^2 . These nondimensional forms are carried out for all stresses and for all solvents. From Figure 5.2.1 it is clear that all t_1 values are negative so compression is affected in X direction. This will cause reduction in width. Some numerical examples will be given in Section 5.3 in Table 5.3.1. Stresses in X direction show a peak at the third station which is located on nearly one third of all widths from the inner side. This is valid between 90° and 180° of flexures. For flexures less than 90° , the peak point moves very slightly outwards while the distribution of t_1 gets more scattered and the peak value drops as the degree of flexure is reduced. t_1 stresses are zero at the boundaries r_1 and r_2 as expected. This is the general behaviour of t_1 . When the solvent or χ changes, the t_1 distribution pattern will not show much difference, as observed from solutions

of our problem. These relations are given in the following figures.

Figure 5.2.1 for $\chi = 1.0$

Figure 5.2.2 for $\chi = 0.75$

Figure 5.2.3 for $\chi = 0.63$

Figure 5.2.4 for $\chi = 0.50$

Figure 5.2.5 for $\chi = 0.25$

Figure 5.2.6 for $\chi = 0.00$

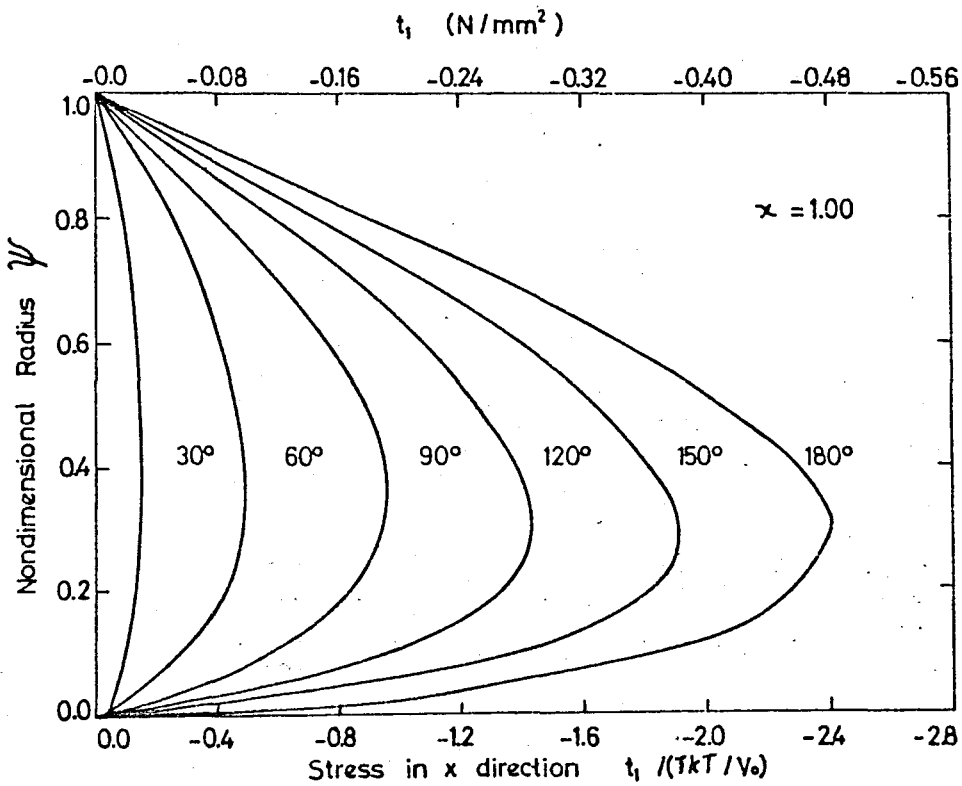


Figure 5.2.1 - Radial distribution of t_x for $\chi = 1.0$.

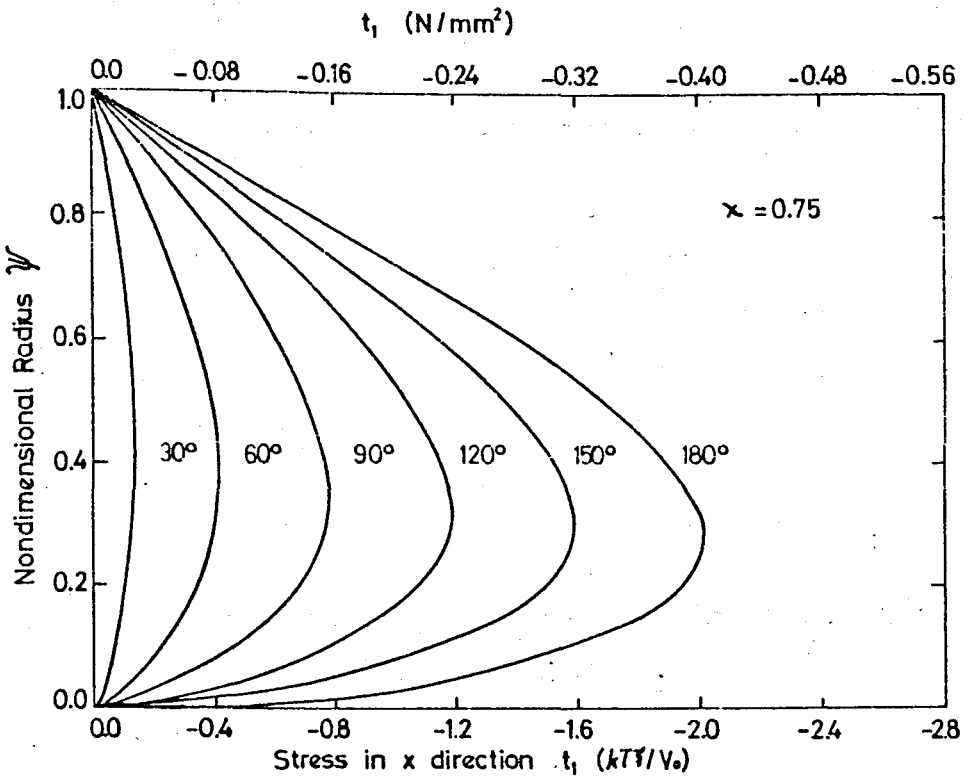


Figure 5.2.2 - Radial distribution of t_1 for $\chi = 0.75$

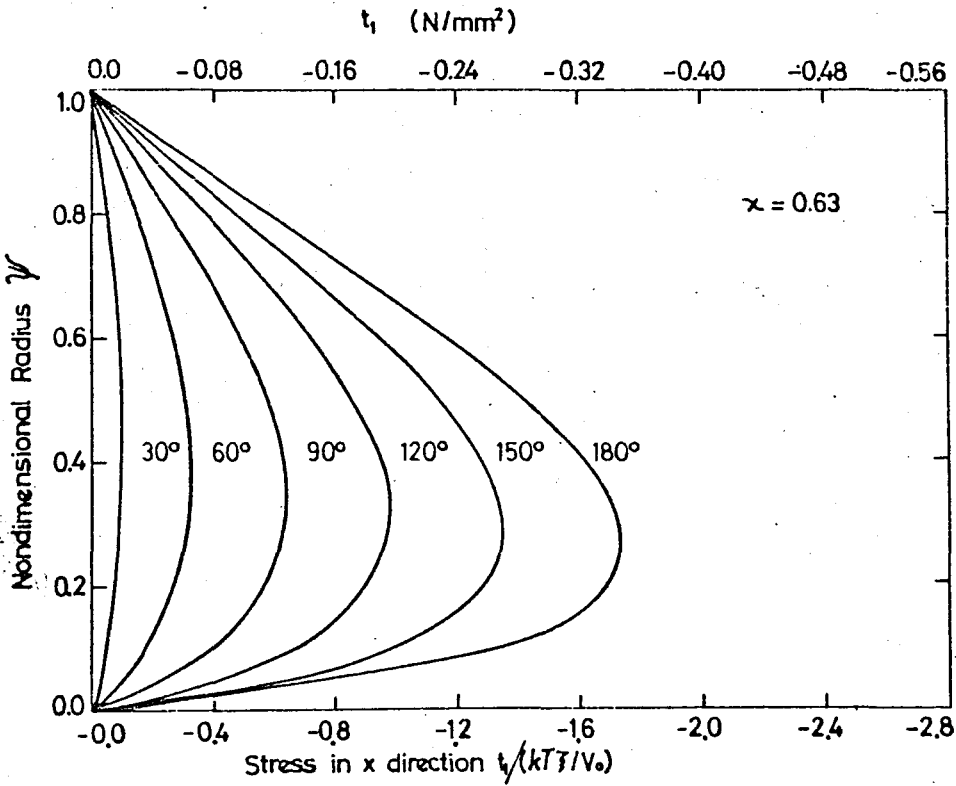


Figure 5.2.3 - Radial distribution of t_1 for $\chi = 0.63$

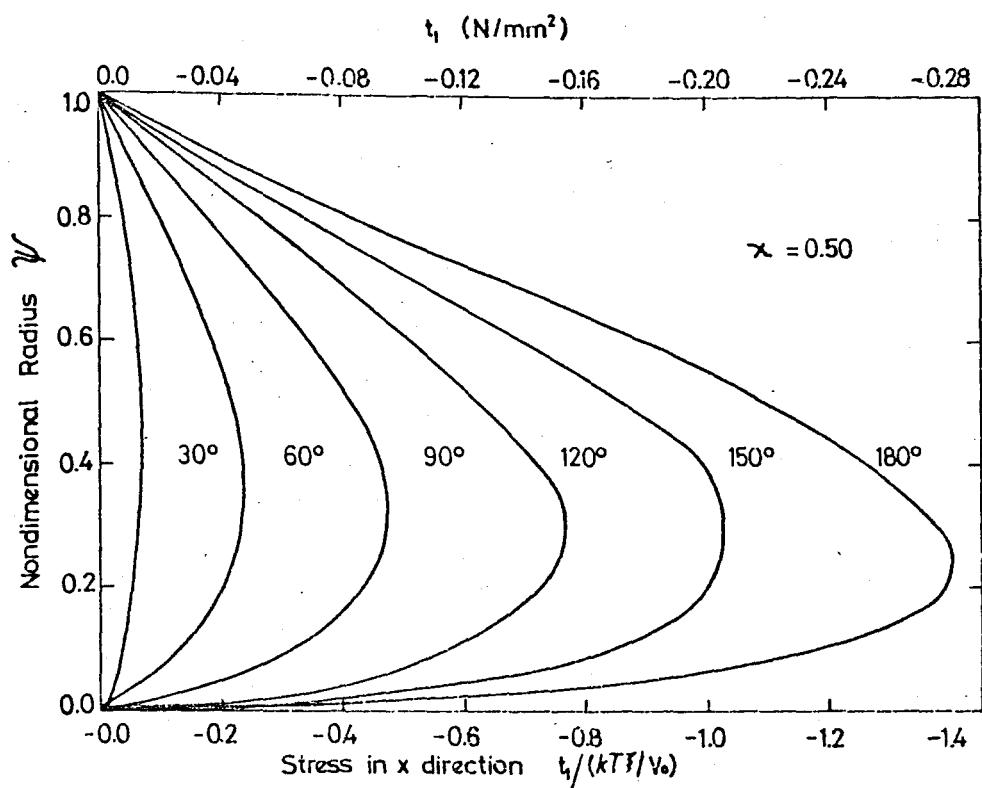


Figure 5.2.4 - Radial distribution of t_1 for $\chi = 0.50$.

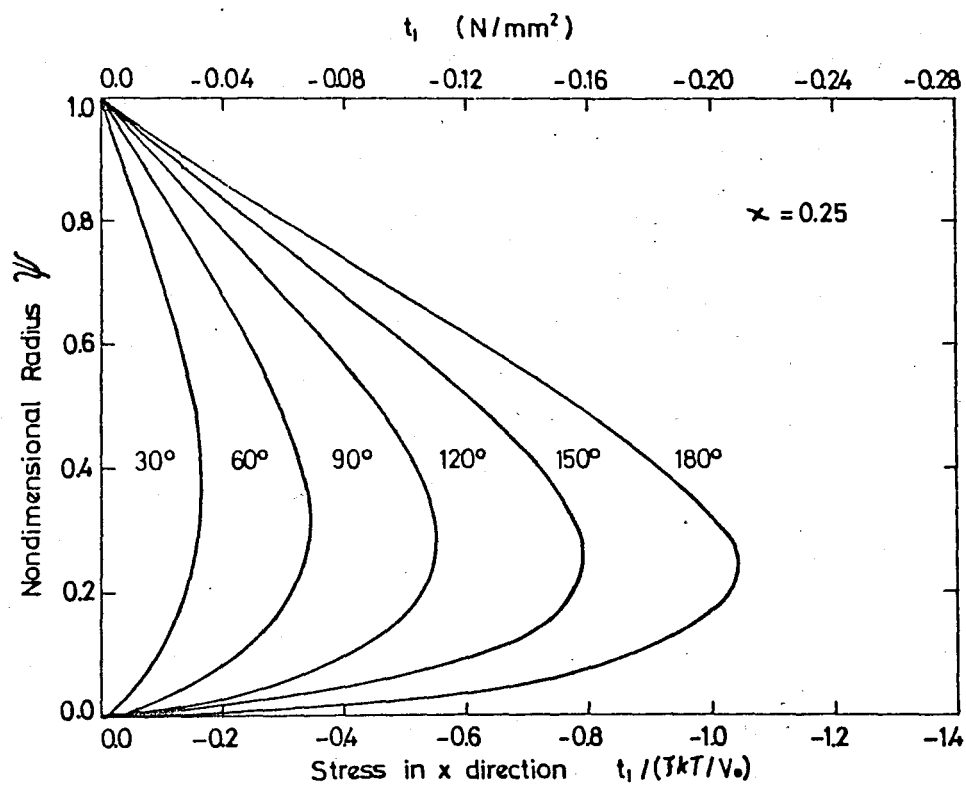


Figure 5.2.5 - Radial distribution of t_1 for $\chi = 0.25$.

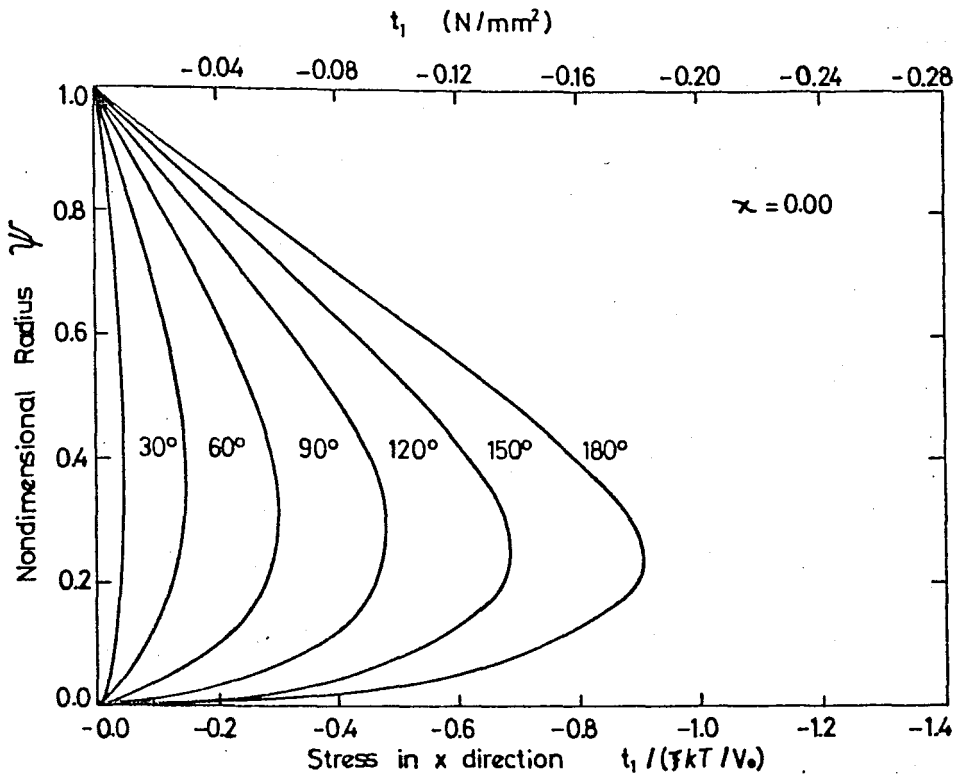


Figure 5.2.6 - Radial distribution of t_1 for $\chi = 0.00$

5.2.2 Stress t_2 in Y Direction

Figure 5.2.7 shows the stresses in Y direction which are denoted by t_2 . This graph also contains the absolute and nondimensional value of t_2 . It is observed that the neutral axis is at about the middle of the beam. The upper part of beam shows increasing tension with increasing degree of flexure and lower part shows increasing compression, and they both reach their maximum values at r_1 and r_2 . Following figures give general solutions for t_2 for different χ 's and flexure degrees.

Figure 5.2.7 for $\chi = 1.0$

Figure 5.2.8 for $\chi = 0.75$

Figure 5.2.9 for $\chi = 0.63$

Figure 5.2.10 for $\chi = 0.50$

Figure 5.2.11 for $\chi = 0.25$

Figure 5.2.12 for $\chi = 0.00$

In these figures there is one point that shows little differences from the general characteristics mentioned above. For a large bending degree, usually above 90° the t_2 stress at outer fibers starting from eight station up to the last station shows different behaviour as the solvent changes. When $\chi = 1.0$ at specified region t_2 increases nonlinearly and for $\chi = 0.75$, t_2 increases almost linearly but for $\chi = 0.63$ and the smaller χ 's it shows a small increase then a decrease towards the boundary. As χ goes down this decrease becomes sharper but less in magnitude.

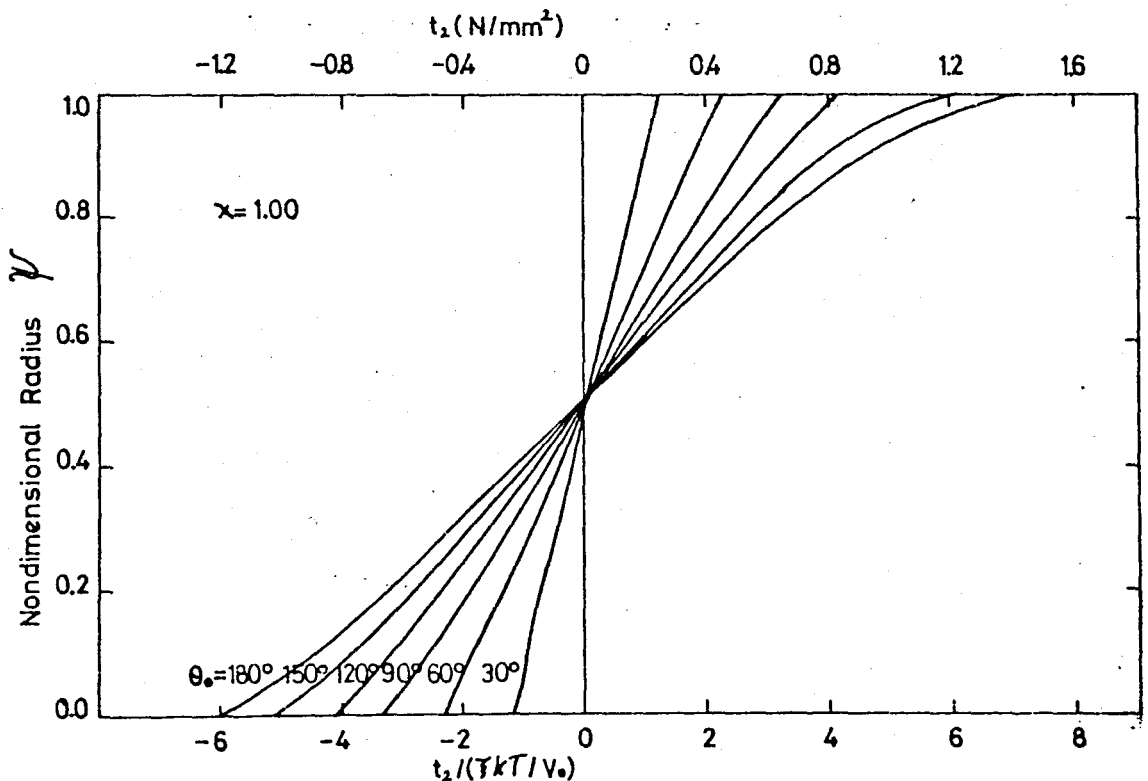


Figure 5.2.7 - Stress t_2 distribution for $\chi = 1.0$.

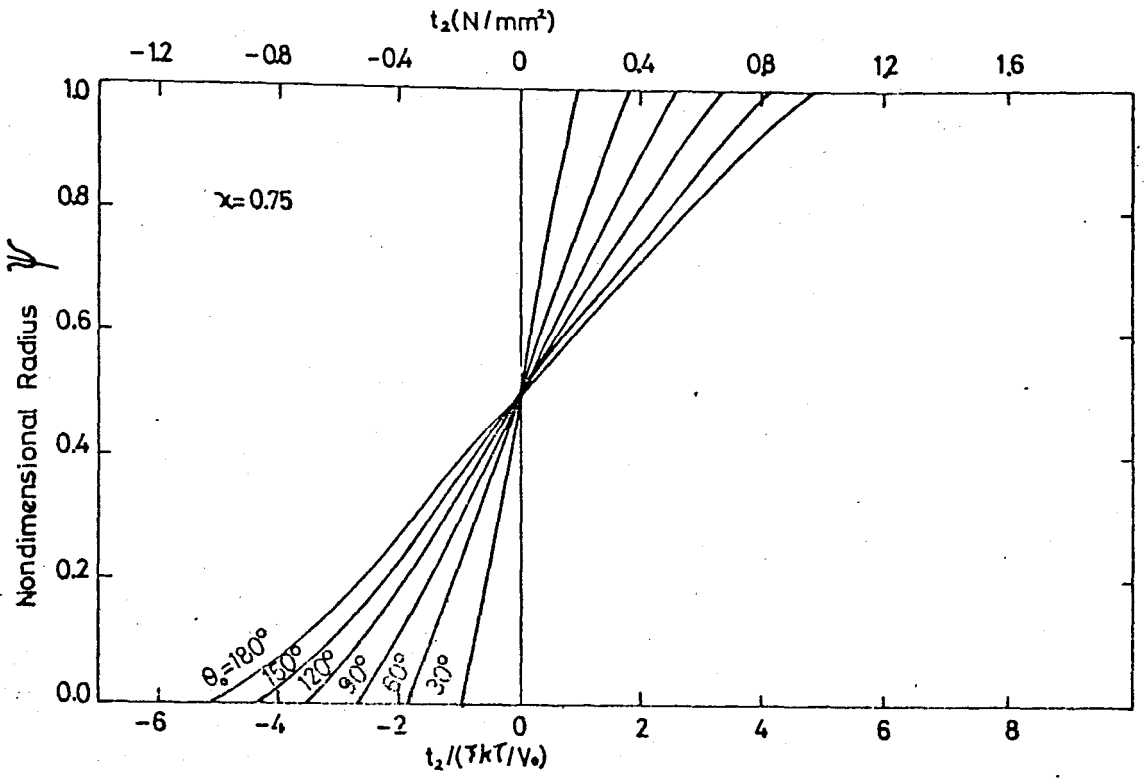


Figure 5.2.8 - Stress t_2 distribution for $\chi = 0.75$.

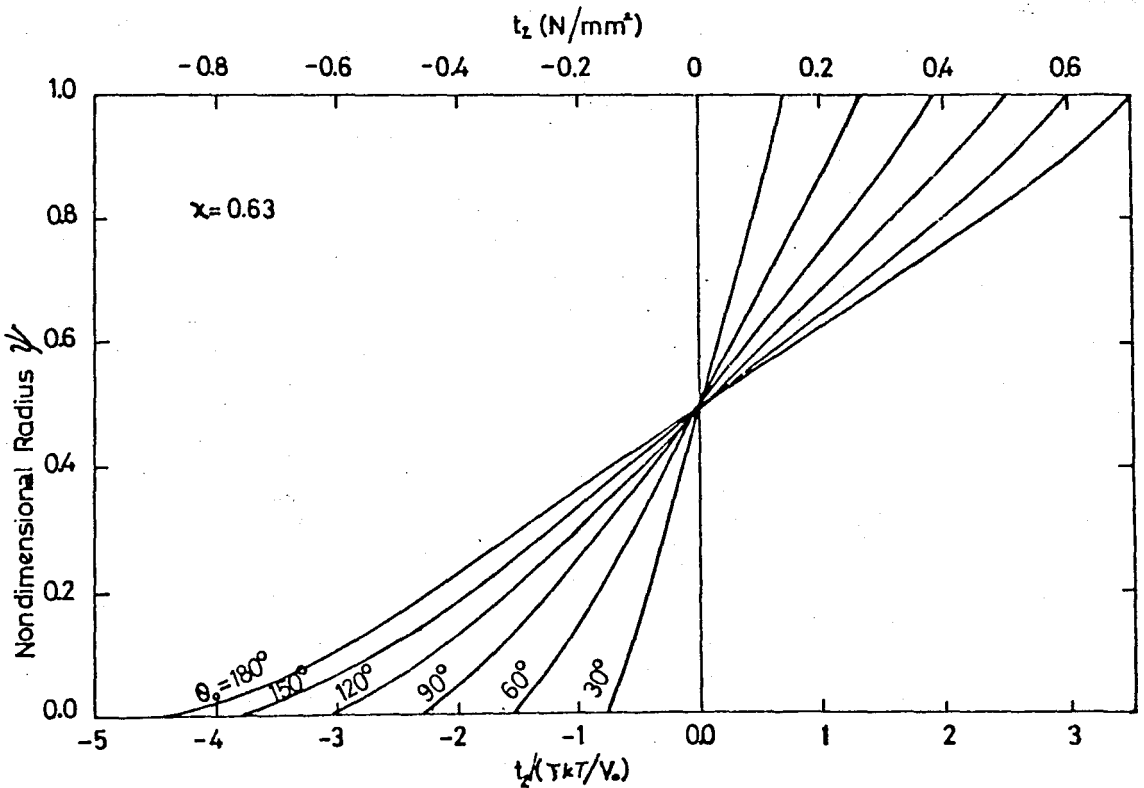


Figure 5.2.9 - Stress t_2 distribution for $\chi = 0.63$.

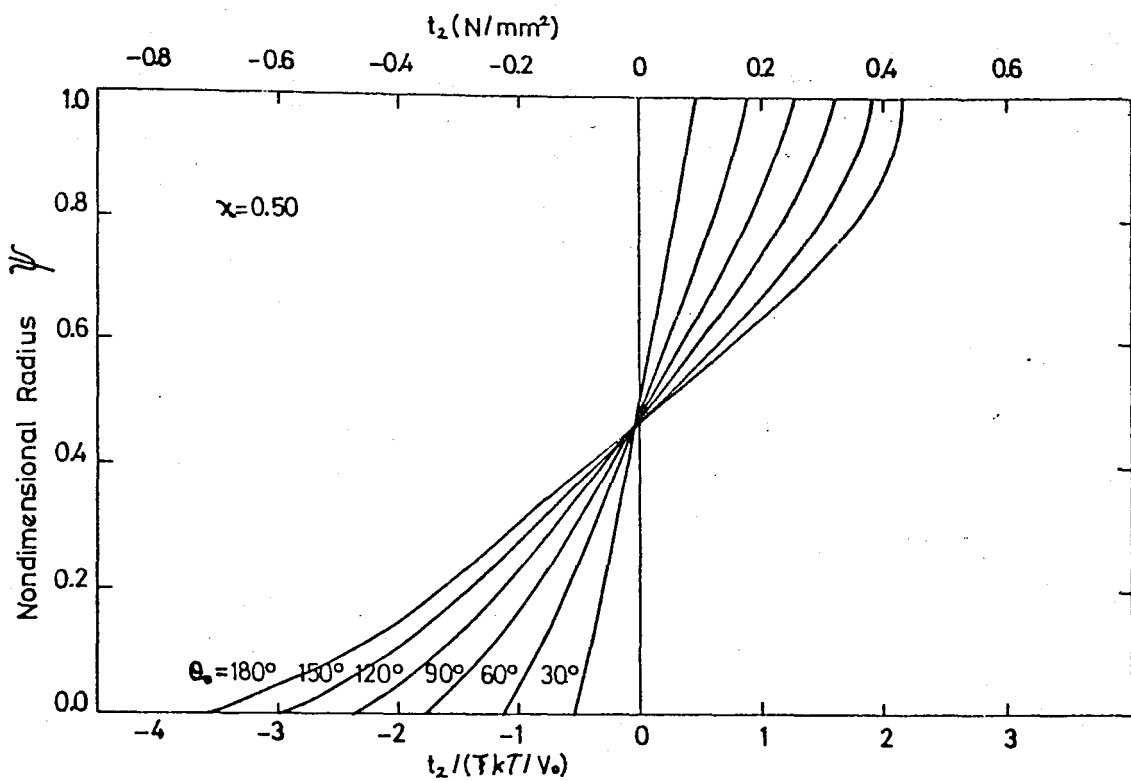


Figure 5.2.10 - Stress t_2 distribution for $\chi = 0.50$.

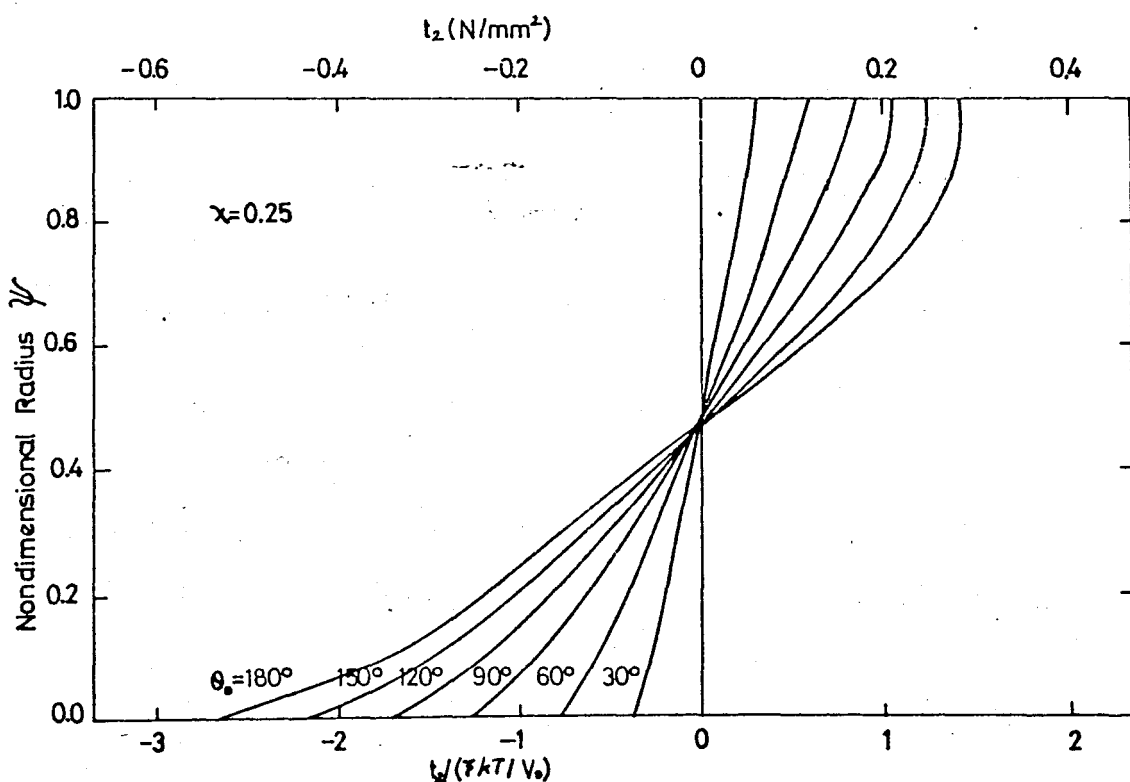


Figure 5.2.11 - Stress t_2 distribution for $\chi = 0.25$.

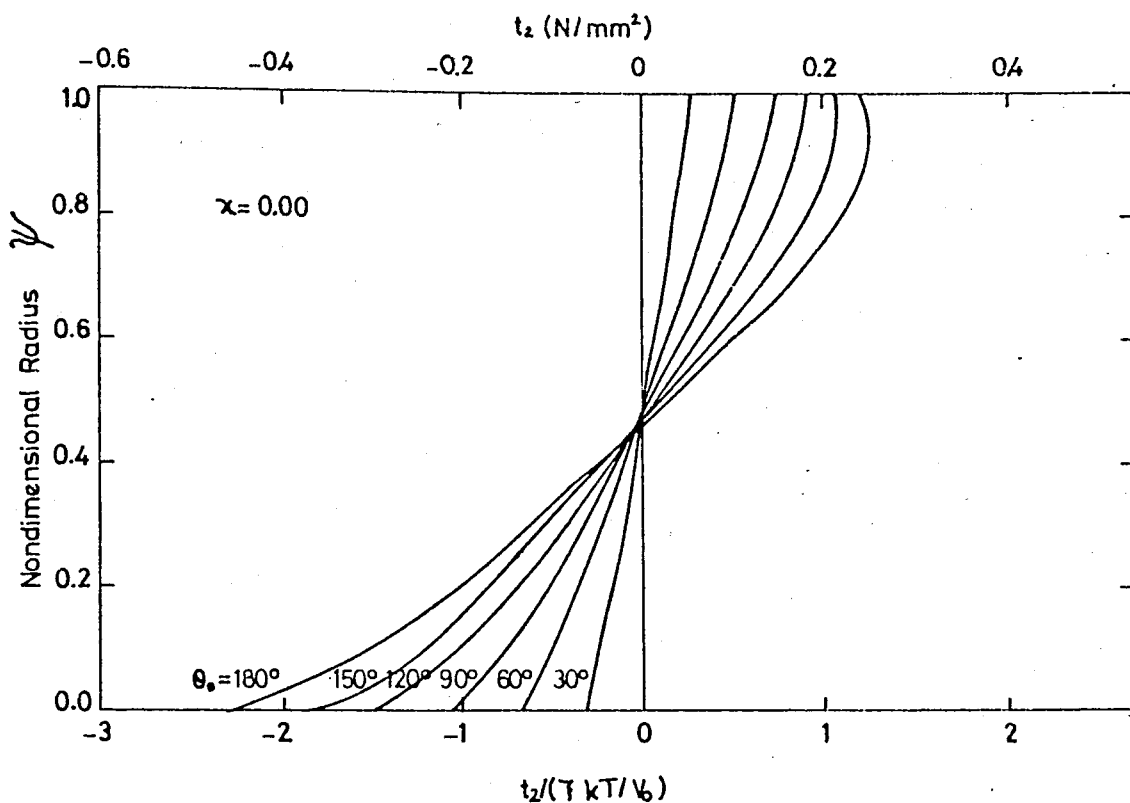


Figure 5.2.12 - Stress t_2 distribution for $\chi = 0.00$

5.2.3 Stress t_3 in Z Direction

The stress t_3 which is known the Poising effect from Section III may be analysed with the same approach that is used for other stresses. The distribution of t_3 values are given in the following figures.

- Figure 5.2.13 for $\chi = 1.0$
- Figure 5.2.14 for $\chi = 0.75$
- Figure 5.2.15 for $\chi = 0.63$
- Figure 5.2.16 for $\chi = 0.50$
- Figure 5.2.17 for $\chi = 0.25$
- Figure 5.2.18 for $\chi = 0.00$

The Pointing effect appears positive or as tension at the outer surface and compression at the inner surface. From r_2 to r_1 it sharply reduces to zero and then starts to increase in the negative direction and reaches its final compressive value at r_1 which is much larger than the maximum tension value. The point where the effect is zero becomes close to the outer surface as the degree of flexure increases.

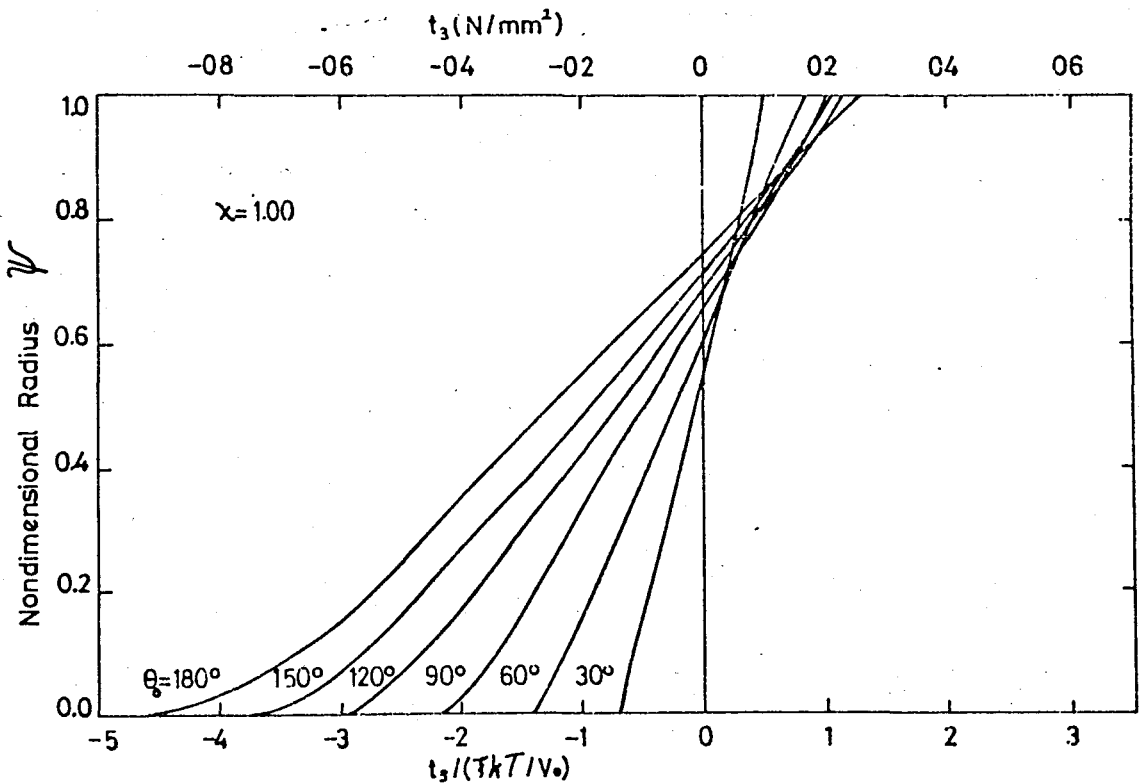
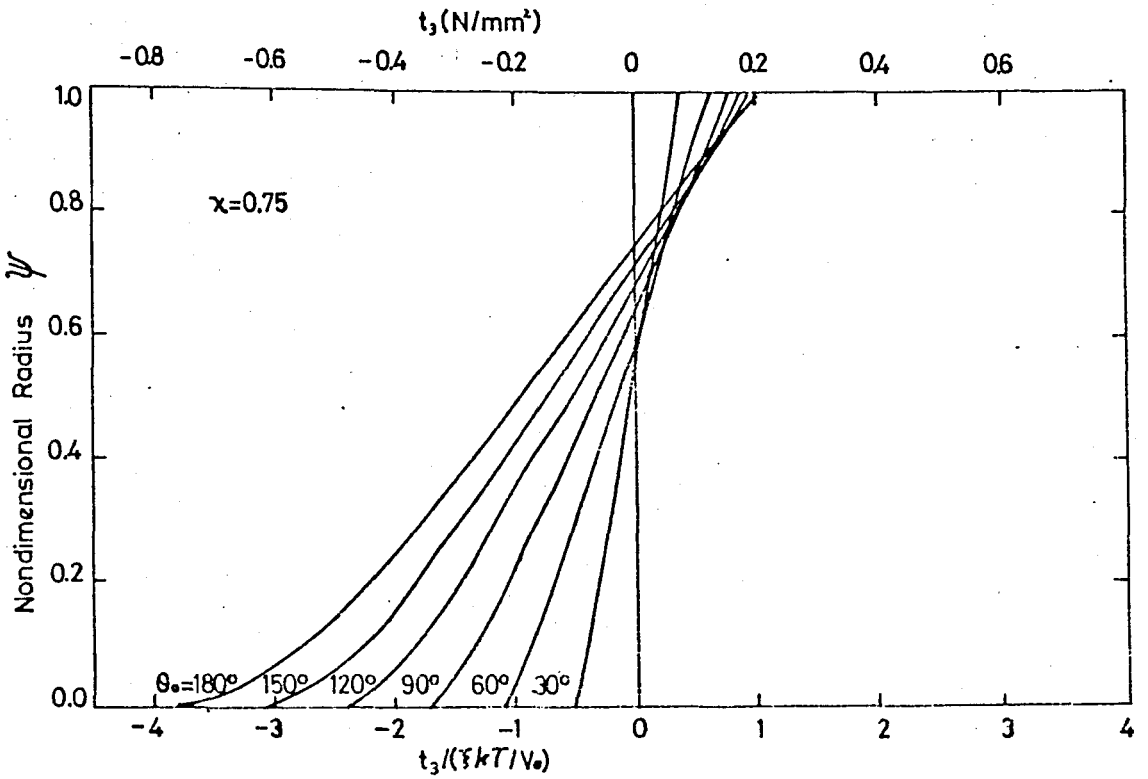
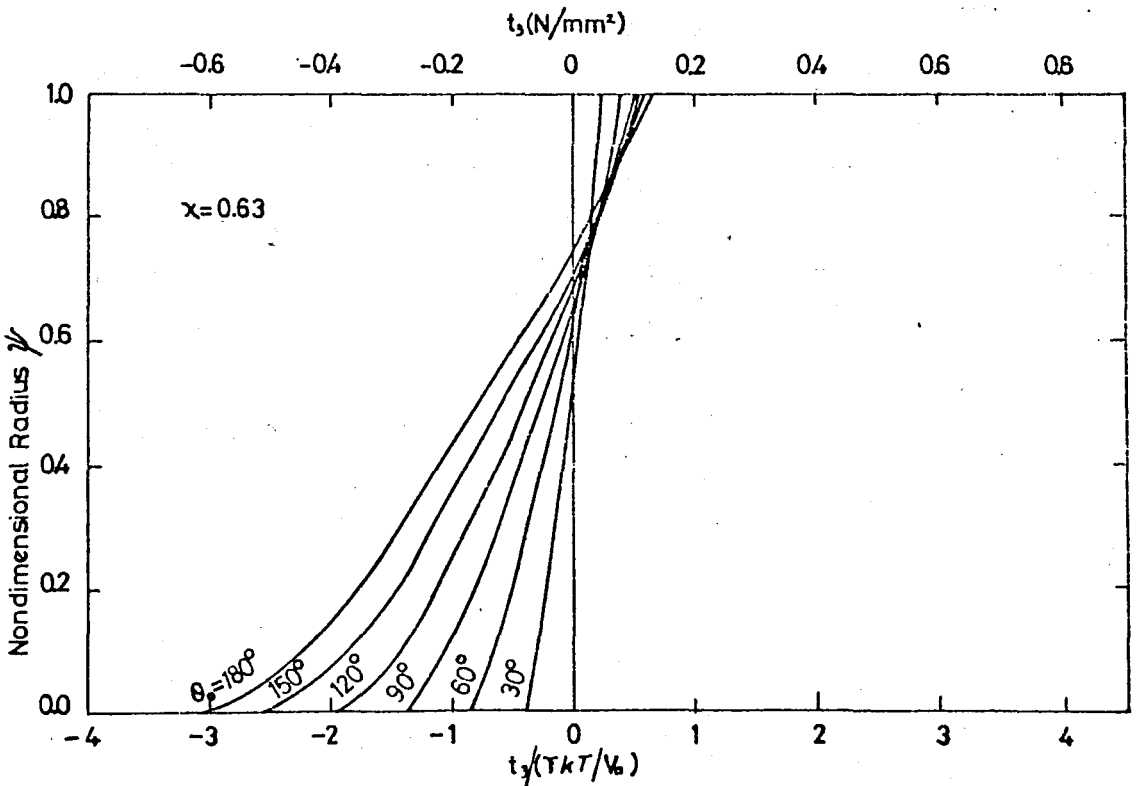


Figure 5.2.13 - Pointing effect for $\chi = 1.0$.

Figure 5.2.14 - Pointing effect for $\chi = 0.75$.Figure 5.2.15 - Pointing effect for $\chi = 0.63$.

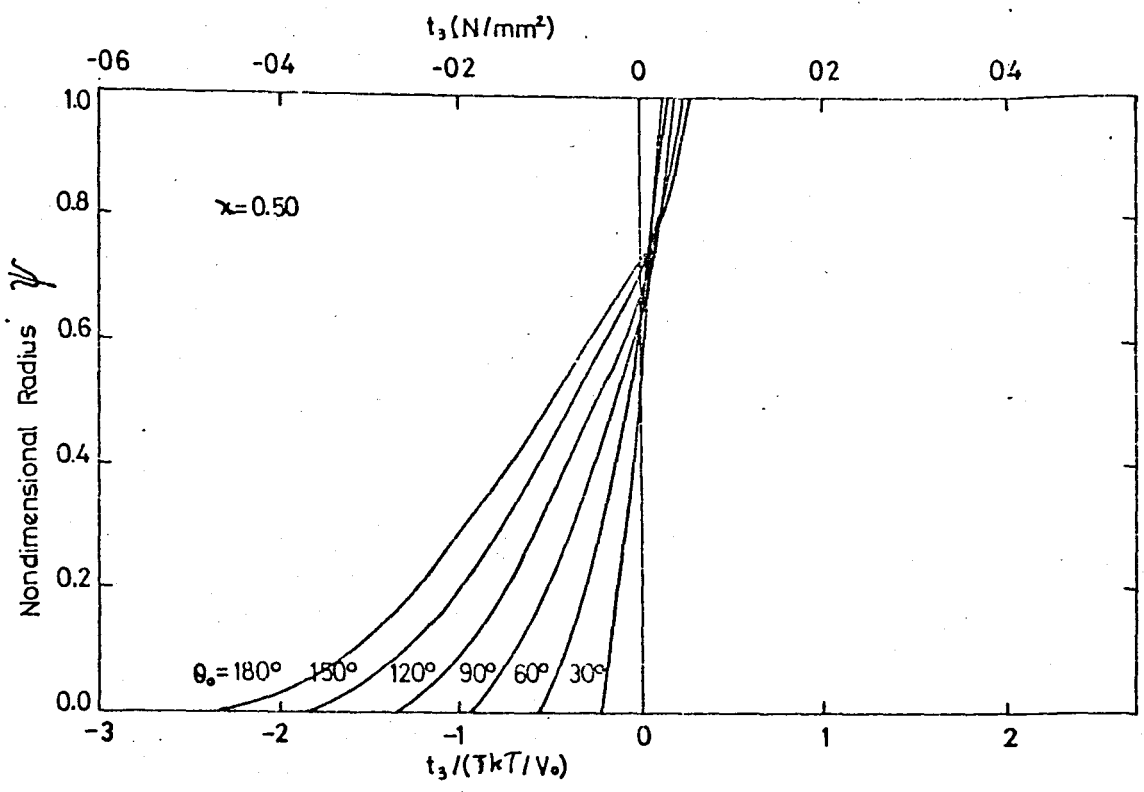


Figure 5.2.16 - Pointing effect for $\chi = 0.50$.

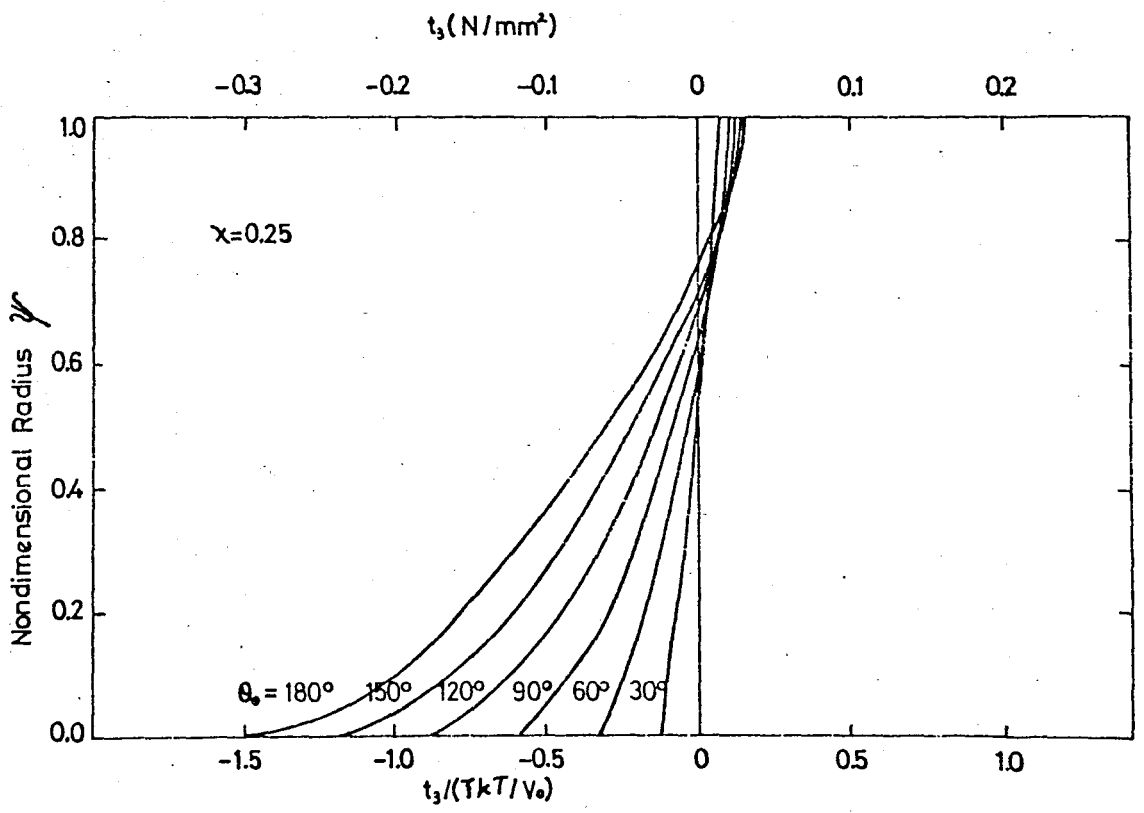


Figure 5.2.17 - Pointing effect for $\chi = 0.25$.

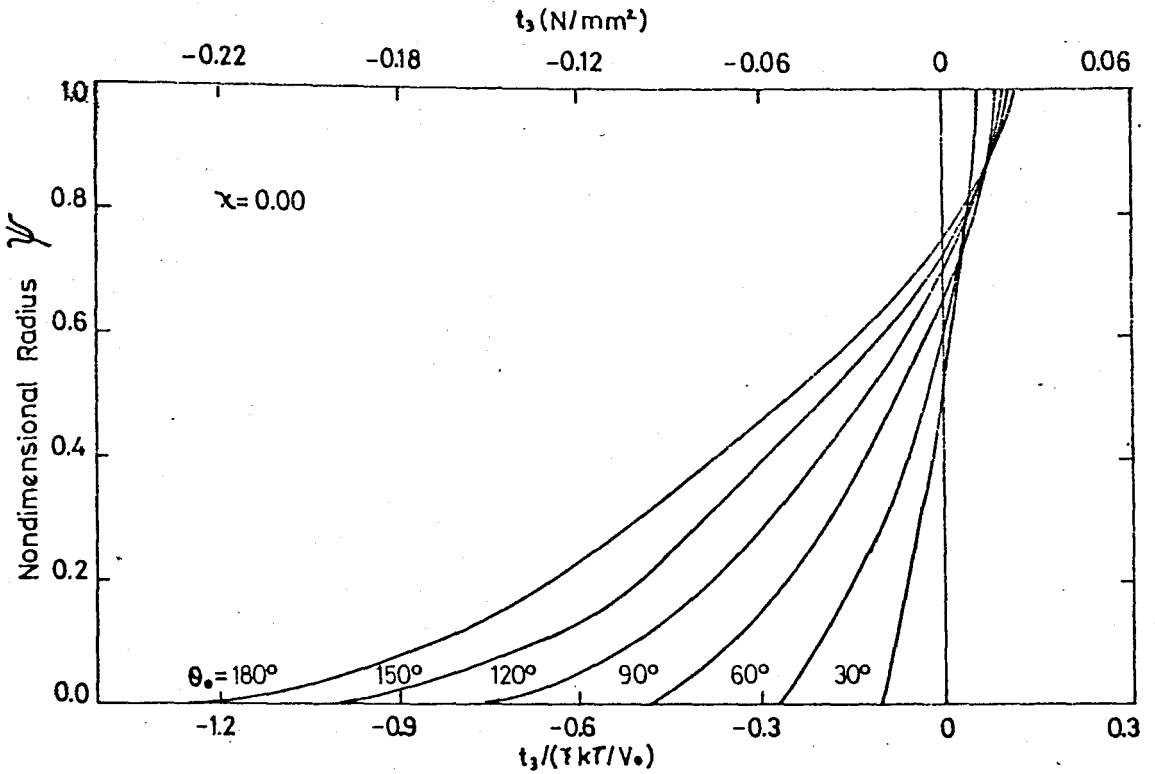


Figure 5.2.18 - Pointing effect for $\chi = 0.00$

5.2.4 Stresses and χ Parameter

In order to examine the stress versus χ parameter relation, some numerical values which are provided by keeping flexure degree constant while χ is changed, are used.

Figure 5.2.19 gives the stress t_1 for every χ at 90° flexure. It is shown that when χ decreases, swelling increases and correspondingly magnitudes of t_1 decreases. During swelling more solvent is absorbed in the mixture so it will be possible to bend the beam with less stress. Therefore, the peak value of t_1 stress drops to a lower value, it also shifts slightly towards the inner radius as χ decreases.

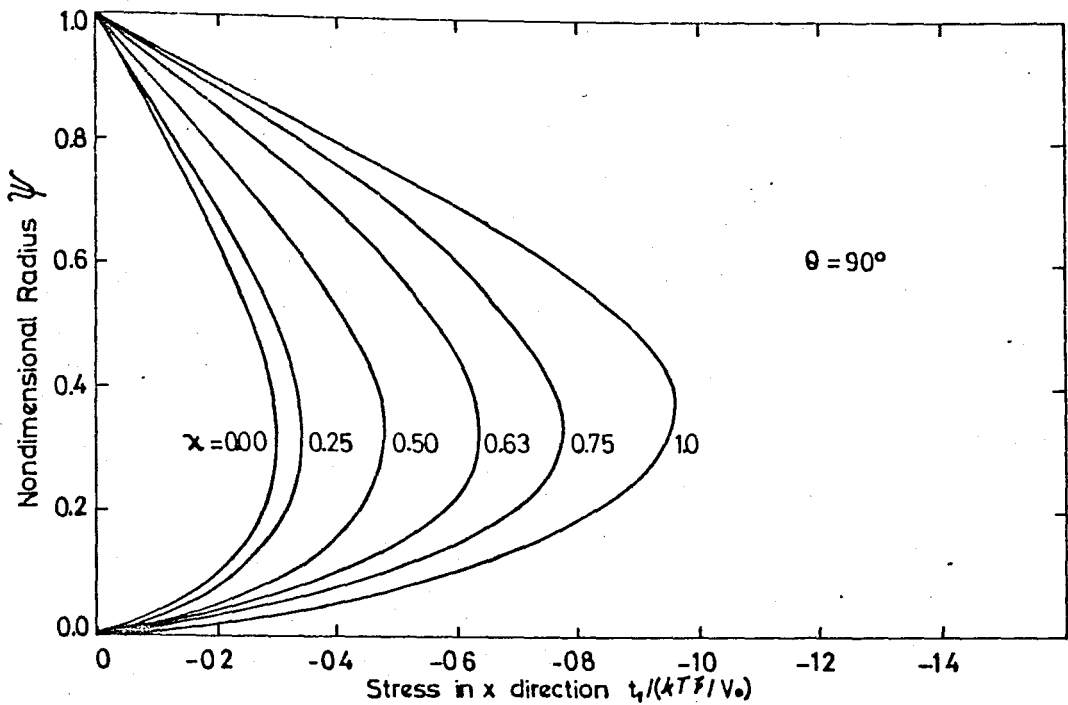


Figure 5.2.19 - t_1 curves for different χ 's at $\theta_0 = 90^\circ$.

Although χ parameter is decreased in equal steps, drop in t_1 peak is not evenly spaced. This is because of swelling degree. Figure 5.1.4 also shows the relation between the χ parameter and the swelling degree v_{20} .

In Figure 5.2.20 we have stress t_2 distribution which is in Y direction. When the $\chi = 1.0$, t_2 stress has larger magnitude than other cases where χ is smaller than 1.0. All the t_2 values drop as χ decreases or when swelling increases. The neutral axis move close to the outer radius as χ increases.

Figure 5.2.21 is plotted for nondimensional radius ψ versus non-dimensional stress t_3 similar to Figure 5.2.20 and 5.2.19 and it shows the Pointing effect against the χ parameter for $\theta_0 = 90^\circ$. Its behaviour is almost the same as t_2 .

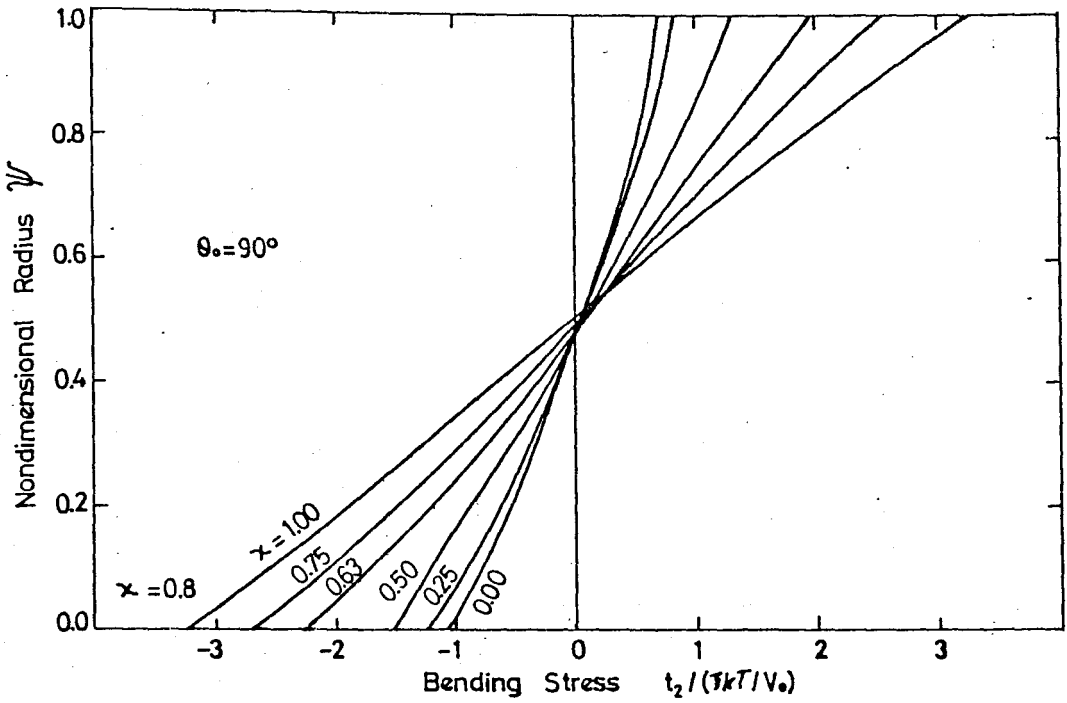


Figure 5.2.20 - t_2 curves for different χ 's ($\theta_0 = 90^\circ$).

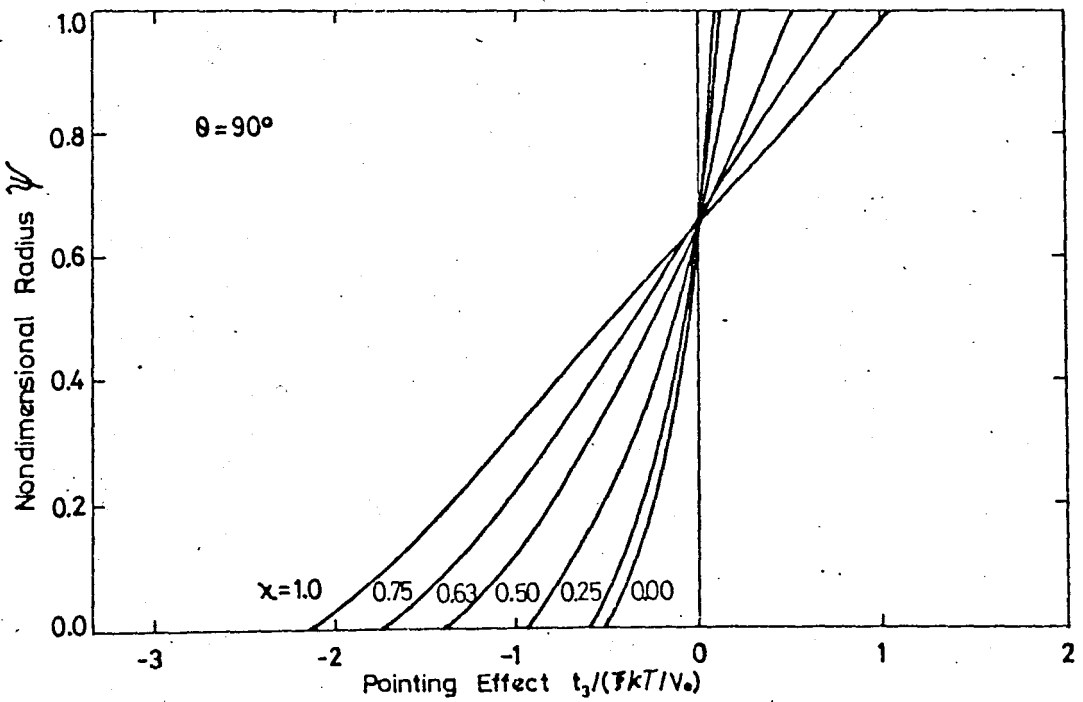


Figure 5.2.21 - t_3 for different χ 's $\theta_0 = 90^\circ$.

We know that as we increase the degree of flexure, the neutral axis of t_3 moves outwards. It is interesting that for different χ 's the axis of t_3 stays at almost the same point for same degree of flexure like in Figure 5.2.21, so neutral axis of t_3 is not effected by the swelling ratio but it is affected mainly by the degree of flexure.

5.3 GENERAL RESULTS

Since the presentation of stresses and solvent actions in beam are completed, we will examine the other variables, energy constant ΔE_0 which is equal to the minimum free energy level, swollen width a_s , swollen and deformed width a_D , radii r_1 , r_2 in Table 5.3.1. Further on, we will examine the dependency of these variables on each other.

From Table 5.3.1 the following common variations are apparent.

During the deformation when the flexure is increased, the radius of curvature is decreased which can be observed from r_1 values.

We also know that t_1 stresses are compressive which cause reduction in width. Reduced or swollen and deformed width is shown in Table 5.3.1 in column a_D . Reduction of width, as t_1 increases, is apparent from columns a_D and a_s . In the same table, the third column gives the minimum free energy which is equal to negative of energy constant ΔE_0 . For every χ the lowest energy level decreases while bending is increased. This happens because of solvent motion and elastic effects. When the solvent is exchanged with better soluable solvents, energy values shift to higher values. From Eq. (3.25) it is known that t_1 stress is proportional to the difference between

TABLE 5.3.1 - General Results.

X	θ_0	v_{20}	$-\Delta E_0$	a_s	a_D	r_1	r_2
	Deg		N-mm/mm ³	mm	mm	mm	mm
1.00	30	0.693125	-5.2730	2.260	2.193	3.350	5.543
	60	0.693125	- 5.1704	2.260	2.044	1.362	3.406
	90	0.693125	- 5.0436	2.260	1.890	0.773	2.663
	120	0.693125	- 4.9088	2.260	1.753	0.509	2.262
	150	0.693125	- 4.7720	2.260	1.637	0.367	2.003
	180	0.693125	- 4.6361	2.260	1.538	0.280	1.818
0.75	30	0.506013	- 7.7169	2.510	2.436	3.716	6.152
	60	0.506013	- 7.6048	2.510	2.273	1.503	3.776
	90	0.506013	- 7.4634	2.510	2.101	0.848	2.948
	120	0.506013	- 7.3109	2.510	2.947	0.555	0.502
	150	0.506013	- 7.1555	2.510	1.815	0.397	2.212
	180	0.506013	- 6.9994	2.510	1.703	0.300	2.003
0.63	30	0.375889	- 9.3864	2.771	2.694	4.093	6.787
	60	0.375889	- 9.2661	2.771	2.518	1.643	4.161
	90	0.375889	- 9.1112	2.771	2.328	0.718	3.246
	120	0.375889	- 8.9423	2.771	2.154	0.595	2.749
	150	0.375889	- 8.7701	2.771	2.004	0.428	2.425
	180	0.375889	- 8.5969	2.771	1.874	0.317	2.191
0.50	30	0.237868	-11.6444	3.228	3.147	4.739	7.886
	60	0.237868	-11.5081	3.228	2.950	1.873	4.823
	90	0.237868	-11.3290	3.228	2.722	1.029	3.751
	120	0.237868	-11.1338	3.228	2.514	0.656	3.170
	150	0.237868	-10.9334	3.228	2.323	0.459	2.782
	180	0.237868	-10.7344	3.228	2.163	0.341	2.504
0.25	30	0.118836	-16.8833	4.068	3.971	5.938	9.909
	60	0.118836	-16.6555	4.068	3.728	2.299	6.027
	90	0.118836	-16.4073	4.068	3.429	1.232	4.661
	120	0.118836	-16.1397	4.068	3.136	0.771	3.907
	150	0.118836	-15.8730	4.068	2.877	0.531	3.408
	180	0.118836	-15.6155	4.068	2.653	0.390	3.043
0.00	30	0.082270	-22.4643	4.598	4.490	6.702	11.191
	60	0.082270	-22.2300	4.598	4.214	2.581	6.749
	90	0.082270	-21.9206	4.598	3.872	1.372	5.244
	120	0.082270	-21.5862	4.598	3.540	0.850	4.390
	150	0.082270	-21.2637	4.598	3.232	0.585	3.817
	180	0.082270	-20.9444	4.598	2.979	0.427	3.406

minimum free energy and the energy at material point considered so energy distribution is very similar to t_1 distribution except that it is not equal to zero at the boundaries. It starts from a finite value listed at $-\Delta E_0$ column for a given value of χ .

5.4 BENDING MOMENT M

In numerical calculations our last step is bending moment for desired degree of flexure. In Figure 5.4.1 Moment values versus degree of flexure are given where θ_0 is in degrees and Moment is in N-mm. Basically when the χ parameter changes, moment is affected. When χ is equal to 0.75, 0.63, or 0.50, swelling is small compared to smaller values of χ parameter. From Figure 5.4.1 it is seen that the moment curve for $\chi = 1.0$ is at the middle and moment curves, for χ equivalent to 0.75, 0.63 and 0.50 are generally lower than $\chi = 1.0$ curve but for very large flexures, moment values become nearly equal. The curves for χ equals to 0.25 and 0.0 are located above the $\chi = 1.0$ curve. The location of curves strongly depends on elasticity modules and on the size of the beam. If we study the Figure 5.4.2, we can follow location of curves more effectively. In this figure the moment versus v_{20} is given. It is clear that when the swelling is not excessive, the moment decreases as swelling increases for the same degree of flexures. This behaviour of moment becomes constant when the bending is 120° or more. On the other hand when the swelling is large or when the χ is less than 0.50, moment rapidly increases. We know that swelling strongly effects the cross-section. When the cross-section is enlarged, larger forces or moment

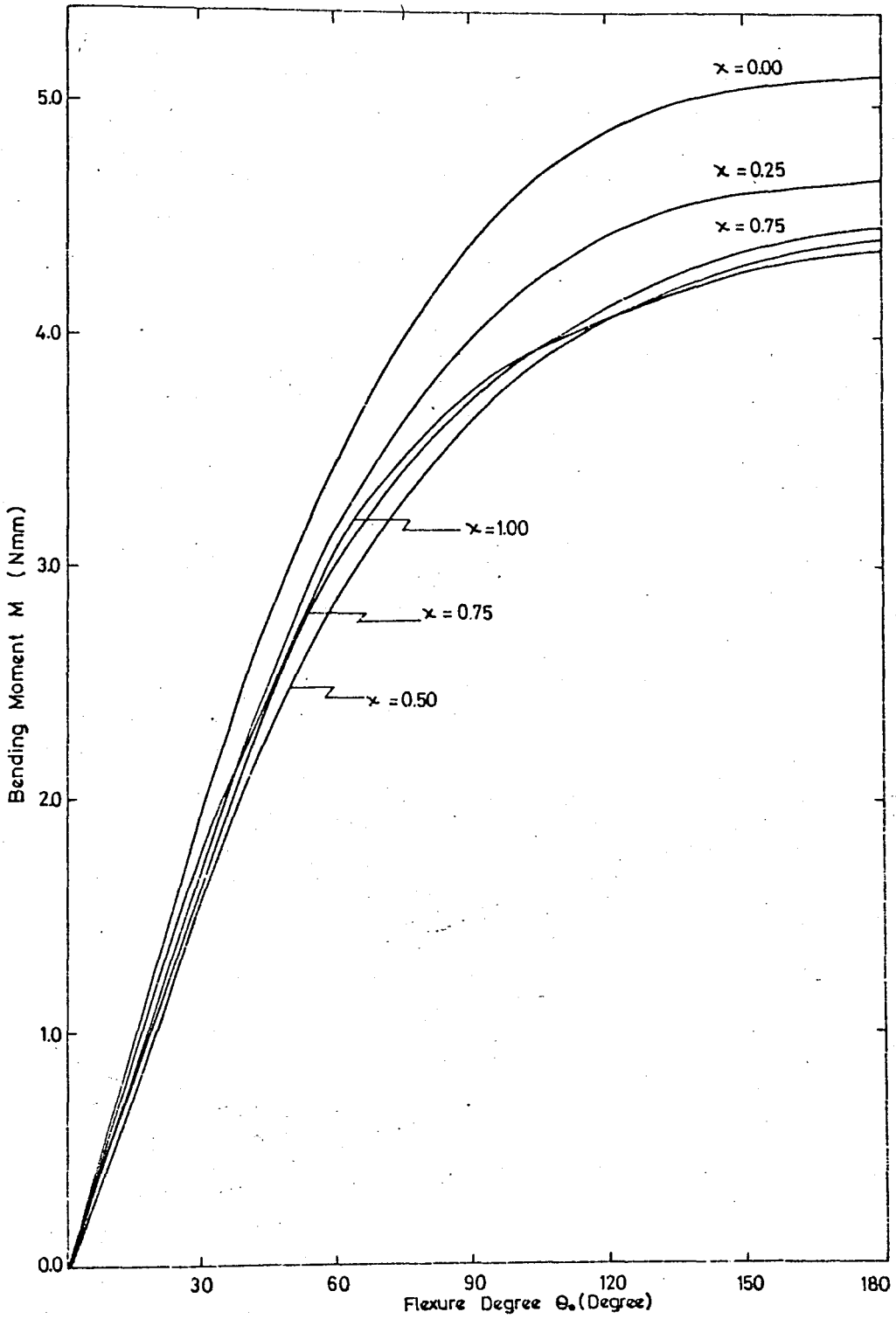


Figure 5.4.1 - Moment values versus θ_0 where θ in degrees M N-mm.

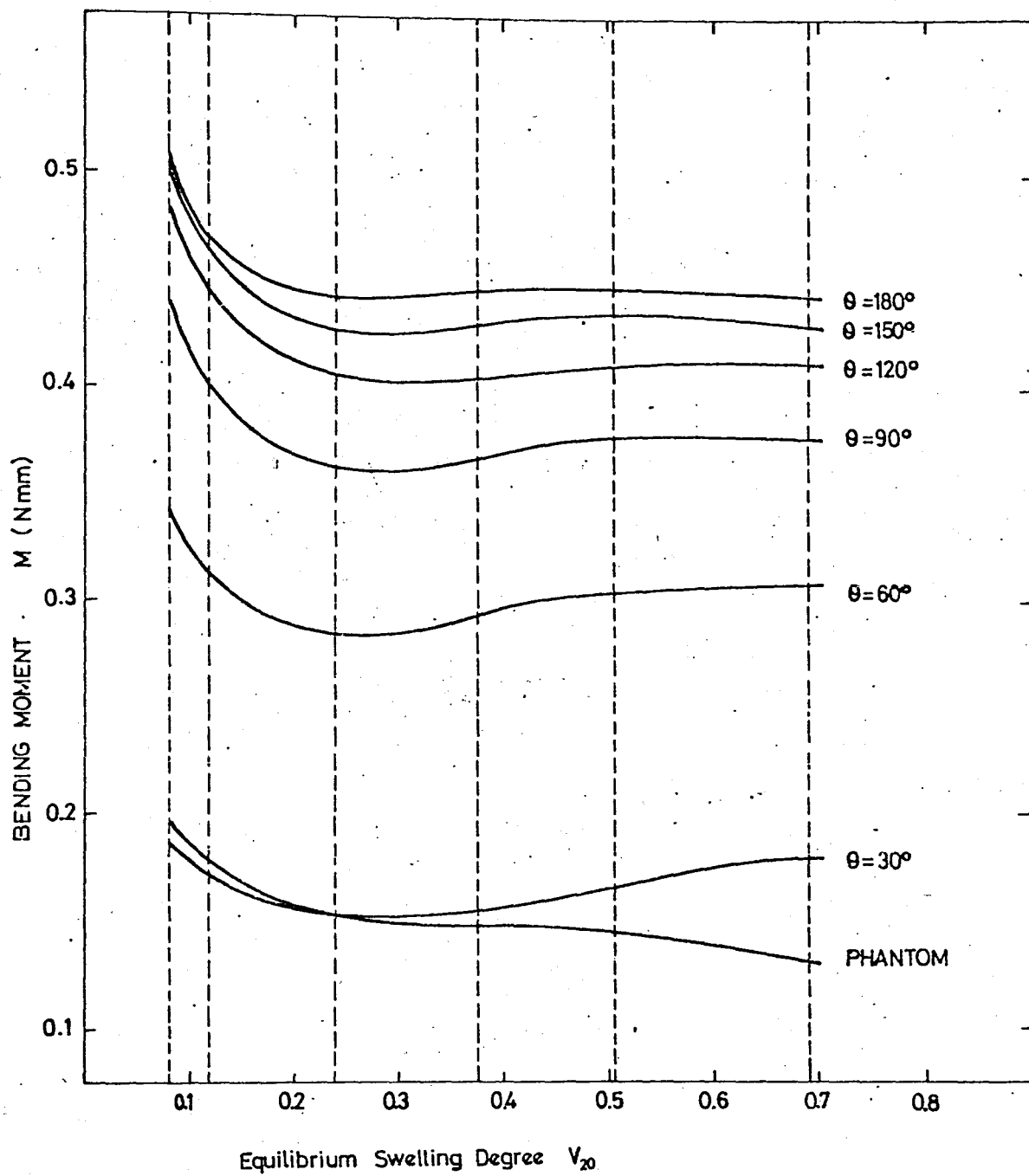


Figure 5.4.2 - Moment versus swelling degree.

arms will be required so moment increases but for cases of less swelling, although the cross-sections do not show much difference, moment drops because of the reduction in the elasticity modulus E . In Figure 5.4.2 the 'phantom case' is plotted for comparison and checking purposes. We have convergence that is, moment values of 'phantom' case get close to 'real' case curve as swelling is increased.

We know that stress t_2 and r are components of moment. The t_2 stress is affected by the length of the beam if the beam is long since it is much easier to bend it. In Figure 5.4.3 maximum t_2 value for different beam lengths is examined at $\theta = 180^\circ$. It is observed that as χ drops t_2 gets smaller because of increasing swelling and as the length of beam increases or a/b ratio decreases t_2 decreases too.

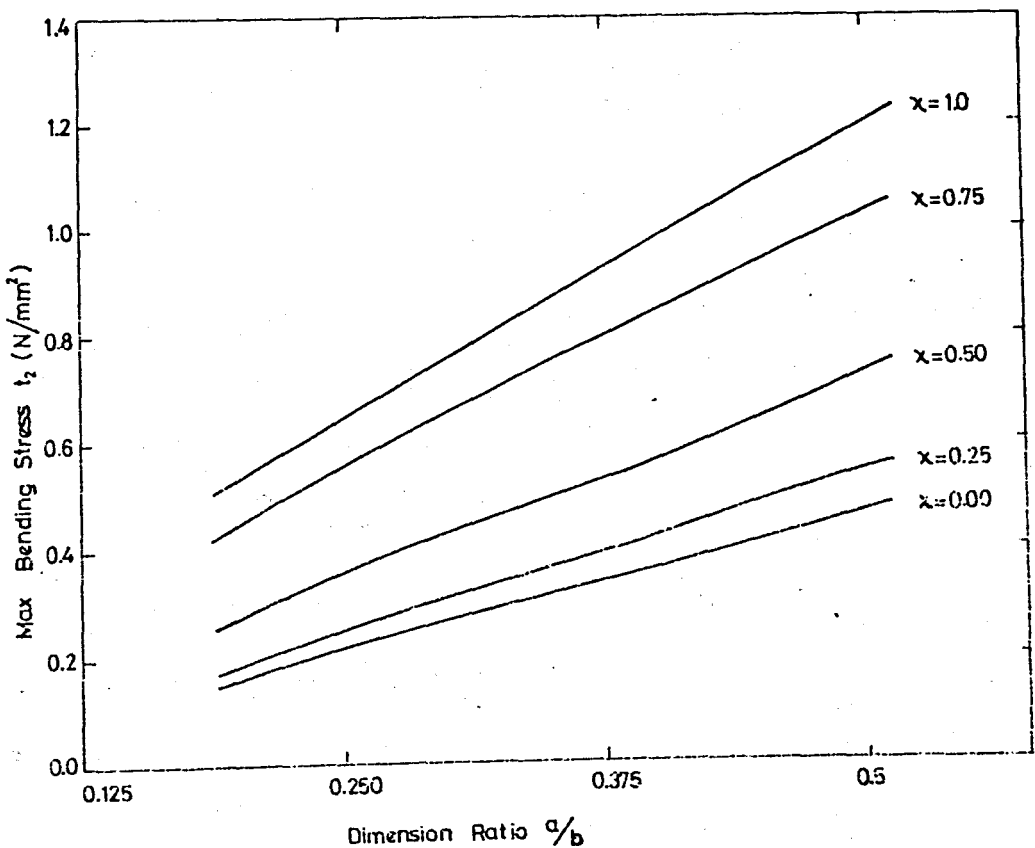


Figure 5.4.3 - Maximum t_2 versus a/b ratio.

VI. LINEAR APPROACH

When the design is considered instead of exact values, sometimes the approximate values may be used. Most of the time it is easier and quicker to get results from linear theory than the nonlinear one. Therefore a comparison between linear and nonlinear theory may be helpful if their common domains of validity are found. Whenever it is possible to find that common limit, then linear theory can be substituted instead of the nonlinear one.

6.1 LINEAR THEORY

In order to understand linear theory, a specimen can be examined under the simple tension and static pressure p . If we consider the specimen shown in Figure 6.1.1 the net constant stress, t , acting on Y surface can be given as

$$t = t_1 - p$$

or

$$t = t_1 - t_2$$

(6.1)

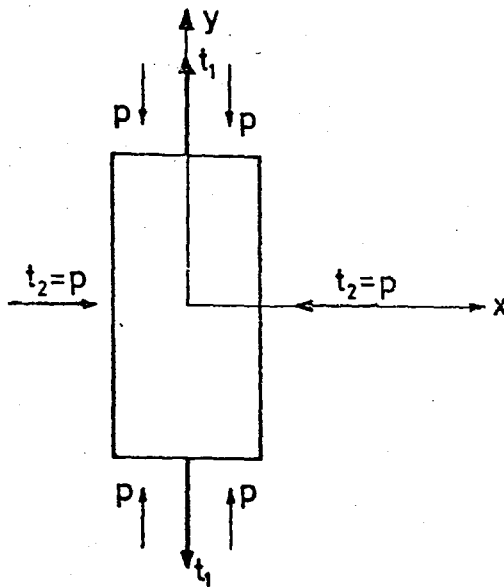


Figure 6.1.1 - Specimen and applied stress for linear treatment.

From the Eq. (2.55) it is known that these stresses can be given in the following forms.

$$t_1 = \frac{RT}{v_1} [\ln(1 - v_2) + v_2 + \chi v_2^2] + \lambda_1^2 v_2 \frac{\xi kT}{v_0} [1 + (\mu/\xi) K(\lambda_1^2)] \quad (6.2)$$

$$t_2 = \frac{RT}{v_1} [\ln(1 - v_2 + v_2 + \chi v_2^2)] + \lambda_2^2 v_2 \frac{\xi kT}{v_0} [1 + (\mu/\xi) K(\lambda_2^2)]$$

Substituting Eq. (6.2) into Eq. (6.1), t will be found as;

$$t = v_2 \frac{\xi kT}{v_0} [\lambda_1^2 + (\mu/\xi) \lambda_1^2 (K(\lambda_1^2)) - \lambda_2^2 + (\mu/\xi) \lambda_2^2 (K(\lambda_2^2))] \quad (6.3)$$

It is advantageous to separate the displacement gradients in two parts as distortion term α and equilibrium swelling term v_2 . Then the stretches

in the X and in the Y direction can be given as

$$\lambda_1 = \alpha v_2^{-1/3}$$

$$\lambda_2 = \alpha^{-1/2} v_2^{-1/3}$$
(6.4)

If we substitute Eq. (6.4) into Eq. (6.3) the net stress, t , will become,

$$t = v_2^{1/3} \frac{kT\xi}{V_0} (\alpha - 1) \left(\frac{\alpha^2 + \alpha + 1}{\alpha} \right) (1 + (\mu/\xi)K(\lambda_1^2))$$
(6.5)

and taking its limit as α goes to unity, the term $(\alpha - 1)$ goes to strain ' ϵ ' and λ goes $v_2^{-1/3}$ then t will be equal to the following;

$$t = 3v_2^{1/3} \frac{kT\xi}{V_0} (1 + (\mu/\xi)K(v_2^{-1/3}))\epsilon$$
(6.6)

From Eq. (6.6) the elastic modulus can be obtained as:

$$E = 3v_2^{1/3} \frac{kT\xi}{V_0} (1 + (\mu/\xi)K(v_2^{-1/3}))$$
(6.7)

On the other hand we know from linear theory that the moment is given by the equation;

$$M = EI \frac{d^2y}{dx^2} = EI \frac{1}{\rho}$$
(6.8)

where E is the elastic modulus, I is the moment of inertia of the beam's cross-section and ρ is the radius of curvature equal to L/θ_0 with L being the length of the half beam. Then the moment may be expressed as;

$$M = \frac{EI}{L} \theta_0 \quad (6.9)$$

The terms in front of the θ_0 term gives the slope of the M versus θ_0 curve and these terms may be denoted as the bending parameter, 'C', defined by;

$$C = EI/L \quad (6.10)$$

During the evaluation of the 'Bending parameter' the final swollen dimensions should be considered. On the other hand the elasticity modulus can be assumed in the following form to see the variation with respect to v_2

$$E = v_2^m f(T, K, \xi, V_0, \dots) \quad (6.11)$$

or taking logarithms of both sides, we have

$$\ln E = m \ln v_2 + \ln f \quad (6.12)$$

This form is useful to obtain a proportionality between E and v_2 as

$$E \propto v_2^m \quad (6.13)$$

where m is the slope of the line whenever $\ln E$ versus $\ln v_2$ is plotted.

6.2 Comparison of Linear and Nonlinear Solutions

As it was explained in the previous section comparison between linear and nonlinear solutions can be useful in design considerations. For this reason in Figure 6.2.1 linear and nonlinear results for $\chi = 1.0$ value are

plotted and it is seen from this figure that linear theory is in agreement with the nonlinear one up to 30° of flexure. If the length of beam is increased by a factor of five this agreement extends up to 90° of flexure. When the value of $\chi = 0.75$ as given in Figure 6.2.2 where moment in Nmm versus to degree of flexure in degrees is plotted, the equality between the linear and nonlinear theories exists only up to 20° of flexure.

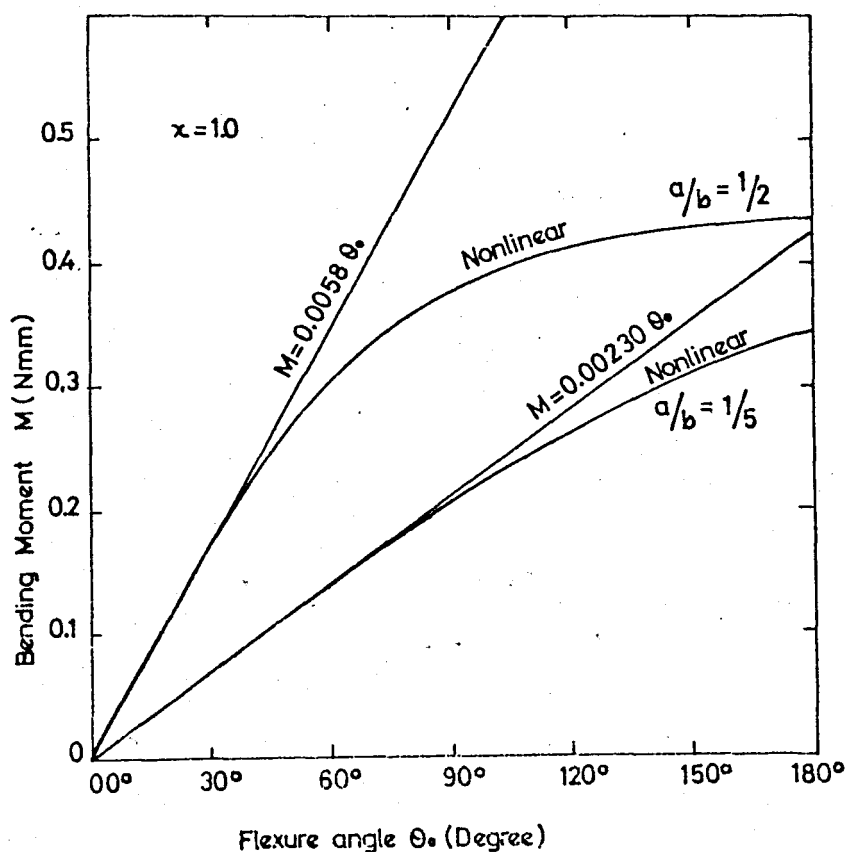


Figure 6.2.1 - Comparison of linear and nonlinear solutions for $\chi = 1.0$.

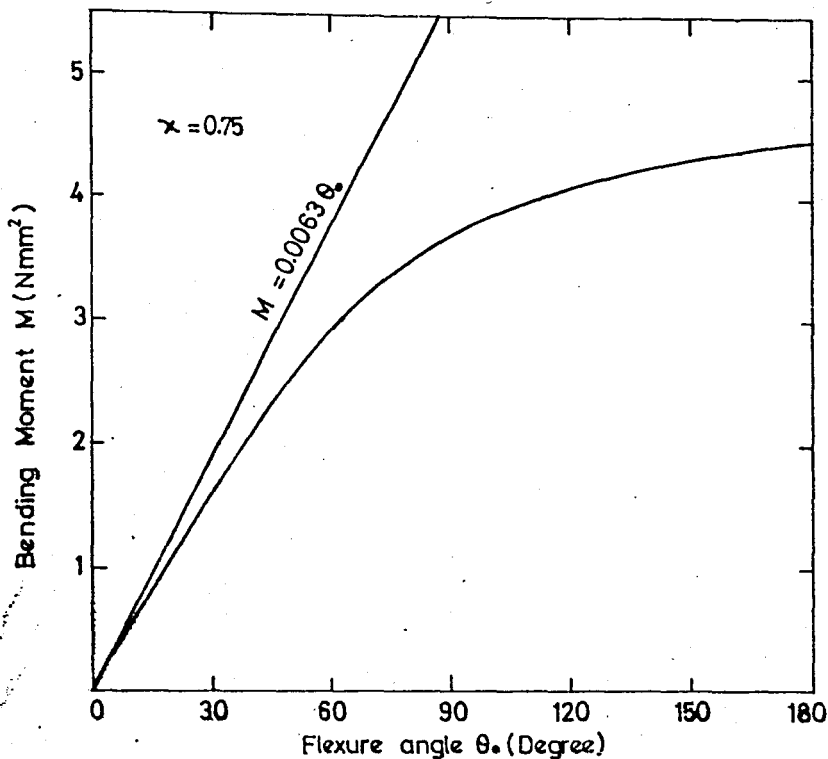


Figure 6.2.2 - Comparison of linear and nonlinear solutions for $\chi = 0.75$.

Similarly in Figure 6.2.3 for $\chi = 0.50$ this equality is reduced further. Figure 6.2.4 and 6.2.5 are for $\chi = 0.25$ and $\chi = 0.00$ respectively. The curves in these figures show agreement only at the origin while in other regions linear and nonlinear solutions diverge from each other. The divergence of solutions may be explained by the help of Figure 6.2.6 where we see that as χ or v_{20} increases, swelling decreases meanwhile elasticity modulus increases but the length of the beam and moment of inertia of beam decreases more rapidly than other components of 'Bending parameter', C , which are plotted in logarithmic values in Figure 6.2.6.

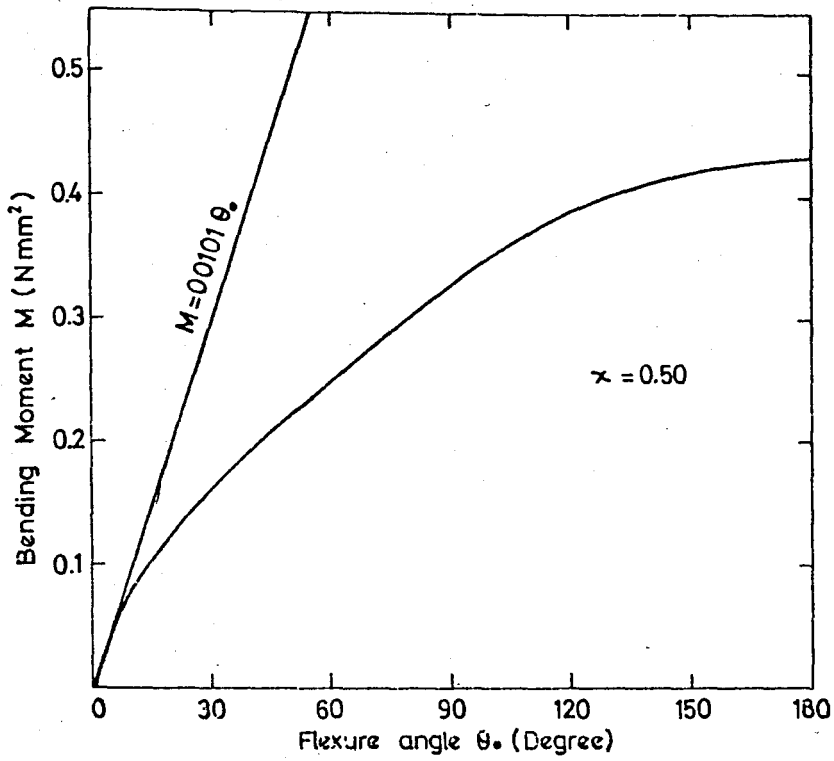


Figure 6.2.3 - Comparison of linear and nonlinear solutions for $\chi = 0.50$.

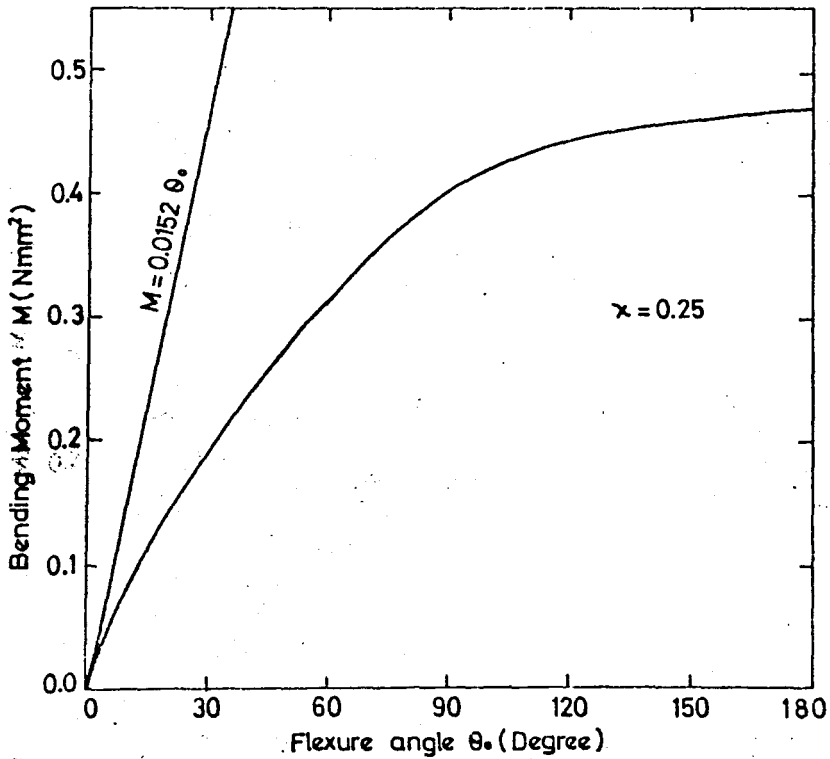


Figure 6.2.4 - Comparison of linear and nonlinear solutions for $\chi = 0.25$.

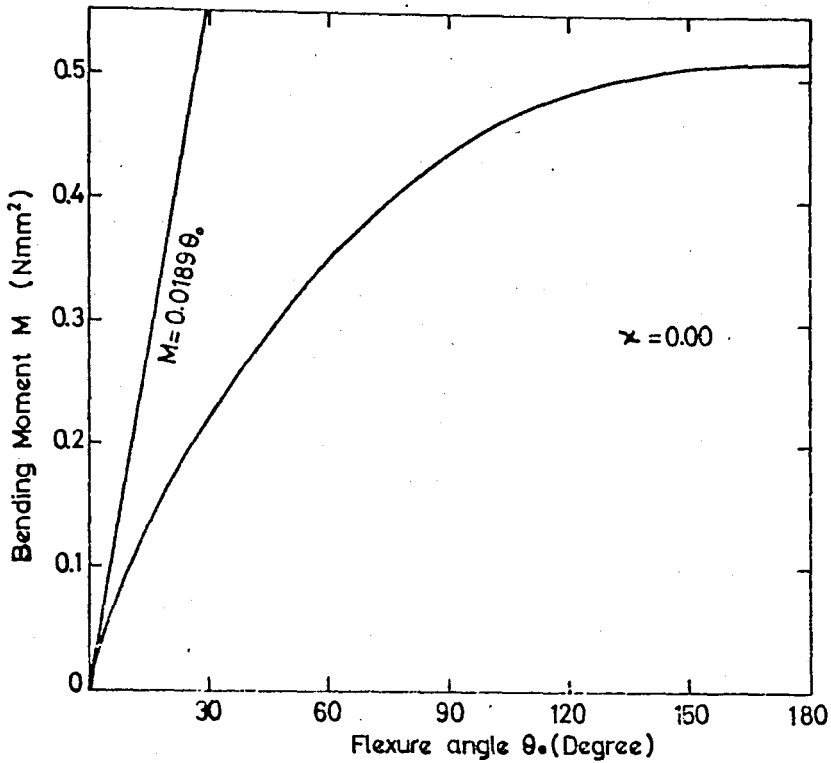


Figure 6.2.5 - Comparison of linear and nonlinear solutions for $\chi = 0.00$.

When χ is less than 0.50, in other words, when v_{20} is less than 0.237 swelling is very effective. As it can be seen from Figure 6.2.6 the moment of inertia term becomes dominant in the case of large swellings. Therefore in the comparison curves when the moment of inertia is large; according to Eq. (6.10) the slope of the linear solution increases but diverges from the nonlinear one.

From Figure 6.2.7 the slope 'm' of curve can be calculated as 0.4090 and the downshift 'ln(f)' comes out as -0.30 accordingly Eq. (6.12) will have the following form;

$$\ln E = 0.4092 \ln v_2 - 0.30 \quad (6.14)$$

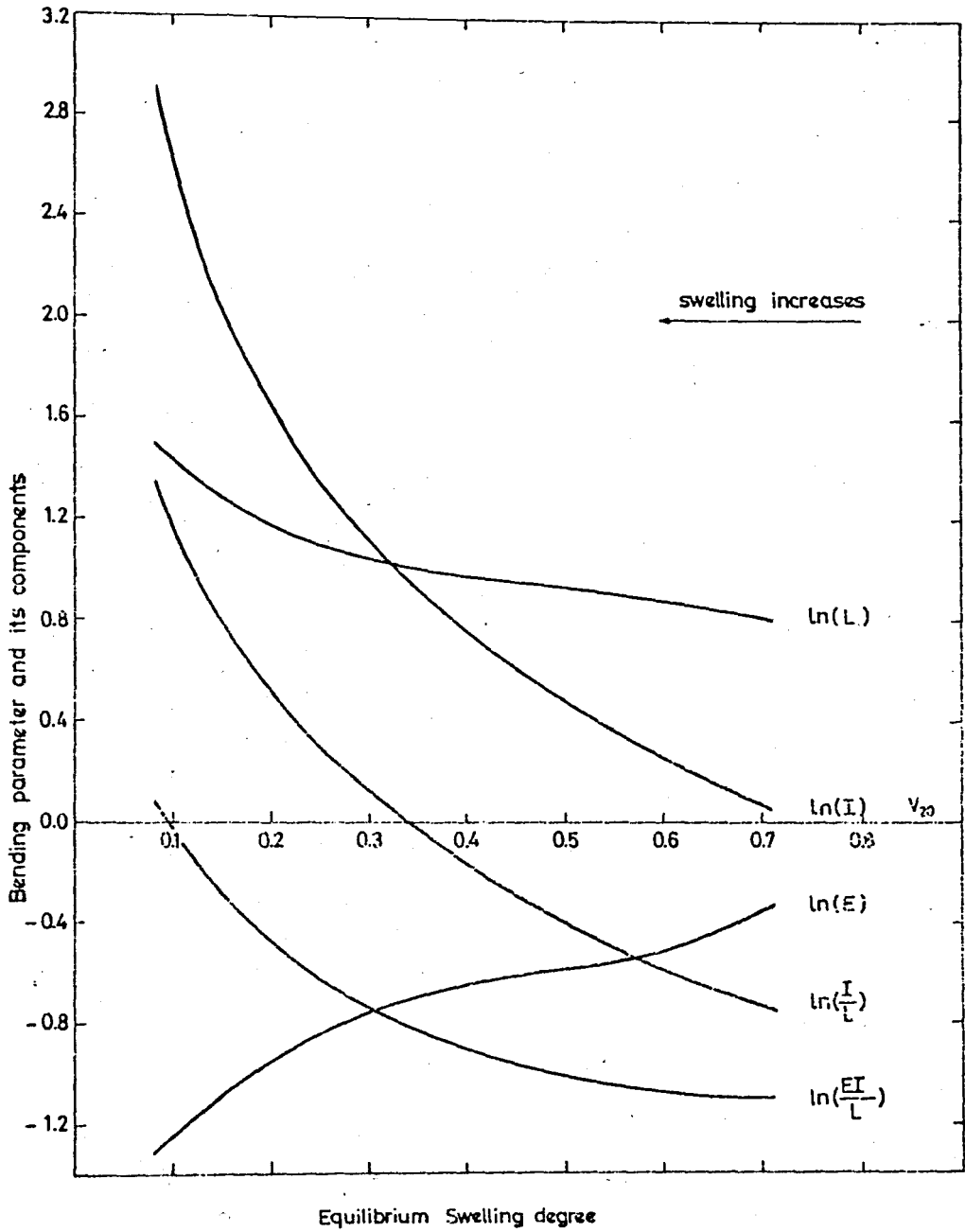


Figure 6.2.6 - Swelling effect on bending parameter and components.

and the proportionality between swelling and elasticity modulus can be expressed as

$$E \propto v_2^{0.4090} \quad (6.15)$$

where the power of v_2 is the slope of the curve in Figure 6.2.7.

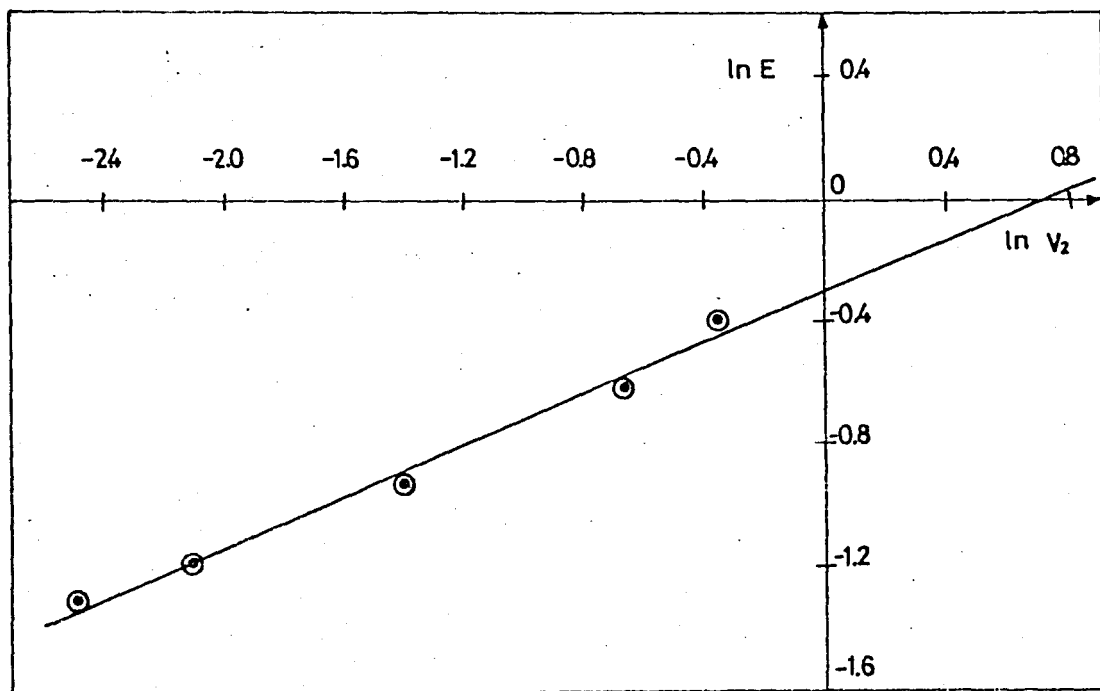


Figure 6.2.7 - The relation between E and v_2 in nonlinear approach.

VII. CONCLUSION

The distribution of stress, strain and amount of solvent are obtained for a cuboid of an amorphous polymeric network bent by couples applied at its ends. Bending is assumed to take place when the cuboid is immersed in a solvent. The effect of different degrees of swelling is investigated by assuming six different solvents of different swelling power. More solvent is seen to enter in a region above the neutral axis. During further deformations solvent moves outwards. The unequal distribution of liquid in the beam diverges from equilibrium position parallel to degree of flexures of the beam. An increase on divergence is observed as the swelling is increased as larger flexure degrees are applied.

The t_1 stress in the radial direction is always negative i.e. compressive and causes reduction in depth of the beam. The t_2 stress in the Y direction which creates the flexural couple has an increasing magnitude depending on the degree of bending. Its tension region implies larger swelling than compression region. Although there is no applied force in the Z-direction, the Poissoning effect, t_3 , becomes necessary to compensate the deformations which will occur in the Z-direction. Required t_3 distributions are also calculated.

Bending moment displays a decrease initially and then an increase against the increasing swelling. At the beginning, swelling is not dominant but the drop in the elasticity modulus causes a reduction in moment up to a point where swelling or indirectly the cross-section becomes dominant, then an increase in moment is observed. For large deformations the drop in elasticity modulus is compensated by an increase in cross-sections until excess swelling occurs.

The comparison of linear and nonlinear solutions indicates that for specific solvents, upto a certain limits, two theories show equality. In certain problems with suitable dimensions, material constants and flexure degree, the linear theory is more readily used than the complex nonlinear one.

APPENDICES

APPENDIX A

A.1 GENERAL DESCRIPTION OF COMPUTER PROGRAM

Basically the solution steps explained in Section IV are followed when the computer program is considered.

The main program starts by reading the input data which include: the material constants, initial values and tolerances. Then the degree of swelling v_{20} is calculated and it is accepted as the initial distribution of the solvent. With this constant distribution, outer radius r_2 is calculated according to assumed r_1 . For the validity of r values, energies at boundaries should be equal, in order to make this comparison, the computer program calculates stretches and energies at r_1 and r_2 . After the equality of energies is obtained these calculations are repeated by including the calculation of t_1 stress according to Eq. (3.25) for 11 stations which are located in the radial direction of the beam. The t_1 values are substituted into Eq. (2.55) to find the new set of v_2 values. Meanwhile the computer program calculates the principal stresses by using final v_2 values.

As a next step, the program compares the final v_2 distribution with the initial v_2 distribution. If these do not match (within an error bound) the final values of v_2 are accepted as the initial distribution of the solvent and the iteration is continued for 11 stations until the equality is satisfied. Up to this point radii are kept constant in fact each radius should be checked for a converged distribution of v_2 so that the program returns back to the beginning and calculates new r_1 and r_2 and repeats iterating on v_2 and compares final r values with previous r values. Iteration on r finishes whenever equal r values are obtained.

The computer program is completed with moment calculations, non-dimensionalizations and output formats.

FLOW CHART

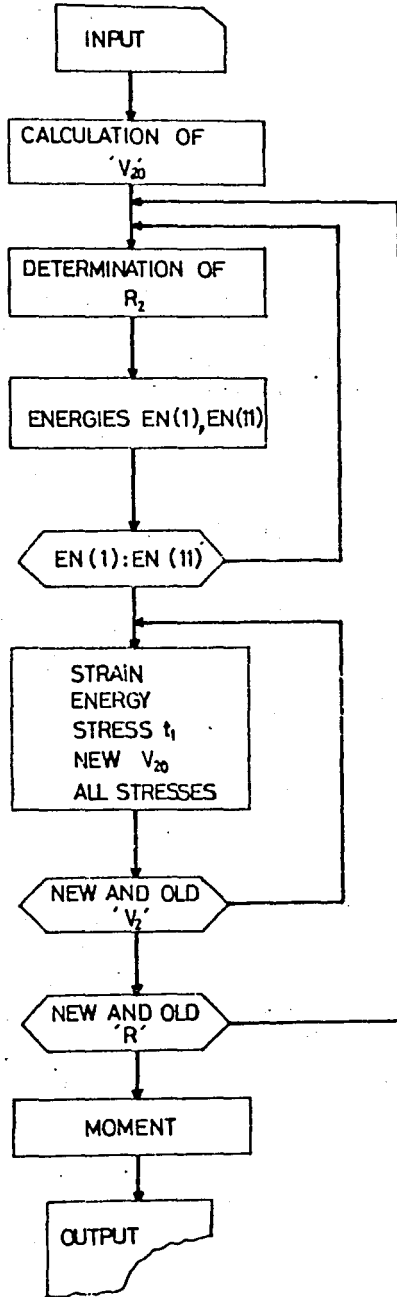


FIGURE A.1

A.2 SUBROUTINE DESCRIPTIONS

In the complete program, the main program calls subroutines meanwhile subroutines reference to other subroutines as can be followed from the following 'Functional Relationship' diagram.

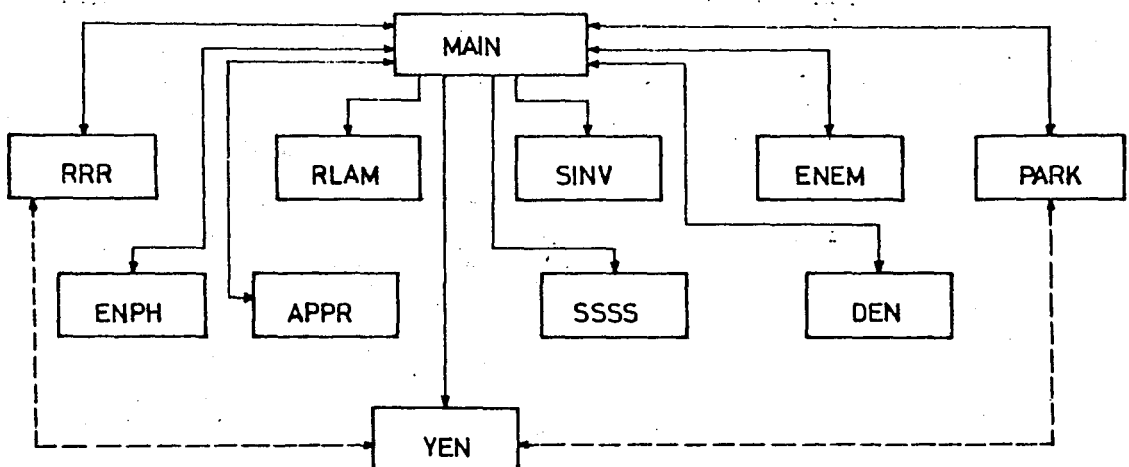


Figure A.2 - Functional relationship between subroutines.

Subroutines with brief explanations are given in the following;

SUBROUTINE PARK: This subroutine calculates the ' $K(\lambda_1^2)$ ' parameter as is given in Eq. (2.51). It receives only the material constants and displacement gradient then calculates energy variable of $K(\lambda_1^2)$ and itself.

SUBROUTINE RLAM: This subroutine calculates the displacement gradients by making use of Eq. (4.3) and swelling degree.

SUBROUTINE SINV: Mainly three invariants of deformation tensor are calculated by the help of the principal stretches.

SUBROUTINE SSSS: The subroutine receives material constants, v_2 distribution, stretches and calculates principal stresses in three directions according to Eq. (2.55).

SUBROUTINE ENEM: By making use of stretches, solvent distributions, and invariants, it obtains mixing free energy, elastic free energy and total free energy.

SUBROUTINE RRR: This subroutine takes the integral given in Eq. (4.7), with extended Simpson's rule and finds the r_2 according to given r_1 .

SUBROUTINE YEN: In this part of the program the stress expression (2.55) is solved for solvent distribution v_2 with the help of the material constants, swelling degree, 'K' parameter and the stress in X direction.

At the beginning of this study, instead of subroutine YEN, subroutine DEN was used. Although subroutine DEN gives good results, it shows unsuccessful convergence for some extreme χ and r values. For diverging points subroutine APPR was used to make an approximation. Since in this program subroutine YEN is considered these following subroutines are not used in calculations but it is noted that these may be necessary in other studies.

SUBROUTINE DEN: This subroutine does the same job as subroutine YEN but differs in the solution method. In subroutine DEN successive approximation method is used.

SUBROUTINE APPR: This subroutine gives a linear distribution of solvent with respect to final and initial stations of the beam.

SUBROUTINE ENPH: This subroutine calculates the energy at 'phantom case'. This can also be done by equating κ to zero or a value which is very close to zero in the conventional program. The latter procedure is preferred in calculations.

A.4 INPUT AND OUTPUT DESCRIPTION

Input format basically includes the followings which are introduced in the list of important variables.

Material constants

Initial values

Tolerances

A sample input data card deck for $x = 0.25$ $\theta_0 = 120^\circ$ is given in Section A.5.

Output gives the results in columns starting from radius, polymer ratio, total free energy, principal stresses in three directions in N/mm^2 and it ends up with nondimensional forms of radius and stresses. After the presentation of this table the moment value in Nmm and its nondimensional form are given before the degree of flexure to which is in radians. Results are finalized with swelling degree and tolerances. The above explanation can be followed from the sample run given in Section A.6.

A.4 LIST OF IMPORTANT VARIABLES

A	: Displacement gradient vector (λ)
A \emptyset	: The width of beam, a_0
B	: Variable of energy expression, B
BD	: Variable of energy expression, \dot{B}
B \emptyset	: The length of beam, b_0
C	: Material constant, ζ
DR1	: Initial value for distance between two stations
E	: Material constant, $1/\kappa$
EN	: Total free energy, ΔE
EN1	: Mixing free energy, ΔE_m
EN2	: Elastic free energy (phantom + constraints), $\Delta E_{ph} + \Delta E_c$
ENA \emptyset	: Energy constant, ΔE_0
F	: Radius function, f
FP	: Derivative of f, f'
G	: Variable of energy, g
GD	: Variable of energy, \dot{g}
GP	: Derivative of displacement in Y direction, g'
H	: Parameter, $K(\lambda_1^2)$
HP	: Derivative of displacement in Z direction, h'
P	: RT/V_1 module
RADII	: Non-dimensional radius, r
RIND	: Difference between both side of integral equality
RINV	: Invariants of deformation tensor

RIN2	:	Increment for r_1 (during the iteration)
RINT	:	Integral from r_1 to r_2
RMO	:	Nondimensional moment value
RMOM	:	Absolute moment value
R1	:	Absolute radius, r
SI	:	Invariant of plastic free energy,
SJ	:	Invariants of elastic free energy,
SSS1	:	Principle stress in X direction, t_1
SSS2	:	Principle stress in Y direction, t_2
SSS3	:	Principle stress in Z direction, t_3
STR1	:	t_1 in nondimensional form
STR2	:	t_2 in nondimensional form
STR3	:	t_3 in nondimensional form
TOL1	:	Tolerance for equilibrium equation solution
TOL2	:	Tolerance for integral related radii
TOL3	:	Tolerance for V_2 iteration
TOL4	:	Tolerance for new V_2 solution
U	:	Material parameter, μ/ξ
V2R	:	Polymer ratio at stations
V20	:	Swelling degree (equilibrium)
X	:	χ parameter
XB	:	$\bar{\chi}$ parameter
Y	:	$\xi kT/V_0$ module
YR1	:	New r_1 values

YT : New t_1 stress expression
YV2R : New polymer ratio at stations
YZ : New initial value for YV20 solution
Z : New swelling degree, v_{20}
ZETA : θ_0 in degrees.

A.5 SAMPLE INPUT DATA CARD

Following data card is used for

$$x = 0.25 \quad \theta_0 = 120^\circ$$

0.125, 0.12, 25., 0.2, 0.25, 0.90, 0.15, 1., 2.0,
2.0994, 0.001, 1., 0.0005, 1.0, 0.6, 0.62, 0.6,
0.001, 0.0001

A.6 - SAMPLE OUTPUT FOR $\chi = 0.25$, $\theta_0 = 120^\circ$

```

** COMPUTER PROGRAM FOR
NONHOMOGENEOUS STATE OF STRESS, STRAIN AND SWELLING
PROBLEM IN AMORPHOUS POLYMER NETWORKS **

```

```

DIMENSION A(3),H(3),B(3),G(3),GD(3),BO(3),Z(3),V2R(11),YV2R(11),R1
#(11),F(11),RINV(3),DIFF(11),FP(11),EN(11),SSS1(11),SSS2(11),SSS3(1
#1),T(2),YR1(11),YDIFF(11),STR1(11),STR2(11),
*STR3(11),RADII(11),YZ(11),YT(11)
EXTERNAL RLAM,PARK
M=1
READ(5,*) F,C,P,Y,X,R1(1),DR1,A0,B0,TET0,TOL2,HP,RIN2,
#U,Z(1),Z(2),Z(3),TOL3,TOL4
DR=DR1

```

```

SOLUTION FOR V20

```

```

TOL1=10.**(-6.)
1 A(1)=Z(1)**(-1./3.)
A(2)=Z(2)**(-1./3.)
A(3)=Z(3)**(-1./3.)
CALL PARK (L,C,A,P,Y,H)
DO 10 I=1,2
WY=ABS(1.-Z(I))
T(I)=P*(ALOG(WY)+Z(I)+X*Z(I)**2.)+Z(I)**(1./3.)*Y*(1.+U*H(I))
II=I
IF(ABS(T(II)).LE.TOL1) GO TO 2
10 CONTINUE
AAA=Z(2)
Z(2)=Z(1)-((Z(1)-Z(2))/(T(1)-T(2)))*T(1)
Z(1)=AAA
GO TO 1
2 I=11
V20=Z(I)
DO 20 J=1,11
YR1(J)=0
20 V2R(J)=Z(I)

```

```

DETERMINATION OF R1 AND R2

```

```

3 DR1=DR
CALL RRR (R1,DR1,V20,V2R,A0,B0,TET0,TOL2,F)

```

```

DETERMINATION OF ENERGY AT R1 AND R2

```

```

GP=TET0/(BO*V20**(-1./3.))
I=1
FP(I)=(V20/V2R(I))/(GP*F(I))
CALL RLAM (I,F,V20,FP,HP,GP,A)
CALL SINV (A,RINV)
CALL ENEM (I,X,Y,RINV,A,C,E,U,V2R,P,EN)
I=I+10
IF(I.GT.11) GO TO 8
GO TO 9
8 EF=ABS(EN(1)-EN(11))
IF(EF.LE.TOL3) GO TO 4
R1(1)=R1(1)+RIN2
GO TO 3

```

```

80.
81.
82.
83.
84.
85.
86.
87.
88.
89.
90.
91.
92.
93.
94.
95.
96.
97.
98.
99.
100.
101.
102.
103.
104.
105.
106.
107.
108.
109.
110.
111.
112.
113.
114.
115.
116.
117.
118.
119.
120.
121.
122.
123.
124.
125.
126.
127.
128.
129.
130.
131.
132.
133.
134.
135.
136.
137.
138.
139.
140.
141.
142.
143.
144.
145.

      FINDING ENERGY, STRESS, YV20

4  IF(EN(1).GT.EN(11)) ENAO=-EN(1)
   IF(EN(11).GT.EN(1)) ENAO=-EN(1)
12 DO 40 J=1,11
   FP(J)=(V20/V2R(J))/(GP*F(J))
   CALL RLAM (J,F,V20,FP,HP,GP,A)
   CALL SINV (A,RINV)
   CALL ENEM (J,X,Y,RINV,A,C,E,U,V2R,P,EN)
   SSS1(J)=(V20**(.2/.3))*U0/(F(J)*TETO*FP(J))*(FN(J)+ENAO)
   CALL YEH (J,A,H,F,V20,HP,GP,E,C,P,Y,SSS1,X,U,YV2R)
   DIFF(J)=ABS(YV2R(J)-V2R(J))
   CALL SSSS (J,H,V2R,A,P,Y,X,U,SSS1,SSS2,SSS3)
40  V2R(J)=YV2R(J)

      COMPARESION OF NEW AND OLD V2R,S

   DM=DIFF(1)
   J=2
5  IF(DM.LT.DIFF(J)) DM=DIFF(J)
   J=J+1
   IF(J.GT.11) GO TO 6
   GO TO 5
6  IF(TOL4.GE.DM) GO TO 7
   GO TO 12

      COMPARESION OF NEW AND OLD R,S

7  DO 90 M=1,11
   YDIFF(M)=ABS(YR1(M)-R1(M))
90  YP1(M)=R1(M)
   YDM=YDIFF(1)
   K=2
91 IF(YDM.LT.YDIFF(K)) YDM=YDIFF(K)
   K=K+1
   IF(K.GT.11) GO TO 92
   GO TO 91
92 IF((0.01).GE.YDM) GO TO 93
   IF(M.LE.1) R1(1)=R1(1)-.10
   M=M+1
   R1(1)=P1(1)-.05
   GO TO 3

      NON-DIMENSIONALIZATION AND OUTPUT FORMATS FOR STRESS AND RADIUS

93 DO 100 MM=1,11
   STR1(MM)=SSS1(MM)/Y
   STR2(MM)=SSS2(MM)/Y
   STR3(MM)=SSS3(MM)/Y
100 RADII(MM)=(R1(MM)-R1(1))/(R1(11)-R1(1))
   ZETA=TETO*.180/3.1416
   WRITE(6,70) X,ZETA
79  FORMAT(1H,//////,30X,***** SOLUTION FOR X=,F5.2,,AND TETA=,
* F9.1,,D *****
   WRITE(6,21)

21  FORMAT(//////,8X,,RADIUS,,12X,,V2R,,10X,,ENERGY,,11X,,STRESSES
*IN X-Y-Z DIRECTIONS,)
   WRITE(6,32) (R1(I),V2R(I),EN(I),SSS1(I),SSS2(I),SSS3(I),I=1,11)
32  FORMAT(/,7X,F9.6,7X,F9.6,7X,F9.5,7X,3F9.6)
   WRITE(6,77)
77  FORMAT(//////,10X,,NONDIMENSIONAL FORMS:,,//,31X,,RADIUS,,
*17X,,STRESSES IN X-Y-Z DIRECTIONS,)
   WRITE(6,78) (RADII(I),STR1(I),STR2(I),STR3(I),I=1,11)
78  FORMAT(/,30X,F9.6,15X,3F9.6)

      MOMENT CALCULATION

```



```

218. SUBROUTINE SSSG (J,H,V2R,A,P,Y,X,U,SSS1,SSS2,SSS3)
219. DIMENSION SSS1(11),SSS2(11),SSS3(11),V2R(11),H(3),A(3)
220. SSS1(J)=P*(ALOG(1.-V2R(J))+V2R(J)+X*V2R(J)**2.)+(A(1)**2.
221. +*V2R(J)*Y*(1.+U*H(1)))
222. SSS2(J)=P*(ALOG(1.-V2R(J))+V2R(J)+X*V2R(J)**2.)+(A(2)**2.
223. +*V2R(J)*Y*(1.+U*H(2)))
224. SSS3(J)=P*(ALOG(1.-V2R(J))+V2R(J)+X*V2R(J)**2.)+(A(3)**2.
225. +*V2R(J)*Y*(1.+U*H(3)))
226. RETURN
227. END

```

```

228. SUBROUTINE ENEM (J,X,Y,RINV,A,C,E,U,V2R,P,EN)
229. DIMENSION EN(11),R(3),G(3),V2R(11),RINV(3),A(3)
230. DO 10 I=1,3
231. G(I)=A(I)**2.*(E+C*(A(I)-1.))
232. 10 B(I)=((A(I)-1.)*(1.+A(I)-C*A(I)**2.))/((1.+G(I))**2.)
233. SJ=-U*(ALOG((1.+B(1))*(1.+G(1)*B(1)))+ALOG((1.+B(2))*(1.+G(2)*
234. +*B(2)))+ALOG((1.+B(3))*(1.+G(3)*B(3))))
235. SI=U*((1.+G(1))*B(1)+(1.+G(2))*B(2)+(1.+G(3))*B(3))
236. EN1=0.5*Y*((RINV(1)-3.)*SI+SJ)
237. V1R=1.-V2R(J)
238. XR=X
239. E12=P*(V1R/V2R(J))*(ALOG(V1R)+XB*V2R(J))
240. EN(J)=EN1+EN2
241. RETURN
242. END

```

```

243. SUBROUTINE RRR (R1,DR1,V20,V2R,A0,B0,TETO,TOL2,F)
244. DIMENSION F(11),R1(11),V2R(11)
245. 2 DO 10 J=2,11
246. 10 R1(J)=R1(1)+(J-1)*DR1
247. RINT=(DR1/3.)*(1./(V20**2.*A0*V20**(-1./3.)))*(V2R(1)*R1(1)+
248. +*V2R(2)*R1(2)
249. +*2*V2R(3)*R1(3)+4*V2R(4)*R1(4)+2*V2R(5)*R1(5)+4*V2R(6)*R1(6)
250. +*2*V2R(7)*R1(7)+4*V2R(8)*R1(8)+2*V2R(9)*R1(9)+4*V2R(10)
251. +*R1(10)+V2R(11)*R1(11))
252. RINT=ABS(RINT)-(B0*V20**(-1./3.)/TETO)
253. IF (RINT-TOL2) 1,1,3
254. 3 DR1=DR1+.0001
255. GO TO 2
256. 1 DO 20 I=1,11
257. 20 F(I)=R1(I)
258. RETURN
259.
260.
261.
262. END

```

```

263. SUBROUTINE RLAM (I,F,V20,FP,HP,GP,A)
264. DIMENSION A(3),FP(11),F(11)
265. A(1)=V20**(-1./3.)*FP(I)
266. A(2)=V20**(-1./3.)*F(I)*GP
267. A(3)=V20**(-1./3.)*HP
268. RETURN
269. END
270.

```

```

271. SUBROUTINE YEN (K,A,H,F,V20,HP,GP,E,C,P,Y,SSS1,X,U,YV2R)
272. DIMENSION F(11),SSS1(11),YV2R(11),YZ(11),YT(11),FP(11),
273. *A(3),H(3)
274. Y7(K)=0.05
275. FP(K)=(V20/YZ(K))/(GP*HP*F(K))
276. CALL RLAM (K,F,V20,FP,HP,GP,A)
277. CALL PARK (E,C,A,P,Y,H)
278. YT(K)=P*(ALOG(1.-YZ(K))+YZ(K)+X*YZ(K)**2.)+A(1)**2.
279. *YZ(K)*Y*(1.+U*H(1))-SSS1(K)
280. IF (YT(K)-0.0) 1,1,2
281. 1 FP(K)=(V20/YZ(K))/(GP*HP*F(K))
282. CALL RLAM (K,F,V20,FP,HP,GP,A)
283. CALL PARK (E,C,A,P,Y,H)
284. YT(K)=P*(ALOG(1.-YZ(K))+YZ(K)+X*YZ(K)**2.)+A(1)**2.
285. *YZ(K)*Y*(1.+U*H(1))-SSS1(K)
286. IF (YT(K).GT.0.0) GO TO 33
287. YY=YZ(K)
288. Y7(K)=YZ(K)+0.0005
289. GO TO 1
290. 2 FP(K)=(V20/YZ(K))/(GP*HP*F(K))
291. CALL RLAM (K,F,V20,FP,HP,GP,A)
292. CALL PARK (E,C,A,P,Y,H)
293. YT(K)=P*(ALOG(1.-YZ(K))+YZ(K)+X*YZ(K)**2.)+A(1)**2.
294. *YZ(K)*Y*(1.+U*H(1))-SSS1(K)
295. IF (YT(K).LT.0.0) GO TO 33
296. YY=YZ(K)
297. Y7(K)=YZ(K)+0.0005
298. GO TO 2
299. 33 YV2R(K)=(YY+YZ(K))/2.
300. RETURN
301. END
302.
303.
304.
305.
306.

```

OPTIONAL AND APPROXIMATION SUBROUTINES

```

307. SUBROUTINE DEN (K,V20,H,A,FP,SSS1,P,Y,X,U,TOL1,R1,YV2R)
308. DIMENSION YZ(3,3),YT(3,3),FP(11),F(11),A(3),H(3),
309. *YV2R(11),P1(11),SSS1(11)
310. YZ(K,1)=V20
311. YZ(K,2)=V20+0.01
312. DO 42 L=1,2
313. WW=ABS(1.-YZ(K,L))
314. YT(K,L)=P*(ALOG(WW)+YZ(K,L)+X*(YZ(K,L)**2.))
315. *A(1)**2.*YZ(K,L)*Y*(1.+U*H(1))-SSS1(K)
316. II=L
317. IF (ABS(YT(K,L)).LE.TOL1) GO TO 41
318. CONTINUE
319. 42 AAA=YZ(K,2)
320. YZ(K,2)=YZ(K,1)-((YZ(K,1)-YZ(K,2))/(YT(K,1)-YT(K,2)))
321. *YT(K,1)
322. Y7(K,1)=AAA
323. GO TO 44
324. 41 L=11
325. YV2R(K)=YZ(K,L)
326. RETURN
327. END

```

```

328. SUBROUTINE APPR (V2R,R1)
329. DIMENSION V2R(11),R1(11)
330. DO 70 K=2,10
331. 70 V2R(K)=(V2R(1)-V2R(11))*((R1(K)-R1(1))/(R1(1)-R1(11)))+V2R(1)
332. RETURN
333. END

```

***** SOLUTION FOR X= .25 AND TETA= 120.00 *****

RADIUS	V2R	ENERGY	STRESSES IN X-Y-Z DIRECTIONS		
.770498	.207250	-16.13900	-.000594	-.340050	-.175758
1.084097	.188250	-16.57277	-.081719	-.232981	-.122179
1.397695	.175250	-16.75015	-.106665	-.159324	-.090852
1.711294	.164250	-16.81449	-.110474	-.096658	-.067555
2.024892	.153750	-16.81660	-.104048	-.037504	-.047947
2.338491	.142750	-16.77926	-.091016	.019868	-.030054
2.652089	.131250	-16.71055	-.074744	.074152	-.014131
2.965688	.119250	-16.61345	-.057027	.123645	-.000422
3.279286	.106250	-16.48969	-.037962	.165832	.011227
3.592885	.092250	-16.33518	-.018686	.197106	.020223
3.906483	.077250	-16.13975	-.000021	.213475	.025986

NONDIMENSIONAL FORMS;

RADIUS	STRESSES IN X-Y-Z DIRECTIONS		
.000000	-.002969	-1.700252	-.878790
.100000	-.408593	-1.164907	-.610897
.200000	-.533326	-.796620	-.454261
.300000	-.552369	-.483289	-.337773
.400000	-.520238	-.187518	-.239735
.500000	-.455080	.099342	-.150272
.600000	-.373720	.370761	-.070654
.700000	-.285135	.618223	-.002109
.800000	-.189812	.829160	.056135
.900000	-.093430	.985529	.101116
1.000000	-.000106	1.067373	.129929

MOMENT: .446251 .808083

TETA: 2.094400

V20= .118836

TOLARANCE FOR V20= .000001

TOLARANCE FOR R INTEGRAL= .001000

TOLARANCE FOR ENERGIES= .001000

TOLARANCE FOR V2R S= .000100

APPENDIX B

SOLVENT DISTRIBUTIONS

Figure 5.1.11 may be examined in a better way with the help of Figure B.1 and B.2 and Table B.1.

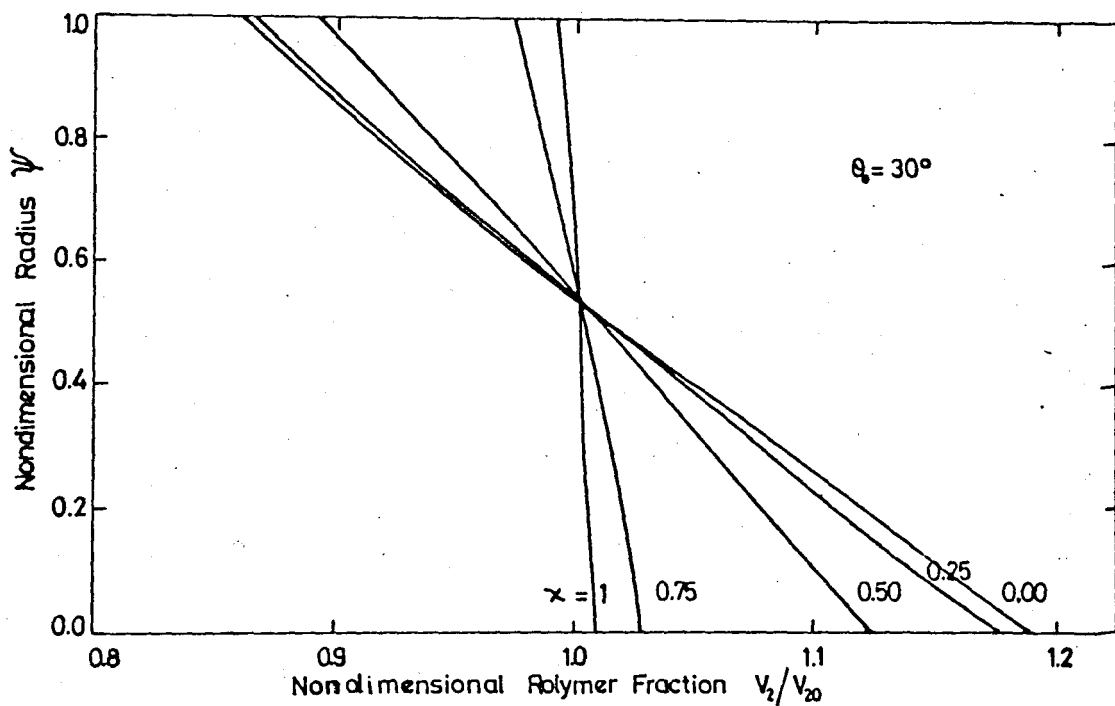


Figure B.1 - Solvent distribution along the X direction at 180° flexure for energy χ parameter.

In these figures radius and polymer fraction are both in nondimensional forms. Radius is introduced in conventional presentation ψ , polymer ratio is nondimensionalized by dividing it into equilibrium swelling ratios V_{20} , which are given in Table B.1.

TABLE B.1

χ	V_{20}
1.0	0.6931
0.75	0.5060
0.63	0.3758
0.50	0.2378
0.25	0.1188
0.00	0.0822

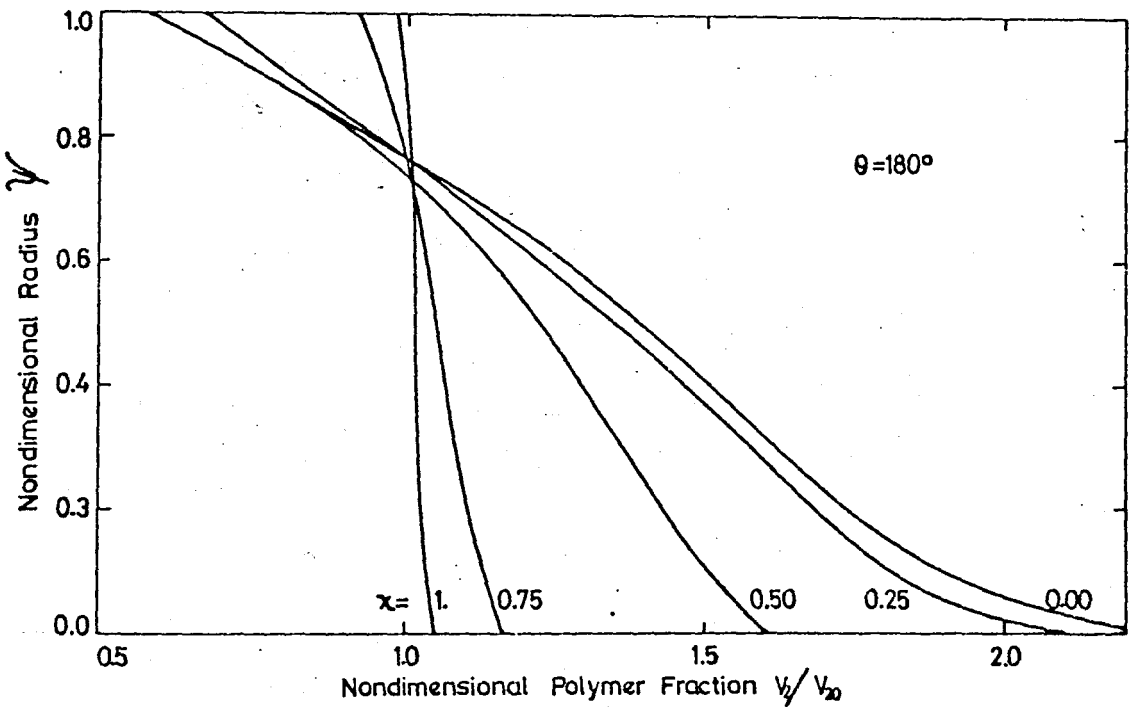


Figure B.2 - Solvent distribution along the X direction for different solvents (χ 's) at 30° flexure.

BIBLIOGRAPHY

1. P.J. Flory and J. Rehner, Journal of Chemical Physics, Vol. 11, pp. 521, 1943.
2. L.G.R. Treloar, The Physics of Rubber Elasticity, 3rd. Ed., Clarden, Oxford, 1975.
3. P.J. Flory, Principles of Polymer Chemistry, Cornell University, Ithaca, N.Y. 1953.
4. P.J. Flory, Discussion notes: "Statistical Thermodynamics of Random Networks", Proc. R. Soc. London Ser. A, A351, pp. 351, 1976.
5. J.P. Flory, "The Elastic Free Energy of Dilation of a Network", Macromolecules, Vol.12, pp. 119, Jan. 1979.
6. P.J. Flory and B. Erman, "Theory of Elasticity of Polymer Networks, 3", Macromolecules, Vol. 15, pp. 800, 1982.
7. P.J. Flory, "Theory of Elasticity of Polymer Networks", The Journal of Chemical Physics, Vol. 66, No. 12, June 1977.
8. B. Erman, "Nonhomogeneous State of Stress, Strain and Swelling in Amorphous Polymer Networks", Journal of Polymer Science, Vol. 21, pp. 893, 1983.
9. P.J. Flory and Yoh-Ichi Tatora, "The Elastic Free Energy and the Elastic Equation of State: Elongation and Swelling of Polydimethylsioxane Networks", Journal of Polymer Science, Vol. 13, pp. 683, 1975.
10. A.C. Eringen, Nonlinear Theory of Continuous Media, McGraw-Hill, New York, 1962.
11. A.E. Green and J.E. Adkins, Large Elastic Deformations, 2nd Ed., Clarendon, Oxford, 1970.
12. A.E. Green and W. Zerna, Theoretical Elasticity, 2nd. Ed., Clarendon, Oxford, 1968.

REFERENCES NOT CITED

- B. Erman, W. Wagner, P.J. Flory, "Elastic Modulus and Degree of Cross-linking of Poly(ethyl acrylate) Networks", Macromolecule, Vo. 13, pp. 1554, 1980.
- K.C. Valais and R.F. Landel, "The Strain-energy Function of a Hyperelastic Material in Terms of the Extension Ratios", Journal of Applied Physics, Vol. 38, No.7, pp. 2997, June 1967.
- P.J. Flory, "Elasticity of Polymer Networks Cross-linked in States of Strain", Mellon Institute, Pittsburgh, Pa., 1959.
- A.C. Eringen, Mechanics of Continua, John Wiley and Sons, Inc., Princeton University, 1967.